Title
Regulation of Cytokinetic Protein FtsZ in *Caulobacter crescentus* by Elements of the Chromosome Partitioning System

Author
Graf, Matthew Allan Gaffney

Publication Date
2014

Peer reviewed|Thesis/dissertation

UNIVERSITY OF CALIFORNIA

Los Angeles

Regulation of Cytokinetic Protein FtsZ in *Caulobacter crescentus* by Elements of the Chromosome Partitioning System

A dissertation submitted
in partial satisfaction of the requirements of the degree
Doctor of Philosophy in Biochemistry and Molecular Biology

by

Matthew Allan Gaffney Graf

2014

ABSTRACT OF THE DISSERTATION

Regulation of cytokinetic protein FtsZ in

Caulobacter crescentus by elements of the

chromosome partitioning system

by

Matthew Allan Gaffney Graf

Doctor of Philosophy in Biochemistry and Molecular Biology

University of California, Los Angeles, 2014

Professor James Gober, Chair

The coordination of essential cell cycle events is necessary to maintain the viability of a species over many generations; two core processes to any replicative cell is the duplication of chromosomal DNA and the division of a growing cell into two functional daughters. The crescent-shaped α-proteobacteria, *Caulobacter crescentus*, has a distinct biphasic life cycle making it ideal to study such cell cycle linked events. The core protein of cell division in *C. crescentus* is the essential, and highly conserved tubulin-homologue, FtsZ. Prior to FtsZ directed cell division, duplicating chromosomes are quickly sequestered to opposing regions of the replicative cell such that each daughter will contain a complete chromosome after division. The three-component partitioning complex, ParAB/*parS*, is homologous to plasmid segregation systems and essential to the viability of *C. crescentus*. Previous work has shown that changes to

the cellular levels of partitioning complex proteins have a drastic effect on the cell cycle, including the loss of FtsZ ring structures associated with cell division. Using a biochemical approach with purified protein components, the interplay between the partitioning complex proteins and cytokinetic protein FtsZ was addressed. The work presented in this dissertation clearly demonstrates the ability of the partitioning complex to directly regulate FtsZ assembly. The data shows that the ATP-bound form of ParA is a potent stimulator of FtsZ assembly and capable of lowering the critical concentration of FtsZ required for filamentation. Additionally, ParA seems capable of changing the nature of assembled FtsZ, causing an overall elongation of filaments and inducing distinct curvatures into their structure. ParA is a member of a superfamily of ATPase proteins, which comprises two known negative regulators of FtsZ filamentation. It is therefore proposed that ParA is a physiologically relevant activator of FtsZ assembly based on previous cytological results, the relation of ParA to known FtsZ regulators and biochemical results presented within this work. The activation of FtsZ assembly by the partitioning protein ParA is a novel example of stimulatory FtsZ regulation by an essential and active participant in a core, chromosomally linked process.

The dissertation of Matthew Allan Gaffney Graf is approved.

Carla Marie Koehler

Beth Ann Lazazzera

James W Gober, Committee Chair

University of California, Los Angeles

2014

To my Mother, who taught me the value of commitment and perseverance;

To my Father, who nurtured in me a love of learning, and the stars;

To my Sister, who exemplifies what it is to be a great teacher;

To my Niece and God-daughter, who has shown me what it is to truly love;

and to my Husband, for whom I do it all.

TABLE OF CONTENTS

FIGURES

FIGURES (Continued)

ACKNOWLEDGEMENTS

First and foremost, I would like to thank my advisor James Gober for his help, guidance, and mentorship throughout my graduate work; also, for his unbelievable and inspirational brilliance. I would also like to acknowledge the members of my committee Carla Koehler, Beth Lazazzera, Joe Loo, and Alison Frand for their guidance through this process and their critical reading of this manuscript. A special acknowledgement to Carla Koehler who has been supportive beyond duty and extended to me the opportunity to manage the Shared Biochemistry Instrumentation Facility; furthermore, I would like to acknowledge Margot Quinlan and Catherine Clarke who were wonderful supervisors in that capacity. An additional acknowledgment to Margot Quinlan must be made for her valuable insights and commentary on the experimental results presented here, as well as the use of her instruments and laboratory space in the sedimentation experiments presented within. Similarly, I would like to acknowledge Albert Courey for allowing the use of his laboratory and systems during the size-exclusion chromatography steps of the protein purification performed for these experiments. I must also to acknowledge Martin Phillips, both friend and mentor, who was instrumental in the gathering and understanding of the electron microscopy data. I would thank all the members of the Gober lab for their expertise, insights, mentorship and friendship during my graduate work. Finally, a special acknowledgement to my friend Heather McFarlane, who beyond being indispensible for guidance during the protein purifications discussed in this dissertation, is simply a phenomenal person.

VITA

2002	Hope for Hearing Foundation Research Fellow
	House Ear Institute, Los Angeles
2006	B.S. Creative Studies: Emphasis Chemistry & Biochemistry
	College of Creative Studies
	University of California, Santa Barbara
2007-2011	Teaching Assistant, Chemistry and Biochemistry
	University of California, Los Angeles
	154: Biochemistry Laboratory
	153C: Metabolism and Regulation
2008	Presentation: American Society of Microbiology Annual Conference
	The Role of GidA in Chromosome Partitioning and Cytokinesis
2010	Presentation: American Society of Microbiology Annual Conference
	Role of Condensins in Chromosome Segregation in Caulobacter
2011	Recipient, Samson H. Cheng Biochemistry Teaching Award
2012	Presentation: Experimental Biology Conference
	Cell Cycle Coordination in Caulobacter crescentus
2012-2014	Manager of the Biochemistry Shared Instrumentation Facility
	Department of Chemistry and Biochemistry
	University of California, Los Angeles

CHAPTER 1

The Role of FtsZ in Bacterial Cell Division
and the Mechanisms of its Regulation

The *ftsZ* gene product is an essential and widely conserved player in bacterial cell division.

Regions of the *Escherichia coli* K-12 genome controlling cell division and cell shape were first identified through the selection of mutants extremely deficient in cell division when grown at elevated temperatures: the mutants were ultimately termed *fts*, for the filamentous temperature-sensitive growth observed [1-4]. Subsequent genetic analysis found that one mutant among a phenotypically similar subset mapped not to the previously identified *ftsA* locus, but to a separate gene, identified as *ftsZ* [5]. Concurrently, a series of mutants were being studied as having a critical role in cell division due to their delayed recovery from filamentation after exposure to ultraviolet light, which induces an SOS-response in *E. coli* [6, 7]. Mutations in a gene believed to be a regulator of this phenotype, termed either *sfiB* or *sulB*, were shown to have dominant phenotypes and produce filamentous cells even in the absence of UV light treatment [8, 9]. Ultimately, both *sulB* and *sfiB* mutants were mapped to the same locus as *ftsZ* [10, 11]. The mapping study linking *sulB* to *ftsZ* also showed that the introduction of an additional wild-type *ftsZ* gene was sufficient to complement temperature-sensitive filamentation [10]. Later work probing the links between cell elongation and septation introduced mutations in division or elongation genes into *E. coli* and monitored growth. FtsZ was demonstrated to be an early and essential player in cell division as *ftsZ* mutants consistently showed in inability to form division septa. In contrast, many other *fts* gene mutations showed the formation of cell division septa, though were unable to complete cell division, suggesting a hierarchical assembly of cell division components [12]. Overexpression of *ftsZ* in *E. coli* K-12 produced additional division sites resulting in minicells, though not at the expense of normal cell division. Furthermore, the amount of observed minicells was proportional to *ftsZ* expression levels, suggesting that FtsZ levels have a direct effect on the number of division sites [13].

Following the demonstration of the critical role *ftsZ* plays in the formation of cell division septa, genetic homologues to *E. coli ftsZ* were identified in a wide array of bacterial species using DNA hybridization via Southern blots, including multiple *Enterobacteriaceae* species, *Pseudomonas aeruginosa*, and *Agrobacterium tumefaciens*. Furthermore, antibodies raised against *E. coli* FtsZ produced detectable bands in Western Blots against distantly related species, including the gram-positive *Bacillus subtilis, Streptococcus faecalis,* and *Staphylococcus aureus*, suggesting of a high degree of conservancy in FtsZ proteins [14]. Analysis of the homologous *B. subtilis* gene revealed a 50% identity with the *E. coli* FtsZ at the amino acid level; furthermore, introduction and expression of the *B. subtilis ftsZ* gene was lethal to *E. coli* [15]. Subsequent work in *B. subtilis* confirmed a similar functional role for FtsZ, as it was demonstrated to be essential for both vegetative cell division at the midcell, and asymmetric division associated with sporulation [16]. The conserved role of FtsZ in bacterial cell division was further demonstrated in a pair of papers focusing again on *E. coli*. Electron microscopy of FtsZ visualized with labeled antibodies in dividing cells showed that it localizes along the inner-membrane of the cell, specifically at the site of the cell invagination [17]. Additionally, an *E. coli* strain was created where an inducible promoter controlled *ftsZ* expression: depletion of FtsZ from this strain resulted in markedly increased cell length and a complete cessation of cell division [18]. Since then, it has come to be widely accepted that FtsZ is the core protein of the multi-protein complex that is responsible for most bacterial cell-division mechanisms. Notably, homologues of bacterial FtsZ have also been identified as having a role in organelle fission in certain eukaryotes. Many types of plants, both non-vascular and vascular species, contain FtsZ homologous to that of cyanobacteria within their chloroplast division machinery; mitochondrial fission in certain protista utilizes an FtsZ with homology tracing to the α-proteobacteria [19, 20]. These discoveries are further evidence of

widely distributed and conserved role for FtsZ, and have been used as evidence to support the theory of the endosymbiotic origin of these eukaryotic organelles [reviewed in 21].

FtsZ is a homologue of Eukaryotic tubulin.

Visualizations of purified FtsZ *in vitro* via electron microscopy revealed filamentous structures reminiscent of eukaryotic cytoskeletal proteins [22, 23]. Filament formation was found to be dependent on GTP, in keeping with earlier studies that demonstrated guanosine-nucleotide specific binding and GTP-hydrolysis by FtsZ [24, 25]. The GTP-dependent filamentation of FtsZ and the highly conserved role it plays in bacterial cell division pointed to tubulin, as opposed to Ras-like signaling proteins, as a possible model for FtsZ function [15-17, 26, 27]. FtsZ contains a well-conserved glycine-rich sequence {GGGTGTG} in the N-terminal portion of the protein. This sequence is nearly identical to the {(SAG)GGTG(SA)G} sequence in the GTP binding domain of tubulin, with the exception of the penultimate threonine in FtsZ (Fig. 1.1). Single amino-acid substitutions introduced into this sequence drastically reduces GTP binding and hydrolysis [24, 25, 28, 29]. Despite a low primary sequence homology on the order of 10%, FtsZ and tubulin were revealed to share a strikingly similar tertiary structure upon resolution via X-ray crystallography [22, 23, 30, 31]. The structure of FtsZ revealed that is composed of two primary folding domains which sandwich a long α-helix linking the domains together (Fig. 1.1). The conserved GGGTGTG sequence was found to lie within a grouping of parallel β-sheets linked by α-helices, characteristic of a nucleotide-binding Rossmann motif. The structural analysis also provided an interesting insight into the previously postulated cooperativity in GTP hydrolysis by FtsZ. A short set of conserved residues was exposed on one face of the FtsZ monomer. This sequence sits on an unstructured loop approximately 100 residues from the GGGTGTG

sequence, at the transition between the N- and C-terminal folding domains. This loop, termed T7, contains a conserved NxDxxD motif, and was found on the opposite pole of FtsZ from the GTP binding site of the GGGTGTG sequence (Fig. 1.1, 1.2). In the αβ-tubulin dimer, the equivalent exposed T7-loop from one monomer was in contact with the Rossman-motif sequence of the other dimer, creating a complete GTPase domain. This arrangement absolutely accounts for the GTP-dependent assembly, and the requirement of assembly for GTP hydrolysis, that is observed in both tubulin and FtsZ, since no single monomer can form a complete GTPase domain and bound nucleotide serves as a contact bridge between assembled subunits [32, reviewed in 33].

Distinct differences in the polymerization dynamics have been observed between eukaryotic tubulin and bacterial FtsZ, despite a common ancestry. Notably, tubulin polymers arrange into cylindrical microtubules generally consisting of 13 linear protofilaments through strong lateral interactions between αβ-tubulin dimers. Interestingly, during microtubule disassembly, linear protofilaments are observed to peel away from the microtubule rather than dissociate in rings or discs. This observation suggests that the head-to-tail associations common to FtsZ are more stable than the lateral interactions unique to tubulin [reviewed in 34]. FtsZ by contrast is observed to primarily associate into single subunit filaments [35, 36]. Though lateral interactions and bundling have been observed between polymers *in vitro*, they are generally seen at higher concentrations, or induced by buffer conditions or crowding agents [37-39]. Furthermore, because there is rarely consistency to the bundling patterns observed across the various conditions, lateral self-association of FtsZ is generally viewed to be an artifact [reviewed in 40].

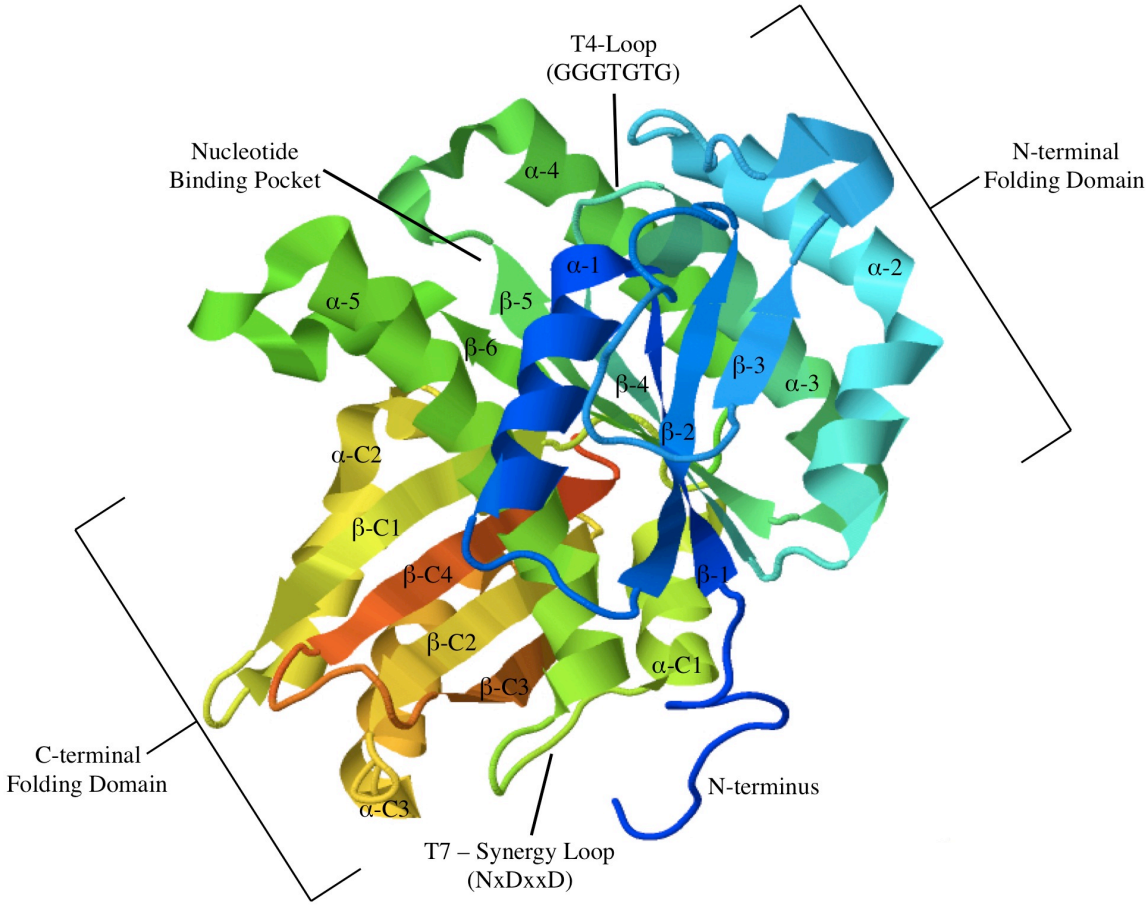

Figure 1.1: The Structure of FtsZ.
Above is the structure of an FtsZ monomer from *Pseudomonas aeruginosa*, lacking the linker region and extreme C-terminal domain. Secondary elements are labeled α or β for helices or sheets, respectively, followed by a number indicating ordering sequence from N- to C-terminals; the numbering restarts after the T7-synergy loop, with the addition of the letter C before the sequential number, corresponding to the switch from the N-terminal to C-terminal folding domains (as in Fig. 1.2). The structure is presented with a color spectrum for easier visibility: beginning with blue at the N-terminus to red at the C-terminus. The T4 loop containing the conserved tubulin GGGTGxG sequence is indicated, as is the T7 loop which completes the GTPase domain upon dimerization [32, 33]. The nucleotide-binding pocket is indicated as well: residues at the start of α-helix 1 and in α-helix 5 mediate recognition of guanine, while residues in β-sheet 5 and α-helix 4 bind to the ribose sugar (see Fig. 1.2).
FtsZ Structure: (PDB ID: 2VAW) Oliva MA, Trambaiolo D, Löwe J. Structural insights into the conformational variability of FtsZ. *J. Mol. Biol.* 373: 1229-1242, 2007.
Note: Labels and annotations were made to the structure by this author.

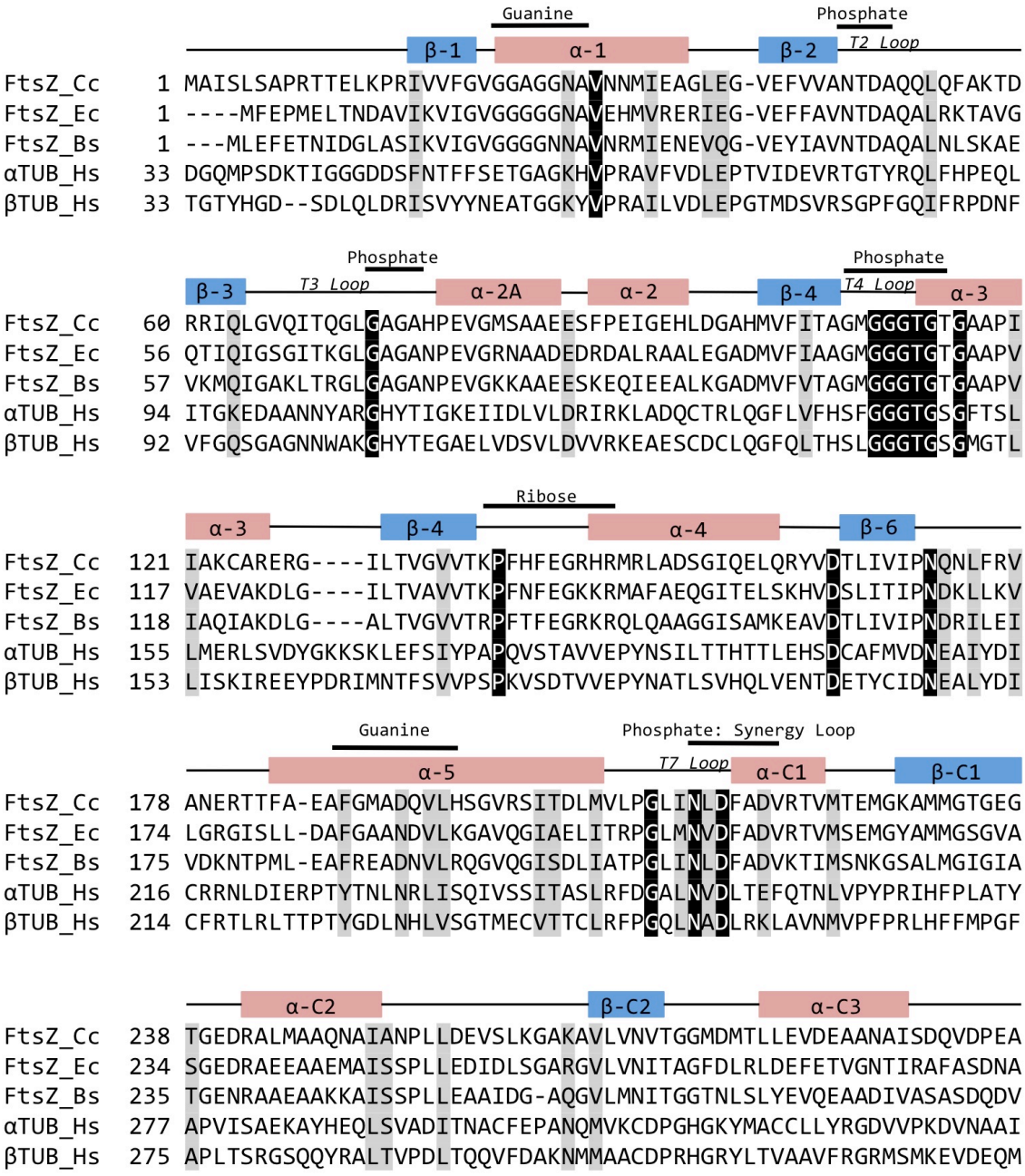

Figure 1.2: Sequence alignment of bacterial FtsZ with human αβ-tubulin.
The partial sequences of three bacterial FtsZ proteins (*C. crescentus*, *E. coli*, *B. subtilis*) were aligned with partial human α- and β-tubulin sequences using Clustal W alignment algorithms. Residues with perfect conservancy are shown in white text with black highlighting, while residues with a lesser degree of conservation are highlighted in gray. Above the alignment is a schematic of the secondary structural elements of FtsZ, as labeled in Figure 1.1. The short HL-1 and HL-2 domains in the T2-loop and after β-6, respectively, are omitted in this schematic for simplicity. Regions that contact guanosine nucleotide are indicated by a thick black bar above the secondary structural schematic, labeled with the contact points on the nucleotide [30].
Clustal W: Larkin MA *et al.*, Clustal W and Clustal X version 2.0. *Bioinformatics* 23: 2947-2948, 2007.
NCBI Sequence Accessions: *C. crescentus* (ACL96088), *E. coli* (BAB96663), *B. subtilis* (AAA22457), α-tubulin (K00558), β-tubulin (J00314)

Polymerization dynamics of FtsZ.

FtsZ binds GTP nucleotide with relatively high binding affinity: observed K_m values range from 10 to 100μM [36, 41]. Nucleotide binding is necessary, but not sufficient to form filaments, as FtsZ has a minimum critical concentration for assembly around 1μM, though calculated values can vary depending on the *in vitro* conditions utilized [42, 50]. Interestingly, it has been shown that FtsZ assembly is a cooperative process: binding of nucleotide stimulates a conformational change in monomers, which stimulates association and the formation of an FtsZ dimer [35, 43, 44, 50]. This dimer acts as a semi-stable nucleator for filament assembly because of the generally slow intrinsic GTP hydrolysis rate of FtsZ, thus assembly is stimulated cooperatively [36, 45, 46].

Fluorescence Recovery after photo-bleaching (FRAP) experiments of FtsZ in both *Escherichia coli* and *Bacillus subtilis* have demonstrated a half-time for recovery on the order of 10 to 20 seconds, suggesting that subunits of FtsZ filaments exchange with the cytoplasmic pool of monomers on this time scale [47-49]. These *in vivo* turnover numbers are in close agreement with turnover rate determined with FRET experiments *in vitro*, which ranged from 4 to 35 seconds depending on the buffering conditions used [36, 50]. Interestingly, subunit exchange *in vitro* still occurred independent of GTP hydrolysis. This raises the possibility that FtsZ monomer cycling from filaments is intrinsic and not entirely dependent on the GTPase activity of FtsZ subunits, and thus may occur both passively and via GTP hydrolysis induced destabilization [36]. The rapid exchange of FtsZ monomers in filaments, occurring on time scales that are a fraction of the assembly and disassembly time of the FtsZ ring during cytokinesis, suggests that a form of dynamic instability or treadmilling of filaments is occurring, as for tubulin or actin

cytoskeletal proteins [47, 51, reviewed in 52]. Some evidence of and directionality in FtsZ assembly into filaments was determined with point mutations at the interface residues around the GTPase domain. Mutations at the GTP binding pocket interface had a slight dominant-negative effect on growth, while interface mutations near the synergy loop had little discernable effect on *E. coli*, with only minor effects on the intrinsic GTP hydrolysis rate of the protein *in vivo*. The stronger effect of mutations at one interface versus the other suggests that the interaction surface at the GTP binding pocket primarily directs association, and therefore incoming monomers will primarily attach to a filament at this exposed end, indicative of directionality to FtsZ filament assembly [53].

FtsZ filament association with the cell membrane and stabilization of the early divisome.

Although FtsZ readily forms polymers capable of membrane constriction in the presence of GTP, FtsZ has no ability to associate with the membrane on its own [22, 24, 54]. Thus, functional divisome assembly requires the recruitment of associative proteins capable of holding FtsZ filaments to the cell membrane. Two such proteins have been identified in *E. coli*, FtsA and ZipA, both necessary for proper divisome assembly. The primary protein responsible for this action is the FtsA protein, highly conserved among bacteria and one of the earliest identified genes of the divisome apparatus [3, 15, 55]. FtsA has significant structural homology to actin and has been shown to bind ATP; additionally, FtsA can form dimers and possibly higher order oligomers [56-59]. FtsA interacts with the extreme C-terminal peptide of FtsZ through a conserved C-terminal region roughly opposite the nucleotide-binding domain, as observed in the structural analysis [56, 60-63]. Despite being highly conserved and essential, discovery of the role of FtsA as a membrane tether for FtsZ has only recently been elucidated. While the structure

of FtsA from *T. maritima* presented no clear membrane associative domains, two mutations in *E. coli* FtsA suggested that such a domain likely exists: the first was a deletion that appeared to reduce FtsZ ring stability but retained the ability to recruit late division proteins, the second was an isolated gain-of-function mutation in the same region that allowed FtsA to completely replace the function of ZipA [62, 64]. These mutations led to the identification of the C-terminal amphipathic helix on FtsA, which was not only essential for FtsA function and cell division, but was able to replace the membrane targeting domain of another essential *E. coli* division regulator [65]. The *E. coli* transmembrane protein, ZipA, serves a similar purpose of membrane attachment for FtsZ and recruitment of late divisome components [65, 66, reviewed in 69]. ZipA associates with the membrane via a trans-membrane helix and is recruited to the division site by FtsZ via an interaction between the C-terminal domains [65-68]. While both ZipA and FtsA are essential for the recruitment of other division components to the FtsZ ring in *E. coli*, the ring is still able to form in the absence of one of the components, although it is far less stable; in the presence of non-functional temperature-sensitive ZipA and FtsA mutants, there is no formation of FtsZ rings at the non-permissive temperature and already formed FtsZ rings quickly disassemble [70]. Thus, in addition to linking FtsZ to the membrane, these proteins play an important role in stabilizing the dynamic filaments so that a fully functional divisome may form.

Many additional factors have been identified which appear to regulate the stability of FtsZ filaments and bundling at the forming divisome. In *B. subtilis*, assembled FtsZ recruits the protein SepF to the division site; SepF directly interacts with FtsZ *in vitro*, and it is proposed that its function is to stabilize assembled FtsZ and promote lateral bundling of filaments through direct interactions [71-73]. Surprisingly, *B. subtilis* also employs a negative regulator of FtsZ

assembly at this stage of divisome formation. The protein EzrA, another membrane associated late recruit to the divisome, interacts with FtsZ directly and reduces its ability to assemble; indeed, *ezrA* mutants show increased FtsZ assembly at existing and aberrant sites [74, 75]. EzrA has recently been found to recruit PBP1 to the division site. PBP1 is involved in septal cell-wall remodeling, a finding that better justifies the role of a negative regulator of FtsZ assembly recruited to the division site [76, 77]. The ZapAB proteins are recruited to the division site in both *B. subtilis* and *E. coli*, where they likely contribute to FtsZ ring stability and bundling [78, 79]. While both proteins appear to interact with FtsZ directly, experiments suggest that ZapA serves to recruit ZapB to the division site, where it serves to promote bundling of FtsZ filaments, suggested by the complex ZapB structures observed via electron microscopy [79, 80]. Additionally, *E. coli* has a third protein, ZapC, which is also recruited to the division site and also serves to bind and bundle assembled FtsZ filaments [81].

Regulation of FtsZ polymerization and cell division site selection.

The most basic form of FtsZ assembly control, but by no means simple, is a tight regulation of protein levels within the cell and during the cell cycle. As previously discussed, FtsZ has a critical concentration of assembly; therefore, levels must be maintained sufficiently high to allow for assembly at the appropriate time [42, 43]. However, if levels become too high, the viability of the cell will be at risk due to aberrant division, as demonstrated by *ftsZ* over-expression experiments [13]. The transcription of *Escherichia coli ftsZ* is under the influence of six identified promoter regions, the majority of which co-translate other essential genes of the divisome, and is regulated by multiple inputs including cell cycle and environmental factors [82, reviewed in 83]. Transcription is tied to the cell cycle and appears to peak roughly in

coordination with the start of DNA replication [84-86]. Additionally, transcription of *ftsZ* and divisome genes are also heavily tied to the growth rate of the cell, such that transcripts increase in faster growing populations [84, 87, 88]. Trans-acting elements have been identified which serve to modulate *ftsZ* expression in response to environmental and metabolic conditions. As *E. coli* enters into the stationary phase, SdiA induces transcription of divisome genes through auto-induction via stimulatory molecules secreted into the media at high population densities [89-91]. Evidence also exists *ftsZ* transcription in *E. coli* is also responsive to the nutrient status and metabolic state of the cell: a two-component system, RcsBC, activates *ftsZ* transcription along with its primary target genes required for the synthesis of the exopolysaccharide colonic acid; additionally, transcription of *ftsZ* is activated by guanosine pentaphosphate, a signaling molecule associated with glutamine metabolism and the stringent response [92, 93]. In species with more complex life cycles, developmental regulation of *ftsZ* transcription is an essential element as well. *Bacillus subtilis* controls expression of *ftsZ* and divisome genes via three promoters, two of which are employed during vegetative growth and a third that is activated as part of the sporulation transcriptional program [94, 95]. The onset of sporulation activates the Spo0A regulator, which in turn activates transcription of sporulation specific σ^H-factor and the *spoIIE* gene [96]. Spo0A is essential for FtsZ asymmetry, which is achieved through an increase in *ftsZ* and divisome gene transcription mediated by both Spo0A and σ^H [97]. The increase in FtsZ levels induces a switch to polar localization of FtsZ rings via a dynamic spiral intermediate structure; the FtsZ ring in the mother cell compartment is destabilized via an independent transcriptional program that produces an assembly inhibitor, MciZ, discussed in detail later [98, 179]. The SpoIIE protein is essential for completion of sporulation and directly interacts with FtsZ; however, it is not necessary for FtsZ asymmetry associated with sporulation. It has been

proposed that the increase in FtsZ levels due to σ^H and Spo0A *ftsZ*-transcriptional increases is sufficient to induce divisome FtsZ-ring reorganization, suggestive of additional unidentified positive factors for assembly at polar regions [99-102]. Similar developmentally regulated and environmentally responsive *ftsZ* transcription programs have been identified in a number of bacterial species, including *Neisseria gonorrhoeae*, *Streptomyces* spp, *Mycobacterium smegmatis*, the cyanobacterium *Anabaena*, and during symbiosis in a species of *Candidatus*, underlying this important aspect of FtsZ regulation and cellular division control [103-108].

Regulation of the spatial positioning of FtsZ assembly is perhaps the most well characterized mechanism. Both *Escherichia coli* and *Bacillus subtilis* utilize two complementary negative regulator mechanisms: the first is associated with the polar regions of the cell, while a second inhibits FtsZ polymerization in regions occupied by the chromosome. Together, these systems ensure that the division septum is formed exclusively at the midcell while protecting the chromosome from physical damage due to a closing divisome. The Min system was the first identified polar-associated regulation system, and so named as *min* mutants divided asymmetrically, producing mini-cells devoid of chromosome [109]. It was proposed early on that the *min* phenotype resulted from a system that drove a division factor from the poles to the medial region of the *E. coli* cell, since *min* mutants have an increased length in the DNA containing cells, complementary to the reduced length of anucleate mini-cells [110]. Once FtsZ had been identified as this primary division factor in bacterial cells, the demonstration that *ftsZ* over-expression produced mini-cells in wild-type *E. coli* supported this polar versus medial competition model [13]. Shortly thereafter, the elucidation of the *minB* locus and the three genes it encodes, *minCDE*, confirmed the previously proposed model. Strangely, both disruptions to

the *min* locus and its overexpression produced the previously observed mini-cell phenotype, indicating a defined range of expression necessary for proper division control [27, 111]. Controlled expression of individual *min* genes in both wild-type and null *minB* genetic backgrounds demonstrated that MinC and MinD are inhibitory factors for cell division, while MinE acts as the spatial determinant for MinCD action [112]. Homologues to *minCD* have also been identified in *Bacillus subtilis*, though the *minE* topological determinant is notably absent from the locus [113, 114]. It was ultimately determined that the primary role of MinD is to enhance division inhibition by MinC and to mediate the action of the MinE localization factor [115]. FtsZ was confirmed as the target of the Min system through genetic experiments showing that the lethality induced by a *minB* locus overexpression was suppressed when *ftsZ* was overexpressed as well [116, 117].

MinC is the primary effector of FtsZ, resulting in an inhibition of assembly and cell division. It has been shown that MinC reduces the extent of filament formation *in vitro*, though it does not act to stimulate the GTPase activity of FtsZ. The N-terminal region of MinC is responsible for the interaction with FtsZ, though the affinity between monomers is relatively weak *in vitro* [118, 119]. Solved crystal structures of MinC from the gram-negative *Thermotoga maritima* revealed that it exists as a dimer, formed through C-terminal domain interactions. Interestingly, two orientations of the N-terminal domain existed relative to the protein as a whole, due to a flexible linker region between the two MinC domains, though the relevance of these conformations has not been addressed [120]. Recent work has focused on the mechanisms of MinC and FtsZ interaction, and the mode of inhibition of FtsZ assembly. Genetic work has determined that the C-terminal peptide of FtsZ, normally associated with FtsA interactions, and residues in the H-9

and H-10 helix regions mediate interactions with MinC. Mutations to these regions conferred resistance to MinC without lowering GTPase activity, which can appear to counteract effectors of FtsZ assembly by stabilizing filaments [121-124]. Finally, recent work has demonstrated that MinC has a higher affinity for FtsZ bound to GDP than to GTP, which has led to the proposal that MinC acts to destabilize FtsZ filaments and sequester recently released monomers from nucleotide-exchange and reassembly [125, 126].

Though MinC is the primary effector of FtsZ assembly, it requires the activity of two factors to actively promote assembly at the midcell, or more accurately, to inhibit assembly at the polar regions of the cell. MinC activity is greatly increased in the presence of MinD, and the interaction between FtsZ and MinC or a MinCD complex has been shown to have notable differences and independent interacting regions [115, 122]. MinD is an ATPase protein, with deviant Walker-A motifs similar to ParA and Soj, which oligomerizes when bound to ATP. Oligomerization causes MinD to associate with the membrane through a C-terminal targeting sequence; furthermore, oligomerized MinD binds MinC and thereby attracts it to the membrane [127-130]. Although MinD has been shown to bind both MinC and MinE, it appears to have a strong preference for MinE *in vitro* [131]. The N-terminal region of MinE stimulates MinD ATPase activity, thus converting it from a membrane associated dimer to monomers with reduced activity [132, 133]. It was initially observed that MinE localized primarily to the medial regions of the cell, where it would serve to deactivate MinD and its membrane association. This would serve to reduce the activity of MinC on FtsZ, allowing FtsZ to assemble in the middle of the cell [134, 135]. It has since been determined that this system actually oscillates from pole to pole with MinE as the primary effector of this switch: MinD-ATP associates with one pole of the

cell, recruiting both MinC, that inhibits FtsZ assembly, and MinE, which deactivates the entire system by dissociating MinD from the membrane [118, 136-138]. As medial proximal MinD is deactivated, it reassembles at the opposite pole, which is the point farthest from ongoing MinE activity. The accumulating MinD at the new pole, along with full dissociation from the previous pole, leads to recruitment of MinC and MinE to the polar region now replete in MinD-ATP initiating another oscillatory cycle. The end result of this oscillation is that MinC and MinD are most active in the polar regions of the cell, and therefore FtsZ is best able to assemble at the medial position [reviewed in 145]. The situation is somewhat different in *B. subtilis*, which lacks MinE, but contains a topological factor DivIVA. MinCD have not been observed to oscillate, but they do create a gradient through the cell with highest concentrations associated with polar regions. This gradient is determined by a MinCD association with DivIVA, mediated by the protein MinJ [139-142]. Molecular determinants for DivIVA localization have not been identified, and it is proposed that DivIVA is localized through interactions with the curved shape of the cellular structure at the poles [113, 143, 144].

The second spatial control mechanism, nucleoid occlusion, involves repression of assembly in regions where chromosome exists, thus delaying cell division until DNA replication is completed and nascent chromosomes are segregated. This mechanism complements medially directed spatial control by preventing assembly over the chromosome that could lead to the cutting of DNA by a dividing cell structure. The first evidence that the physical chromosome has a direct effect on the positioning of the divisome was provided using a series of *E. coli* mutants in *dnaA*, *dnaX*, *gyrA*, and *gyrB*, deficient in either DNA replication or segregation, respectively. In this study, replication deficient mutants showed a decrease in the number of total cell constriction

events when grown at the non-permissive temperature; segregation deficient mutants showed a similar effect, as well as a marked increase in the production of cells lacking DNA [146]. These findings were extended and confirmed using *E. coli parC* and *mukB* temperature sensitive mutants, deficient in chromosome segregation or organization, respectively. In these mutants, FtsZ rings were unable to form in the mid-cell where unsegregated nucleoids were present. It was also observed that FtsZ rings did not form close to the poles in DNA free regions, but appeared to be normally positioned in anucleate cells, presumably due to the action of the still functioning Min system [147]. In mutants lacking MinCDE, FtsZ rings were widely distributed throughout the cells, but were limited to regions free of chromosomal DNA. In cells lacking the membrane anchor FtsA, multiple rings were clustered in nucleoid free regions, suggesting that nucleoid occlusion mechanisms are sufficient to direct Z-ring formation in the absence of other divisome components [148].

The first protein identified as being a direct nucleoid occlusion factor was fortuitously discovered in a double-mutant screen of *min* mutants in *B. subtilis*. Null mutants in the ParB/Spo0J-like gene, *yyaA*, led to severe division defects and filamentous cells in concert with either mutated MinD or suppressed *minD* expression, and failed to form discrete FtsZ rings. YyaA, henceforth referred to as Noc in agreement with the literature, has about 40% homology with the DNA binding protein Spo0J, and Noc-GFP fluorescent fusions were observed to co-localize with the *Bacillus* nucleoid. The clearest evidence of the role of Noc in nucleoid occlusion was the observation that *ftsZ* over-expression in a *noc* null-mutant led to the formation of Z-rings over the nucleoid, as opposed to *minD* mutants, which maintained division sites only in nucleoid free regions [149, 150]. The Noc protein binds to a fourteen base-pair inverted repeat

sequence found at 74 sites throughout the *B. subtilis* chromosome, though these sites are notably absent from the *ter*-region of the DNA, suggesting that FtsZ suppression is diminished toward the end of chromosomal replication [151]. A similar double-mutant screen in *Escherichia coli* yielded a mutant locus that required co-expression of *minCDE* from an inducible promoter in order to grow, and was named *slmA*. In *slmA* mutants, depletion of the Min system leads to filamentous cells and reduced viability. ZipA, which interacts with FtsZ at the division site, localizes normally in a solely mutant *slmA* background, confirming that the division phenotype of the *slmA* mutation is independent of the Min system. SlmA contains a helix-turn-helix DNA-binding motif similar to that of the TetR repressor system, and deletions of this motif led to a diffuse localization of SlmA(ΔHTH) fluorescent fusions. Deletions of the entire *slmA* gene, or the helix-turn-helix region alone, led to cell septa forming directly over the chromosome, and over-expression of *slmA* was able to block FtsZ ring formation and cell division. SlmA was also shown to directly interact with FtsZ *in vitro*, apparently leading to a stimulation of FtsZ polymer formation [152]. This final observation seems to be inconsistent with a nucleoid occlusion mechanism since SlmA stimulation of FtsZ assembly would favor cell division over the nucleoid, and has led other groups to probe the nature of the SlmA interaction with FtsZ. An unresolved debate currently exists regarding the SlmA mechanism, with two research groups championing independent conclusions. The first hypothesis proposes that SlmA forms a dimer of dimers on DNA that promotes FtsZ proto-filaments to form anti-parallel structures by acting as a bridge between protofilaments, and thereby inhibit functional FtsZ-ring formation. This hypothesis was put forward through observations of the SlmA crystal structure and the study of small-angle X-ray scattering of SlmA-FtsZ polymers [153-154]. The second proposal suggests that SlmA forms dimers at specific DNA sequences, and that these dimers promote disassembly

of FtsZ polymers by increasing GTPase activity of FtsZ [155, 156]. While debate about the interaction mechanism is ongoing, both groups identified a roughly twenty-five base pair DNA sequence bound the TetR-like helix-turn-helix motif of SlmA; this sequence is notably absent from the *ter* region of the chromosome as observed for the Noc binding region [153, 155]. Interestingly, there is little identity between the DNA binding regions for Noc and SlmA and the proteins themselves have no homology to each other, suggesting that these two nucleoid occlusion mechanisms likely evolved independently [reviewed in 157]. A homologue to *B. subtilis* Noc has recently been identified gram-positive *Staphylococcus aureus*, a spherical bacterium related to *B. subtilis*, which lacks an identifiable Min system. *S. aureus* cell division is interesting as there are an infinite number of possible division planes that could bisect a sphere, yet cell division occurs only on orthogonal planes in three successive cell cycles [158]. The Noc homologue from *S. aureus* was observed to be closely associated with *ori* proximal regions of the chromosome, using functional fluorescent fusion. Deletions of *noc* led to the formation of multiple division planes within the cell, as observed by fluorescent fusions to FtsZ and EzrA; deletion of *noc* also led to the bisection of the chromosome. The role of the chromosome and Noc in determining the cell division site was further demonstrated with the addition of the antibiotic chloramphenicol, which causes irregular condensation of the chromosome. Under these conditions, formation of FtsZ rings occurred along planes that did not equally bisect the cell [159].

While spatial mechanisms of cell division control are crucial to maintain viability in a normally growing cell, they are insufficient to maintain viability over many generations under the many conditions a bacterial population may encounter. The integration of external and internal

environmental cues into the cell cycle has been widely observed, and unsurprisingly there are factors that can control FtsZ-assembly and the cell cycle as part of this communication. The SOS-response is widely distributed in bacterial cells and is induced by the accumulation of single stranded DNA due to damage or the arresting of chromosomal duplication. In *Escherichia coli,* the RecA protein binds to accumulating single-stranded DNA, promoting auto-cleavage of the LexA transcriptional repressor, leading to the production of a swath of proteins involved in DNA repair and recombination, as well as the inhibition of cell division [reviewed in 160 and 161]. The SOS-response induced protein SulA, was identified in the early days of cell division work in *E. coli*, through a study of mutants resistant to filamentation after treatment with ultraviolet light [7, 162]. Subsequent work identified SulA as being capable and sufficient to block cell division through a direct interaction with FtsZ; in the absence of FtsZ, SulA has a relatively short half-life underlining the transient nature of this control system [134, 163-167]. Initial studies on the mechanism of inhibition suggested that SulA interaction required GTP and Mg^{2+} specifically, followed by later work that clearly showed SulA reducing FtsZ polymerization *in vitro*, and leading to a moderate reduction in the GTP-hydrolysis rate of FtsZ [37, 168, 169]. SulA from *Pseudomonas aeruginosa* has sufficient stability *in vitro* such that the crystal structure of it bound to FtsZ could be solved. The structure showed that SulA contacts the NxD portion of the FtsZ T7-synergy loop (NxDxxD), consistent with the observed reduction in GTP hydrolysis and clearly suggesting a mechanism by which assembly of filaments can be inhibited. Furthermore, SulA dimerized in such manner as to bind two FtsZ monomers, with their orientations opposite that of assembled FtsZ [170]. This mechanism of sequestration has been confirmed by experiments showing that SulA has the effect of increasing the apparent critical concentration of FtsZ *in vitro*, suggesting that there is less free FtsZ available to form polymers in the presence of

SulA [44, 171]. While SOS-induced cell division inhibitors have been identified in a number of species, as yet only SulA has been identified as having a direct interaction with FtsZ. Both the YneA protein of *Bacillus subtilis* and the Rv2719c protein of *Mycobacterium tuberculosis* appear to function outside of the cytoplasm where they associate with the cell wall, despite their constitutive expression leading to a reduction in FtsZ-ring formation and a standard filamentation phenotype [172-174]. Similarly, the overproduction of SOS-induced protein DivS in *Corynebacterium glutamicum* leads to cell elongation and FtsZ misplacement, though no direct interactions with FtsZ have been detected [175].

Another common response to changing environmental conditions among bacteria is the cessation of normal growth to form a spore, a dormant and highly resistant cell type. As nutrient conditions degrade, *Bacillus subtilis* activates the transcriptional regulator Spo0A, leading to a global change in gene expression that ultimately produces a highly compacted chromosome protected by a specialized cell wall structure. The spore is extremely resistant to environmental pressures and will remain dormant until conditions improve, at which time it will differentiate back into a normal, or vegetative, cell and resume regular growth [reviewed in 176-178]. In *B. subtilis*, the onset of sporulation causes the divisome to assemble asymmetrically, as opposed to the medial position observed during vegetative growth. The switch to an asymmetric localization of FtsZ is believed to be primarily a product of increased FtsZ protein levels induced by Spo0A-mediated *ftsZ* transcriptional increases, as previously discussed [98, 101]. Positive localization factors for an asymmetric divisome in *B. subtilis* sporulation have not been definitively identified, and it has been proposed that the divisome assembles at a site pre-determined by the architecture of the cell, as for DivIVA [113, 143, 144]. This theory is supported by the production of an FtsZ

assembly inhibitor, MciZ, which is produced exclusively in the mother cell dependent upon the σ^E transcription factor. In the absence of MciZ, an additional septa forms within the mother cell at an asymmetric position mirroring the normal sporulation septa; conversely, over-production of MciZ produces filamentous cells devoid of identifiable FtsZ rings. Thus, FtsZ does not discriminate between polar localization positions in the absence of MciZ, suggesting that an additional factor exists that determines asymmetrical repositioning; despite extensive searches, no FtsZ-interacting protein capable of directing this localization has yet been identified [179]. MciZ is a small peptide inhibitor of FtsZ assembly both *in vivo* and *in vitro*. Initial studies showed that MciZ reduced GTPase activity, supported by MciZ resistant FtsZ mutants that had an amino acid substitution in the GTP binding pocket. Recent *in vitro* work has proposed that MciZ is in fact a direct competitor with GTP for FtsZ binding, consistent with all previously observed results [179, 180]. A novel sporulation linked system of FtsZ control has been identified in the *Streptomyces* spp., where FtsZ is non-essential for viability during regular filamentous growth [181]. Prior to sporulation, the protein SsgA accumulates between the nucleoids of filamentous cells, and recruits a second protein SsgB to its position; in turn, SsgB stimulates the transition of FtsZ from a diffuse pattern to long helices on the long axis of the cell, and finally to discrete FtsZ rings at the point of SsgAB localization [182]. This SsgAB system is of special note as it is one of the only systems yet identified which is appears to be a recruiter of FtsZ to a discrete location prior to assembly, rather than a repressor preventing mislocalization of the divisome.

Internal cues related to the metabolic status of the bacterial cell have also been shown to interact with FtsZ in order to control cell division. It has long been observed that growth rates and cell

size differ for bacterial cells under different nutrient conditions, requiring a coordination of cell division with nutrient availability [183-185]. Despite the long existing knowledge of this relationship, and of FtsZ as the core protein in the divisome, mechanisms underlying this regulation are only now being understood. Recent work has shown the number of cells with FtsZ rings is inversely proportional to the growth rate in vegetative *Bacillus subtilis*, but that the total FtsZ concentration remains the same under all nutrient conditions. This observation runs contrary to the growth rate dependent transcription of *ftsZ* observed in *Escherichia coli*, and suggests that regulation of FtsZ assembly, rather than protein levels, determines this effect in *B. subtilis* [186]. The *ugtP* gene was identified as an effector of cell division during a screen for mutants with increased cell length, but unaffected FtsZ localization. UgtP is involved in the synthesis of the diglucose diacylglycerol anchor for lipoteichioic acid, a major component of the cell wall in gram-positive bacteria. Purified UgtP was capable of inhibiting FtsZ assembly *in vitro*, and fluorescent fusions localized to the division plane in rich media growth conditions. Interestingly, the inhibitory effect was stimulated in the presence of the UgtP substrate, and mutations in genes controlling the upstream metabolic pathway caused a diffuse localization pattern of the UgtP fusions, suggesting that the flow of metabolites is central to the regulatory effect of FtsZ [187]. It has subsequently been proposed that UgtP forms oligomeric structures that are inhibited in the presence of high levels of its substrate UDP-glucose; thus, UgtP monomers are freed to interact with FtsZ in nutrient rich conditions, an interaction stimulated by the presence of UDP-glucose. Therefore, when metabolite flux is high through this anabolic pathway, UgtP interacts with FtsZ and reduces the amount of FtsZ available for assembly, which in turn increases the cell size; when metabolite flux is low, it interacts primarily with itself leaving FtsZ assembly unaffected [188]. How this effect is ultimately controlled, and

counteracted, such that the *B. subtilis* cell still divides at the proper time under nutrient rich conditions remains unresolved. Recently, a similar system has been identified in *Escherichia coli*, where the UDP-glucose binding enzyme OpgH, has been shown to negatively effect FtsZ assembly exclusively in rich-media. The N-terminal region of OpgH, likely sequestered in the absence of bound substrate, increases the apparent critical concentration of FtsZ for assembly and decreases GTP hydrolysis activity, suggesting that OpgH binds FtsZ monomers. Contrary to the *Bacillus* UgtP enzyme, OpgH does not require substrate for medial localization, as it has a second localization determinant within its membrane spanning domains; however, the determinant that prevents medial localization via the transmembrane regions in nutrient poor conditions has yet to be determined [189]. The existence of these systems in these distantly related bacteria suggests widespread use of UDP-glucose as a signaling molecule to link metabolic state to cell division control, significant as UDP linked metabolites represent an entry point to the production of the cell membrane and cell wall structures [reviewed in 190].

Recent work has identified FtsZ as a target of a member of the toxin-antitoxin (TA) system in *Esherichia coli*. TA systems are widely distributed throughout bacterial species and are a mechanism of population control to aid in species viability. TA systems are expressed as a protein pair with toxin and anti-toxin in a relatively stable complex, and are generally dispensable for normal growth. The free toxin is far more stable than free anti-toxin, so when separated the toxin will persist while anti-toxin is quickly degraded. Under conditions of cellular stress conditions the pair will become separated, leading to growth inhibition or programmed cell death through a diversity of cellular targets and mechanisms [reviewed in 191 and 192] The identified toxin, YeeV, was shown to inhibit cell division and lead to the formation of spherical

cells. This phenotype is more consistent with inhibition of MreB function, which is the bacterial homologue of actin. Indeed, YeeV was shown to directly interact with both FtsZ and MreB, where it inhibited GTP and ATP dependent assembly activities, respectively. YeeV also reduced GTP hydrolysis activity of FtsZ, though it does not have a similar effect on the ATP hydrolysis activity of MreB, suggesting independent mechanisms of action for each target. Interestingly, N-terminal residues of YeeV were shown to specifically inhibit FtsZ function, leaving MreB assembly intact, while the C-terminal residues acted on MreB alone [193]. Conversely, the YeeV anti-toxin, YeeU, was shown to have a direct effect on FtsZ and MreB, rather than simply sequestering and deactivating YeeV. YeeU was capable of stimulating polymer formation *in vitro*, and was able to suppress the phenotype of A22 treatment (an MreB inhibitor) or over-expression of SulA, suggesting a powerful stimulatory effect on assembly [194].

The ClpXP chaperone-protease system [reviewed in 201] has also been identified as being capable of inhibiting FtsZ assembly both *in vivo* and *in vitro*, a mechanism of regulation conserved among *Bacillus subtilis*, *Escherichia coli*, and *Mycobacterium tuberculosis*. In *B. subtilis*, the ClpX chaperone is sufficient for FtsZ interaction and assembly inhibition both *in vivo* and *in vitro*, though it does not appear to affect the GTP-hydrolysis rate of FtsZ. Interestingly, inhibition does not require ATP-hydrolysis by ClpX (though *in vivo* evidence suggests that ATP binding may stimulate the interaction), nor does ClpX promote proteolysis of FtsZ via ClpP. The exact mechanism of this interaction has not been fully elucidated, but likely involves sequestration of FtsZ monomers or destabilization of existing filaments [195, 196]. A similar ClpX sufficient inhibition of FtsZ assembly has been observed in *M. tuberculosis*, though the ATP dependence and proteolysis of FtsZ were not addressed [197]. While evidence in *E. coli*

suggests that ClpX alone is capable of inhibiting FtsZ assembly *in vitro*, it has additionally been demonstrated that the ClpP serine-protease is also capable of degrading FtsZ, unlike in *B. subtilis*. Furthermore, it has been proposed that ClpXP interacts with and degrades assembled FtsZ more readily than it does individual monomers, suggesting a mechanism by which a specific ratio of FtsZ filaments to FtsZ subunits might be maintained [198-200]. Despite the differences that seem to exist between the mechanisms of FtsZ regulation by the ClpXP system, the wide conservation of both FtsZ and ClpXP in bacteria likely suggests that this mechanism of cell division control is rather common.

There is evidence of even more factors involved in the control of FtsZ assembly during the cell cycle. It has been observed that FtsZ rings continue to form at the mid-cell in regions devoid of DNA in *Bacillus subtilis* cells lacking the Min system and nucleoid occlusion protein Noc, though at a time later than in wild-type cells, suggesting other systems of mid-cell determination [202]. It has been proposed that structures within the cell membrane or peptidoglycan layers themselves act to mark the possible division sites [113, 144]. As yet there is no direct evidence confirming this model, or any identification of mechanisms responsible for attracting FtsZ to these positions in the absence of other assembly factors. A recent model has linked the events of DNA replication itself with division site selection in *B. subtilis*, as replication initiation and segregation mutants show an increased misplacement of division septa, independent of SOS-response or nucleoid occlusion factors [203, 204]. In *B. subtilis* cells where replication blocks are induced through the introduction of *tetR* binding regions, cell division is transiently blocked. This division block was not induced as part of an SOS-response nor dependent on the nucleoid occlusion protein, Noc. Interestingly, this study showed in increase in septa formation over the

chromosome when Spo0J, a ParB homologue, was deleted [204]. Additionally, in *E. coli*, it has been shown that conditions that lead to a single, replication-blocked chromosome are effective at inhibiting FtsZ assembly and cell division at the mid-cell. This effect was also shown to be independent of the known FtsZ regulators SlmA (nucleoid occlusion), SulA (SOS-response) or the spatial determining Min system [205]. A weakly DNA-binding protein, YvcL, has been identified as having a role in cell division in *B. subtilis*, where genetic evidence shows interplay between it and the known Min and Noc systems; over-expression of *ftsZ* was able to suppress the phenotype of a *yvcL* mutant. YvcL is similar to the protein WhiA, a sporulation specific transcriptional regulator of *ftsZ* in *Streptomycese coelicolor,* though no evidence of transcriptional regulation in *B. subtilis* is observed as would be expected by the homology [206]. Cell division has also been studied in the rod-shaped gram-positive *Corynebacterium glutamicum*, which does not divide strictly at the mid-cell and lacks clear homologues of either Min or nucleoid occlusion systems, as well as a lack of other common FtsZ regulators (FtsZ, ZipA, ZapA, and EzrA). *C. glutamicum* utilizes a ParAB/*parS* system in chromosome partitioning [207, 208]. In this study, the deletion of *parA* and *parB* greatly altered both the birth length and elongation length of cells, led to a randomization of cell division timing, and notably, allowed cell division to occur over the nucleoid [209]. Taken together, these findings clearly suggest the existence of other levels of regulation coordinating chromosome duplication and segregation with the events of cell septation. Though the mechanisms remain unclear, replication blocks that lead to an arrest in cell division in both *B. subtilis* and *E. coli*, the identification of additional DNA-associated proteins with cell division effects in *B. subtilis*, and the observed cell division effects of deletions of *par* system genes in *C. glutamicum* and *B. subtilis* (Spo0J) all

point to still more control systems involved in FtsZ assembly by other core bacterial cell cycle events.

FtsZ of *Caulobacter crescentus* and regulation of assembly.

Caulobacter crescentus is a gram-negative, rod-shaped, aerobic and oligotrophic bacterium that undergoes a biphasic cell cycle. The primary cell is non-motile and fixed to surfaces through a strong adhesive excreted at the end of a stalk structure made primarily of peptidoglycan; furthermore, only this cell-type is capable of initiating DNA replication and cell division. Cell division results in a second cell type that is motile and unable to duplicate DNA and undergo cell division. After a certain time lag, a motile *Caulobacter* cell will shed its flagellum and replace it with an adherent stalk, allowing it commence DNA duplication and cell division. This specialized life-cycle allows *Caulobacter crescentus* to efficiently colonize and thrive in environments that are extremely sparse in nutrients [210, 211]. Cell division in *Caulobacter crescentus* is similar to that of most rod-shaped bacteria and occurs via binary fission, with a divisome assembling once per cell cycle, roughly at the mid-cell [212]. The mass doubling time of *C. crescentus* is approximately 90 minutes when grown in standard media at 30°C. This differs from the time necessary for a full cell cycle, due to the temporal lag required for differentiation from a swarmer to a stalked cell type; thus, the entirety of the cell cycle, from formation of one swarmer cell through differentiation, division, and the formation of an additional swarmer cell is roughly 150 minutes [212, 220, 234]. One of the great advantages to *Caulobacter crescentus* as an experimental system is that swarmer cell populations may be easily purified from a mixed culture using density centrifugation, allowing for detailed studies of cell cycle linked events [213].

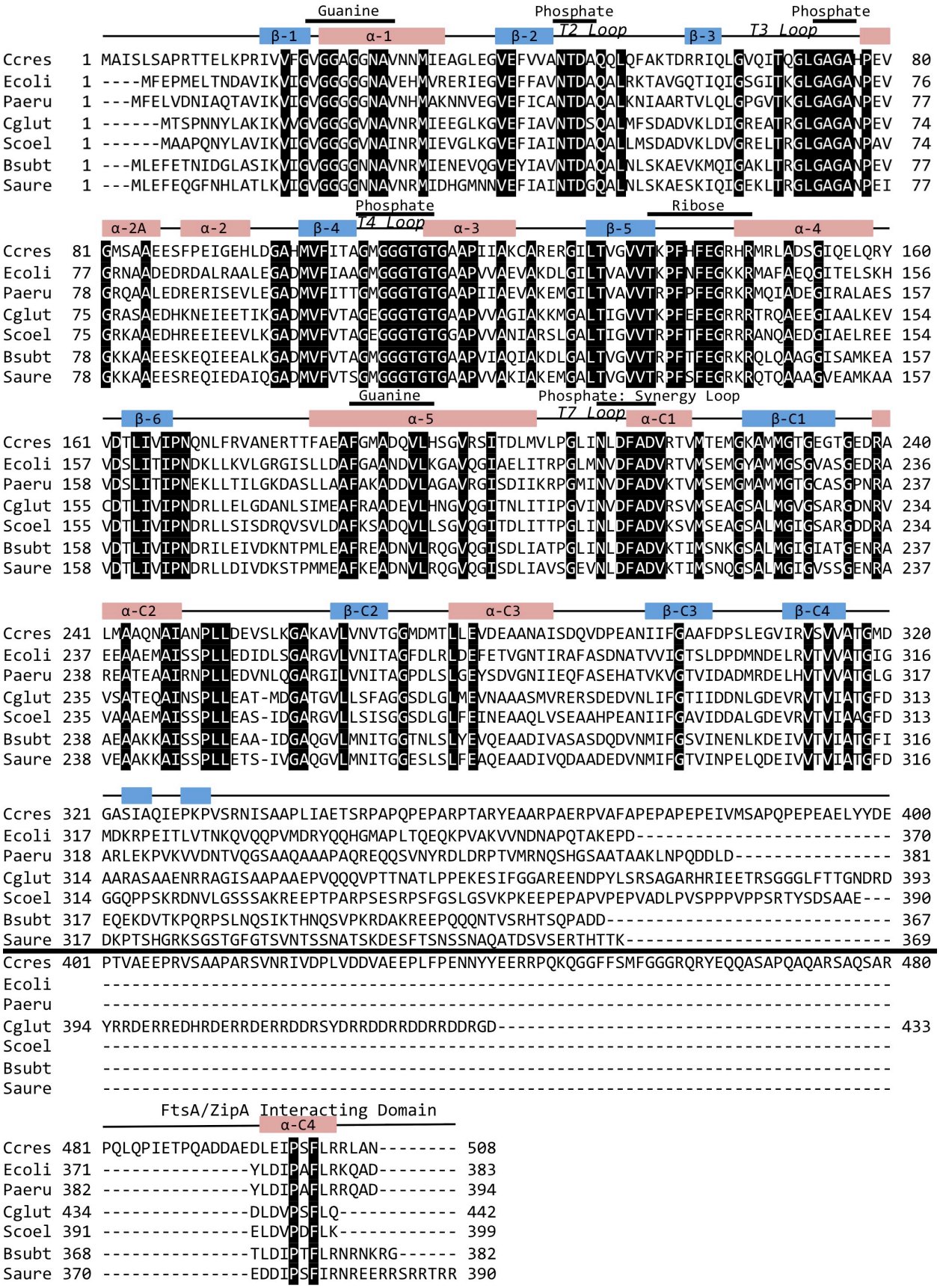
Guanine
Phosphate
Phosphate
β-1
α-1
β-2
T2 Loop
β-3
T3 Loop
Ccres 1 MAISLSAPRTTELKPRIVVFGVGGAGGNAVNNMIEAGLEGVEFVVANTDAQQLQFAKTDRRIQLGVQITQGLGAGAHPEV 80
Ecoli 1 ----MFEPMELTNDAVIKVIGVGGGGGNAVEHMVRERIEGVEFFAVNTDAQALRKTAVGQTIQIGSGITKGLGAGANPEV 76
Paeru 1 ---MFELVDNIAQTAVIKVIGVGGGGGNAVNHMAKNNVEGVEFICANTDAQALKNIAARTVLQLGPGVTKGLGAGANPEV 77
Cglut 1 ------MTSPNNYLAKIKVVGVGGGGVNAVNRMIEEGLKGVEFIAVNTDSQALMFSDADVKLDIGREATRGLGAGANPEV 74
Scoel 1 ------MAAPQNYLAVIKVIGVGGGGVNAINRMIEVGLKGVEFIAINTDAQALLMSDADVKLDVGRELTRGLGAGANPAV 74
Bsubt 1 ---MLEFETNIDGLASIKVIGVGGGGNNAVNRMIENEVQGVEYIAVNTDAQALNLSKAEVKMQIGAKLTRGLGAGANPEV 77
Saure 1 ---MLEFEQGFNHLATLKVIGVGGGGNNAVNRMIDHGMNNVEFIAINTDGQALNLSKAESKIQIGEKLTRGLGAGANPEI 77
Phosphate
T4 Loop
Ribose
α-2A
α-2
β-4
α-3
β-5
α-4
Ccres 81 GMSAAEESFPEIGEHLDGAHMVFITAGMGGGTGTGAAPIIAKCARERGILTVGVVTKPFHFEGRHRMRLADSGIQELQRY 160
Ecoli 77 GRNAADEDRDALRAALEGADMVFIAAGMGGGTGTGAAPVVAEVAKDLGILTVAVVTKPFNFEGKKRMAFAEQGITELSKH 156
Paeru 78 GRQAALEDRERISEVLEGADMVFITTGMGGGTGTGAAPIIAEVAKEMGILTVAVVTRPFPFEGRKRMQIADEGIRALAES 157
Cglut 75 GRASAEDHKNEIEETIKGADMVFVTAGEGGGTGTGAAPVVAGIAKKMGALTIGVVTKPFEFEGRRRTRQAEEGIAALKEV 154
Scoel 75 GRKAAEDHREEIEEVLKGADMVFVTAGEGGGTGTGGAPVVANIARSLGALTIGVVTRPFTFEGRRRANQAEDGIAELREE 154
Bsubt 78 GKKAAEESKEQIEEALKGADMVFVTAGMGGGTGTGAAPVIAQIAKDLGALTVGVVTRPFTFEGRKRQLQAAGGISAMKEA 157
Saure 78 GKKAAEESREQIEDAIQGADMVFVTSGMGGGTGTGAAPVVAKIAKEMGALTVGVVTRPFSFEGRKRQTQAAAGVEAMKAA 157
Guanine
Phosphate: Synergy Loop
T7 Loop
β-6
α-5
α-C1
β-C1
Ccres 161 VDTLIVIPNQNLFRVANERTTFAEAFGMADQVLHSGVRSITDLMVLPGLINLDFADVRTVMTEMGKAMMGTGEGTGEDRA 240
Ecoli 157 VDSLITIPNDKLLKVLGRGISLLDAFGAANDVLKGAVQGIAELITRPGLMNVDFADVRTVMSEMGYAMMGSGVASGEDRA 236
Paeru 158 VDSLITIPNEKLLTILGKDASLLAAFAKADDVLAGAVRGISDIIKRPGMINVDFADVKTVMSEMGMAMMGTGCASGPNRA 237
Cglut 155 CDTLIVIPNDRLLELGDANLSIMEAFRAADEVLHNGVQGITNLITIPGVINVDFADVRSVMSEAGSALMGVGSARGDNRV 234
Scoel 155 VDTLIVIPNDRLLSISDRQVSVLDAFKSADQVLLSGVQGITDLITTPGLINLDFADVKSVMSEAGSALMGIGSARGDDRA 234
Bsubt 158 VDTLIVIPNDRILEIVDKNTPMLEAFREADNVLRQGVQGISDLIATPGLINLDFADVKTIMSNKGSALMGIGIATGENRA 237
Saure 158 VDTLIVIPNDRLLDIVDKSTPMMEAFKEADNVLRQGVQGISDLIAVSGEVNLDFADVKTIMSNQGSALMGIGVSSGENRA 237
α-C2
β-C2
α-C3
β-C3
β-C4
Ccres 241 LMAAQNAIANPLLDEVSLKGAKAVLVNVTGGMDMTLLEVDEAANAISDQVDPEANIIFGAAFDPSLEGVIRVSVVATGMD 320
Ecoli 237 EEAAEMAISSPLLEDIDLSGARGVLVNITAGFDLRLDEFETVGNTIRAFASDNATVVIGTSLDPDMNDELRVTVVATGIG 316
Paeru 238 REATEAAIRNPLLEDVNLQGARGILVNITAGPDLSLGEYSDVGNIIEQFASEHATVKVGTVIDADMRDELHVTVVATGLG 317
Cglut 235 VSATEQAINSPLLEAT-MDGATGVLLSFAGGSDLGLMEVNAAASMVRERSDEDVNLIFGTIIDDNLGDEVRVTVIATGFD 313
Scoel 235 VAAAEMAISSPLLEAS-IDGARGVLLSISGGSDLGLFEINEAAQLVSEAAHPEANIIFGAVIDDALGDEVRVTVIAAGFD 313
Bsubt 238 AEAAKKAISSPLLEAA-IDGAQGVLMNITGGTNLSLYEVQEAADIVASASDQDVNMIFGSVINENLKDEIVVTVIATGFI 316
Saure 238 VEAAKKAISSPLLETS-IVGAQGVLMNITGGESLSLFEAQEAADIVQDAADEDVNMIFGTVINPELQDEIVVTVIATGFD 316
Ccres 321 GASIAQIEPKPVSRNISAAPLIAETSRPAPQPEPARPTARYEAARPAERPVAFAPEPAPEPEIVMSAPQPEPEAELYYDE 400
Ecoli 317 MDKRPEITLVTNKQVQQPVMDRYQQHGMAPLTQEQKPVAKVVNDNAPQTAKEPD---------- 370
Paeru 318 ARLEKPVKVVDNTVQGSAAQAAAPAQREQQSVNYRDLDRPTVMRNQSHGSAATAAKLNPQDDLD---------- 381
Cglut 314 AARASAAENRRAGISAAPAAEPVQQQVPTTNATLPPEKESIFGGAREENDPYLSRSAGARHRIEETRSGGGLFTTGNDRD 393
Scoel 314 GGQPPSKRDNVLGSSSAKREEPTPARPSESRPSFGSLGSVKPKEEPEPAPVPEPVADLPVSPPPVPPSRTYSDSAAE--- 390
Bsubt 317 EQEKDVTKPQRPSLNQSIKTHNQSVPKRDAKREEPQQQNTVSRHTSQPADD---------- 367
Saure 317 DKPTSHGRKSGSTGFGTSVNTSSNATSKDESFTSNSSNAQATDSVSERTHTTK---------- 369
Ccres 401 PTVAEEPRVSAAPARSVNRIVDPLVDDVAEEPLFPENNYYEERRPQKQGGFFSMFGGGRQRYEQQASAPQAQARSAQSAR 480
Ecoli ----------
Paeru ----------
Cglut 394 YRRDERREDHRDERRDERRDDRSYDRRDDRRDDRRDDRGD---------- 433
Scoel ----------
Bsubt ----------
Saure ----------
FtsA/ZipA Interacting Domain
α-C4
Ccres 481 PQLQPIETPQADDAEDLEIPSFLRRLAN-------- 508
Ecoli 371 ---------------YLDIPAFLRKQAD-------- 383
Paeru 382 ---------------YLDIPAFLRRQAD-------- 394
Cglut 434 ---------------DLDVPSFLQ------------ 442
Scoel 391 ---------------ELDVPDFLK------------ 399
Bsubt 368 ---------------TLDIPTFLRNRNKRG------ 382
Saure 370 ---------------EDDIPSFIRNREERRSRRTRR 390

Figure 1.3 [Previous Page]: Sequence alignment of bacterial FtsZ proteins.
The sequence alignment of *Caulobacter crescentus* FtsZ with six additional FtsZ proteins was performed using the ClustalW algorithm. Only perfectly conserved residues are indicated, with white-type and black highlighting. Secondary structural elements are shown above the sequences and labeled in accordance with the literature [30, 33]. The short HL- and HL-2 domains found in the T2-loop and after β-6 have been omitted in this schematic for simplicity. Regions that directly contact guanosine nucleotide are indicated by a black bar and labeled with the interacting nucleotide moiety. Due to the extreme variability of sequences, the C-terminal domains beginning after β-C4 (VxAxG), were separately aligned using the same algorithm. Alignment attempts produced variable and inconsistent results save for the terminal FtsA interacting helix (data not shown), thus the C-terminal linker regions are presented unaligned and contiguous with the rest of the FtsZ sequences to highlight the difference in linker region lengths. Two short β-sheet regions observed in the crystal structure are indicated, however, they are left unlabeled since subsequent work showed no apparent secondary structure in the linker [217]. The FtsA interacting region is shown as aligned by ClustalW. The α-helical nature of this C-terminal domain was demonstrated in a co-crystal with ZipA [68].
ClustalW: Larkin MA *et al*., ClustalW and ClustalX version 2.0. *Bioinformatics* 23: 2947-2948, 2007.
NCBI Sequence Accessions: *C. crescentus* (ACL96088), *E. coli* (BAB96663), *P. aeruginosa* (AAA95993), *C. glutamicum* (CCH25295), *S. coelicolor* (AAD10553), *B. subtilis* (AAA22457), *S. aureus* (AAA16512)

Caulobacter crescentus encodes an FtsZ homologue that is 508 amino acids in length with a predicted molecular weight of about 54,207 daltons. Sequence analysis of FtsZ from *Caulobacter crescentus* shows a high conservancy in major domains with other bacterial FtsZ proteins [30, 214]. The tubulin-like domain roughly spans residues 15 through 330, with strong sequence conservancy at all important secondary structural elements. The GGGTGTG sequence of the split GTPase domain begins at residue 109; the T-7 synergy loop begins at residue 211 with the sequence NLDFAD, identical to both *Escherichia coli* and *Bacillus subtilis* (Fig. 1.2). Studies that substituted wild-type residues to alanines at either of these positions were lethal to *Caulobacter* and produced atypical cell morphologies even in the presence of wild-type FtsZ. Additional charged to alanine substitutions that also proved to be dominant-lethal were located in the C-terminal region of the tubulin-like domain at residues 237 (**DR**) and 278 (**EVDE**) [215]. These mutations align with the HC2 and HC3 α-helices of the *Methanocaldococcus jannaschii*

structure, which bind four β-sheets that interact with the central H5 helix [30]. The substitution at residues 237 and 238 (HC2 equivalent) produced cells that were filamentous, though not entirely smooth, suggesting that this mutation interferes with the assembly of FtsZ and activation of cell division. Conversely, the substitution to residues 278-281 produced cells that were partially filamentous, but linked by an extended and highly constricted cell structure, suggesting an inability to complete cell division, and perhaps a reduced ability to initiate FtsZ assembly. The differences in these phenotypes is notable since the mutated residues should be very near each other on the surface of FtsZ, based on the structure of the *M. jannaschii* FtsZ [30, 215].

The final conserved domain at the extreme C-terminal spans residues 497 to 503 and is homologous to the FtsA binding domain of other bacteria. This region has a minor substitution at residue 498 of glutamate for an aspartate found in the equivalent position in both *E. coli* and *B. subtilis*. The short tail following the conserved portion of the FtsA binding domain is of equivalent length to *E. coli* FtsZ; however, the third position after the domain contains a leucine residue in *C. crescentus*, whereas most aligned bacterial FtsZ proteins have a basic or amide residue at this positions (R, K, or Q) [214]. The identity of this region as an FtsA binding motif in *C. crescentus* has been confirmed using yeast two-hybrid analysis [216]. Deletions of the region containing the FtsA binding helix have a dominant-lethal phenotype to *C. crescentus*, and greatly reduced viability of the cell when expressed in coordination with normal FtsZ. Expression of FtsA region truncations produce extremely long, filamentous cells, with multiple discrete FtsZ rings distributed along the length of the cells when visualized with labeled antibodies. These two phenotypes suggest that this region is not required for normal assembly of

FtsZ, but is necessary for the continuation of normal cell division, similar to observations in other bacteria [12, 61, 216].

The most obvious difference between the FtsZ of *Caulobacter crescentus* and that of *Escherichia coli* and *Bacillus subtilis* is the larger size of the protein, due to a linker region between the tubulin-like domain and FtsA binding domain that is greatly extended by comparison. While *E. coli* and *B. subtilis* have linker regions of approximately 57 and 54 amino acids in length, respectively, the linker of *Caulobacter crescentus* FtsZ is approximately 178 amino acids, based on sequence alignments [214]. An analysis of the linker region, primarily in *E. coli*, suggested that the length of the linker is the major determinant in function. Notably, a construct in which the *E. coli* linker was replaced with an equivalent length truncation from the *C. crescentus* linker was able to complement an *E. coli ftsZ* deletion, while a similar construct with the full-length *C. crescentus* linker was not able to rescue the *ftsZ* deletion mutant. Circular dichroism of the *C. crescentus* linker in this study showed no identifiable secondary structural elements [217]. In a different study, four charged residues within the linker were substituted for alanines (EERR at residue 441), with no discernable effects on viability or morphology of *Caulobacter crescentus* [215]. It would seem that due to the lack of observed secondary structure within this region and the mutability of an introduced mutation, that this region acts as a similarly disordered peptide as it does in *E. coli*. An additional difference in this region is the overall negative charge of the linker sequence, which is -11 in *C. crescentus* compared with a minor positive charge of about +1 and +3 in the linkers of *E. coli* and *B. subtilis*, respectively. This negative charge is notably lower than that of the *Rhizobium meliloti* linker region that is also greatly extended, but has a slight positive charge similar to *E. coli* [217]. Some evidence of a uniquely important role for the

linker is suggested by differences observed between truncations in the FtsA binding region alone, versus truncations in the entire linker and FtsA binding region. When the extreme terminal region was deleted starting at residue 485, the resultant cells were division inhibited and produced filamentous cells when overexpressed. A similar phenotype was observed for a truncation mutant beginning at residue 281, which deletes the entire linker region as well. However, this extended truncation produced many fewer transconjugants during genetic crossover than the shorter truncation (~$1x10^2$ less). When the extended truncation was expressed along with normal FtsZ, few functional FtsZ rings were observed while the shorter truncation beginning at residue 485 showed multiple FtsZ rings throughout the cell when expressed with normal FtsZ in a similar fashion. This could suggest that regions within the linker aid in the formation of a stable FtsZ ring structure [216]. To date however, no directed studies have addressed the developmental and functional significance of the extended length and greater negative charge of the FtsZ linker region in *C. crescentus*.

The FtsZ of *Caulobacter crescentus* shows all the functional hallmarks of homologues in other bacteria, and some notable differences related to its unique development. Expression of *C. crescentus ftsZ* in *Escherichia coli* produces filamentous cells, similar to the phenotype observed for constitutive overproduction of the endogenous FtsZ in *E. coli*, suggesting a conservation of functionality between the homologues [13, 214]. In *vitro* assembly requires the addition of GTP and produces both straight and curved filament structures observable by electron microscopy [218, 234]. *In vivo*, FtsZ localizes into a single band at the midcell prior to the onset of cell division, a localization that precedes the medial localization of all other cell division and peptidoglycan remodeling proteins [219-221]. Observations of this medial band have shown that

it contains multiple smaller filaments which predominantly gird the midcell perpendicular to the long axis, suggestive of a mechanism by which GTP hydrolysis and the resultant protofilament curvature serve to provide the concerted force needed for cell septation [222, 223]. In addition to the common medial localization, a transient localization at one pole of a cell has been observed, immediately following differentiation of a swarmer cell type into a stalked cell capable of replication and division. The transient polar localization of *C. crescentus* FtsZ is at the same pole where the flagellum was located and shed and the nascent stalk begins to develop [219, 224]. Notably, overexpression of *ftsZ* in *C. crescentus* produces multiple stalk structures or stalks with bifurcations along their length, suggesting a functional role for this transient localization in the formation of the stalk [214]. Additionally, overexpression of *ftsZ* in *C. crescentus* produces a distinct phenotype defined by multiple thin and elongated regions connecting cells [215, 216].

FtsZ in *Caulobacter crescentus* is under distinct cell-type specific control, through regulation of *ftsZ* transcription and proteolytic degradation of FtsZ protein. Immunoblots of synchronized populations of *C. crescentus* consistently show that there is no detectable FtsZ protein in division inhibited swarmer cells [214, 219, 224]. In one such study, even when FtsZ was over produced throughout the cell cycle, swarmer cells showed little FtsZ localization despite detectable protein within the cells. This could suggest the presence of an assembly inhibitor in swarmer cell populations, though no such protein has been identified [224]. Proteolysis of FtsZ has also been suggested as a control mechanism for FtsZ in *C. crescentus*. It has been observed that the half-life of FtsZ is greatly reduced following the onset of cell division, when FtsZ levels begin to decline. Furthermore, FtsZ levels in the swarmer cell are consistently lower than stalked cells, even when transcribed from native promoters not linked to the cell cycle, or overexpressed from

additional inducible promoters. This suggests that mechanisms in addition to transcriptional regulation exist that are capable of reducing FtsZ levels in the swarmer cell [219]. While *C. crescentus* does have a ClpXP serine protease system that is essential, and ClpXP is capable of degrading FtsZ in *E. coli*, as yet a proteolytic system directly responsible for FtsZ degradation has not been identified in *C. crescentus* [200, 225]. Control of FtsZ levels in *C. crescentus* is also accomplished by transcriptional regulation, which proceeds from a single promoter, unlike the multiple promoters utilized by *E. coli* and *B. subtilis* [85, 94, 219]. Transcription from *C. crescentus ftsZ* promoter is under cell cycle control and is repressed in swarmer cell populations, recommencing shortly after the initiation of DNA replication following differentiation into a stalked cell, and peaking just prior to cell division [219]. Cell-type specific transcription from this promoter is regulated by the CtrA response regulator of *Caulobacter crescentus*, which is present specifically in swarmer cell populations and is degraded by the ClpXP serine-protease system shortly after differentiation into a stalked cell. CtrA production begins shortly after the onset of DNA replication and accumulates in the pre-divisional cell, coinciding with a reduction in *ftsZ* transcription. However, *ftsZ* transcription is not entirely shut off since CtrA is quickly cleared from the stalked portion of the predivisional cell, allowing continued production of FtsZ in the nascent stalked cell. This cell-type specific control allows for continuous *ftsZ* transcription in the stalked cell so that another round of cell division may begin directly following cell division [219, 225, 226].

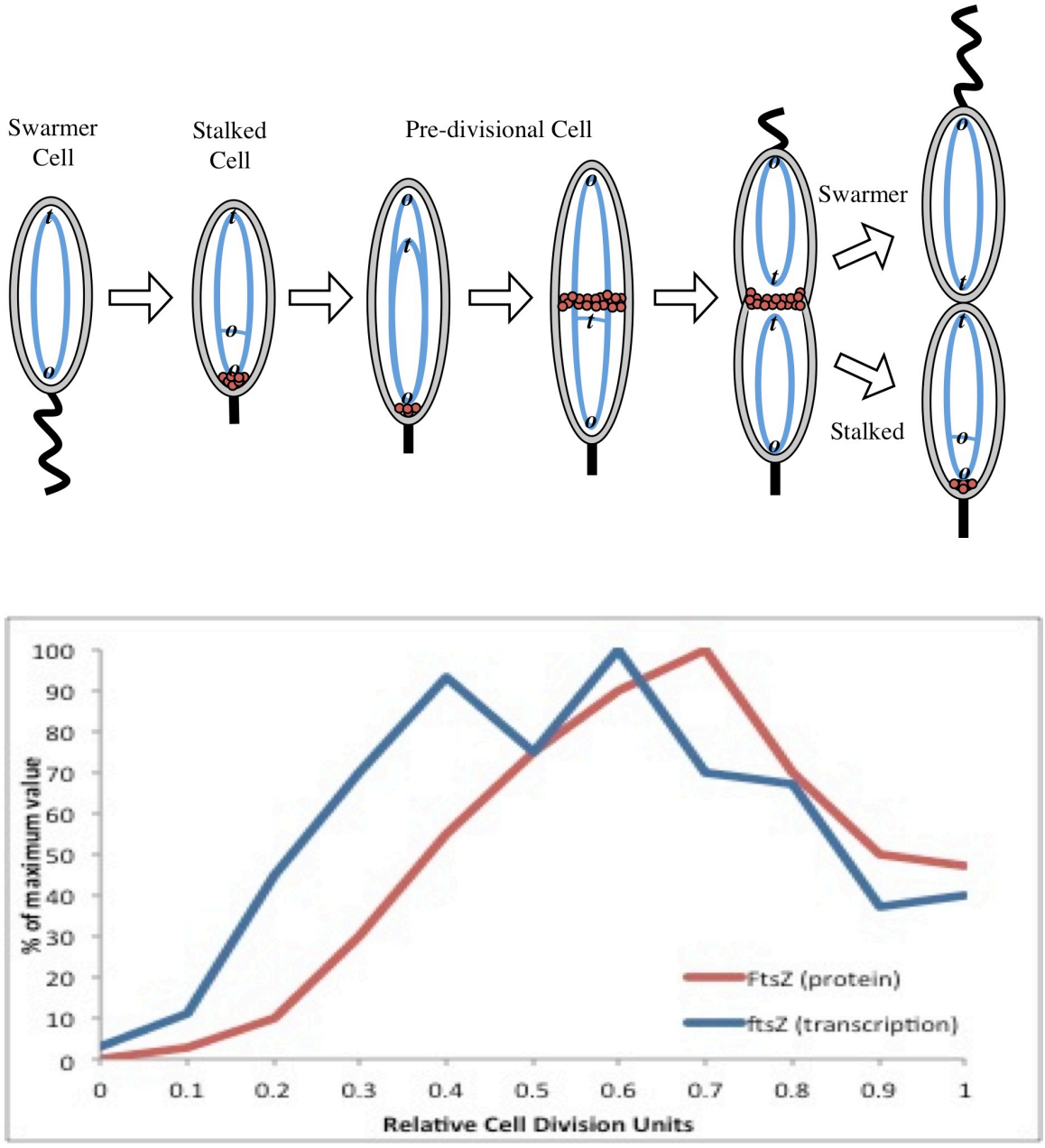

Figure 1.4: FtsZ in the cell cycle of *Caulobacter crescentus*.
Important phases of the cell cycle of *C. crescentus* are diagrammed, beginning with a swarmer cell and traced through division into nascent stalked and swarmer cells. The chromosome is represented by the blue lines, with the approximate locations of the origin and terminus of replication indicated by italicized letters, *o* and *t*, respectively. Localized FtsZ protein is marked with red circles. A representative graph of levels of FtsZ protein and transcription from the *ftsZ* promoter through the cell cycle is also presented, adapted from data presented in References 214, 219, and 236. The swarmer cell in the diagram above is relative to 0 division units on the graph; each subsequent cell diagram represents an additional 0.2 division units into the cell cycle. Chromosome and FtsZ localization are adapted from data presented in References 219, 220, 224 and Chapter 2: 3, 4.

Research into the control of FtsZ assembly in *Caulobacter crescentus* has identified a few systems with mechanisms reminiscent of those seen in other bacterial species. These include spatial regulatory systems that limit assembly at non-medial positions, regulatory systems tied to the progression of DNA replication and segregation, as well as systems that may be responsive to the metabolic state of the cell. Assembly of FtsZ at the midcell is intricately tied with DNA replication and segregation, though many of the mechanism underlying these observations remain unidentified. The midcell localization of FtsZ requires the onset of DNA replication, and in cells lacking the DnaA replication initiator, FtsZ rings form exclusively at the stalked pole of predivisional cells. Notably, overexpression of FtsZ does not rescue this phenotype suggesting that inhibition of FtsZ assembly is powerful enough to continue under increased protein levels. It was also noted in this study that FtsZ rings formed exclusively in regions with the lowest DNA content in cells, reminiscent of a type of nucleoid occlusion system [227]. A powerful nucleoid occlusion mechanism, though not yet identified, would be consistent with the finding that no FtsZ assembly was observed in swarmer cell populations even when FtsZ is overproduced, since studies have shown that the entirety of the swarmer cell is filled with nucleoid [224, 228].

Caulobacter crescentus also employs an FtsZ filament bundling and organizing system similar to that of ZapB or SepF in *E. coli* and *B. subtilis*, respectively. The protein FzlA, is well conserved among α-proteobacteria, and is essential for cell division in rich media. FzlA has been shown to interact directly with FtsZ *in vitro* using co-sedimentation assays; furthermore, FzlA increases light scattering of FtsZ and reduces the GTP hydrolysis rate, consistent with a role in stabilizing filaments. When FzlA is over-expressed, multiple FtsZ foci are seen throughout the cell, in contrast, depletions of FzlA yield fuzzy multiple FtsZ bands at the midcell. Overall, however,

FzlA has a limited effect on cell division, consistent with phenotypes seen for similar FtsZ stabilizers SepF and ZapB. When FtsZ assembly is monitored with electron microscopy, the presence of FzlA produces highly coiled FtsZ filaments that are thicker than normal filaments, suggesting that FzlA promotes lateral bundling in a manner producing large helices of FtsZ *in vitro* [229].

A mechanism of FtsZ assembly inhibition accomplished by a NADH-binding enzyme, regulated in a cell cycle dependent manner, has recently been proposed [230]. KidO was identified in a genetic screen focused on the identification of SpmX-independent activators of the DivJ protein, which mediates differentiation of a *Caulobacter crescentus* swarmer cell into a replicative stalked cell. The DivJ kinase, when activated in a differentiating swarmer, phosphorylates and activates the DivK cell fate determinant, which leads to the proteolytic destruction of the CtrA transcription factor. The clearance of CtrA results in the activation of DNA-replication and the transcription of a wide array of genes, including *ftsZ* [219, 225, 226, 231-233]. KidO is proteolytically degraded following swarmer to stalk differentiation by the ClpXP system, and it was noted that accumulation of KidO caused by inhibition of proteolysis led to inhibition of cell division, leading to an investigation of the role of KidO in FtsZ regulation. Evidence linking FtsZ to KidO is primarily cytological and genetic: overexpression of *kidO* led to slightly elongated cells with fluorescent fusions to FtsZ dispersed or located at non-medial foci; a non-specific mutagenic screen for suppression of cell elongation under *kidO* overexpression yielded mutant FtsZ with amino acid substitutions near the GTP binding domain or T7-synergy loop. A direct interaction between FtsZ and KidO was observed through tandem-affinity purification of KidO followed by FtsZ-directed immunoblots, as well as surface plasmon-resonance analysis of

binding using the same affinity purification construct. Notably, KidO constructs with mutations in residues that bind NADH did not lead to inhibition of cell division when overexpressed, suggesting that the binding of the co-factor is necessary for FtsZ interaction, similar to UgtP and OpgH in *E. coli* and *B. subtilis*, respectively [230].

Spatial regulation of FtsZ assembly at the midcell is proposed to occur via a Min-like mechanism, though polar direction of the inhibitor is mediated through the chromosome in *C. crescentus*, rather than the polar architecture as for *E. coli* and *B. subtilis*. The *mipZ* gene was identified during a bioinformatics screen for highly conserved proteins among a-proteobacteria that have cell cycle regulated promoter sequences nearby. MipZ shows some homology to MinD and ParA, primarily in the deviant Walker-A motif characteristic of these ATPases. Depletion and constitutive expression of *mipZ* cause cells to filament or produce smaller than normal swarmer cells, respectively. Fluorescent fusions to FtsZ are dispersed throughout the cell into discrete foci that do not appear as complete rings when MipZ is depleted; conversely, when MipZ is overproduced, fusions to FtsZ are found exclusively at the cell poles. *In vitro* control of FtsZ assembly was demonstrated via sedimentation assays, GTP hydrolysis assays, and observation of assembled FtsZ via electron microscopy. MipZ reduced FtsZ assembly in a concentration dependent manner, and required bound ATP for inhibition; ATP hydrolysis by MipZ was not necessary for function as MipZ hydrolysis mutants and slowly hydrolysable ATP-analogs produced similar inhibition of FtsZ assembly [234]. Fluorescent fusions to MipZ begin at the flagellated pole, transitioning to bipolar foci following differentiation to a stalked cell. This transition closely mimics the localization of ParB, involved in chromosome partitioning, and a direct interaction between ParB and MipZ was shown via surface-plasmon resonance and

bacterial two-hybrid analysis [234, 235]. Analysis of MipZ, and mutants deficient in ATP binding and hydrolysis, have yielded interesting additional layers to its function. MipZ will form homodimers in an ATP dependent manner, with each monomer bound to an ATP molecule: these dimers are necessary for inhibition of FtsZ, but do not stably interact with ParB. MipZ has a slow ATPase activity, and dissociates from itself when ATP is hydrolyzed. ParB is capable of stimulating the ATPase activity of MipZ, an effect enhanced by ParB being bound to its *parS* recognition sequence. Furthermore, MipZ dimers are capable of binding chromosomal DNA in a non-specific manner [235]. Thus, it has been proposed the MipZ serves to directly repress FtsZ assembly at the polar regions of the cell through an interaction with chromosomal DNA, regulated by the ParB partitioning protein. It is proposed that ParB, while moving to the opposite poles in conjunction with DNA segregation, will drag MipZ monomers behind it, mediated by direct interactions. Nucleotide exchange by MipZ will promote dimer formation, and absent ParB, ATP hydrolysis will be slow and this dimer will be stable enough to bind non-specifically to chromosomal DNA. In the dimerized form near the poles of the cell MipZ will inhibit FtsZ assembly, which will be favored at the medial position away from ParB and the highest concentrations of MipZ [234, 235].

Discussion.

The controlled assembly of the divisome is essential to the viability of a bacterial species, and requires the coordination of a variety of signals to ensure that cell division happens at the proper place, at the proper time, and under the proper conditions. Cell division requires an elaborate array of proteins that must assemble in a highly controlled and hierarchical manner to coordinate cinching of the cell membranes with remodeling of the peptidoglycan cell wall. At the core of

this multi-protein machine is the tubulin homologue, FtsZ. FtsZ has been found in every bacterial species characterized and with few exceptions, is essential for growth and viability. Incredibly, certain Protista still utilize FtsZ homologues in mitochondrial fission, and all plant species contain FtsZ homologues involved in chloroplast division. When one considers the probable common ancestry of FtsZ and eukaryotic tubulin, necessary for mitosis and intercellular trafficking, the evolution of that proto-protein seems almost miraculous.

Control of FtsZ assembly is essential to maintain viability over generations, and although many unique systems have evolved, directed by a species own development and environment, certain hallmarks remain common. Regulators of FtsZ have been identified that respond to the metabolic state of the cell and control FtsZ assembly directly, or through transcriptional or proteolytic means in both gram-positive and gram-negative bacteria. Spatial control mechanisms are widely conserved and ensure that FtsZ assembly can only occur at discrete locations within the cell; furthermore, complementary mechanisms exist that inhibit FtsZ assembly over bacterial chromosomes preventing the division machinery from cutting the genetic contents of the cell. In bacteria with multiple cell types, such as sporulating bacteria or *Caulobacter crescentus*, FtsZ is regulated developmentally through multiple mechanisms.

Despite the many modes and functions of these regulatory mechanisms, proteins that interact directly with FtsZ protein work in surprisingly common ways. Inhibition of assembly usually involves the stimulation of GTP hydrolysis in order to de-stabilize protofilaments, or the binding and sequestration of FtsZ monomers such that attachment to growing filaments is prohibited. Stimulation of assembly is often achieved by binding of FtsZ dimers and protofilaments to

stabilize their interaction, resulting in an apparent decrease in the GTP hydrolysis rate; alternately, lateral associations of FtsZ protofilaments can be stimulated to promote assembly of higher-order FtsZ structures aiding in the assembly of a fully functional divisome. In this work, data is presented that suggests a novel, chromosome-associated mechanism of FtsZ regulation. It is proposed, through biochemical analysis, that the ParAB-*parS* chromosome partitioning system of *Caulobacter crescentus* serves to regulate FtsZ assembly, thereby linking DNA replication and segregation directly to cell division.

References

[1] P. van de Putte, Jeanette van Dillewijn, and A. Rörsch. The selection of mutants of *Escherichia coli* with impaired cell division at elevated temperature. *Mutat. Res*. 1: 121-128, 1964.

[2] Austin L. Taylor and Carol Dunham Trotter. Revised linkage map of *Escherichia coli*. *Bacteriol. Rev*. 31: 332-353, 1967.

[3] Matthieu Ricard and Yukinori Hirota. Process of cellular division in *Escherichia coli*: physiological study on thermosensitive mutants defective in cell division. *J. Bacteriol*. 116: 314-322, 1973.

[4] Gail Fletcher, Carleen A. Irwin, Joan M. Henson, Cynthia Fillingim, Molly A Malone, and James R. Walker. Identification of the *Escherichia* cell division gene *sep* and organization of the cell division-cell envelope genes in the *sep-mur-ftsA-envA* cluster as determined with specialized transducing Lambda bacteriophages. *J. Bacteriol*. 133: 91-100, 1978.

[5] J. F. Lutkenhaus, Hans Wolf-Watz, and W. D. Donachie. Organization of genes in the *ftsA-envA* region of the *Escherichia coli* genetic map and identification of a new *fts* locus (*ftsZ*). *J. Bacteriol*. 142: 615-620, 1980.

[6] John J, Donch, Young Sup Chung, Michael H. L. Green, Joseph Greenberg, and Guylyn Warren. Genetic analysis of *sul* mutants of *Escherichia coli* B. *Genet. Res*. 17: 185-193, 1971.

[7] Jacqueline George, Marc Castellazzi, and Gérard Buttin. Prophage induction and cell division in *E. coli*: III. Mutations *sfiA* and *sfiB* restore division in *tif* and *lon* strains and permit the expression of mutator properties of *tif*. *Molec. Gen. Genet*. 140: 309-332, 1975.

[8] Olivier Huisman, Richard d'Ari, and Jacqueline George. Further characterization of *sfiA* and *sfiB* mutations in *Escherichia coli*. *J. Bacteriol*. 144: 185-191, 1980.

[9] Susan Gottesman, Ethan Halpern, and Patsy Trisler. Role of *sulA* and *sulB* in filamentation by Lon mutants of *Escherichia coli* K-12. *J. Bacteriol*. 148: 265-273, 1981.

[10] Joseph Lutkenhaus. Coupling of DNA replication and cell division: *sulB* is an allele of *ftsZ*. *J. Bacteriol*. 154: 1339-1346, 1983.

[11] C.A. Jones and I.B. Holland. Inactivation of essential division genes, *ftsA*, *ftsZ*, suppresses mutations at *sfiB*, a locus mediating division inhibition during the SOS response in *E. coli*. *EMBO J*. 3: 1181-1186, 1984.

[12] Kenneth J. Begg and William D. Donachie. Cell shape and division in *Escherichia coli*: experiments with shape and division mutants. *J. Bacteriol*. 163: 615-622, 1985.

[13] John E. Ward and Joe Lutkenhaus. Overproduction of FtsZ induces minicell formation in *E. coli*. *Cell* 42: 941-949, 1985.

[14] J. Christopher Corton, John E. Ward, Jr., and Joe Lutkenhaus. Analysis of cell division gene *ftsZ* (*sulB*) from Gram-negative and Gram-positive bacteria. *J. Bacteriol.,* 169: 1-7, 1987.

[15] Bernard Beall, Michael Lowe, and Joe Lutkenhaus. Cloning and characterization of *Bacillus subtilis* homologs of *Escherichia coli* cell division genes *ftsZ* and *ftsA*. *J. Bacteriol*., 170: 4855-4864, 1988.

[16] Bernard Beall and Joe Lutkenhaus. FtsZ in *Bacillus subtilis* is required for vegetative septation and asymmetric septation during sporulation. *Genes Dev*. 5: 447-455, 1991.

[17] Erfei Bi and Joe Lutkenhaus. FtsZ ring structure associated with division in *Escherichia coli*. *Nature*, 354: 161-164, 1991.

[18] Kang Dai and Joe Lutkenhaus. *ftsZ* is an essential gene in *Escherichia coli*. *J. Bacteriol*., 173: 3500-3506, 1991.

[19] Ben R. Kiefel, Paul R. Gilson, and Peter L. Beech. Diverse eukaryotes have retained mitochondrial homologues of the bacterial division protein FtsZ. *Protist* 155:105-115, 2004.

[20] Allan D. Terbush and Katherine W. Osteryoung. Distinct functions of chloroplast FtsZ1 and FtsZ2 in Z-ring structure and remodeling. *J. Cell Biol*. 199: 623-637, 2012.

[21] Katherine W. Osteryoung. Organelle fission in eukaryotes [Review]. *Curr. Opin. Microbiol*. 4: 639-646, 2001.

[22] Amit Mukherjee and Joe Lutkenhaus. Guanine nucleotide-dependant assembly of FtsZ into filaments. *J. Bacteriol*., 176: 2754-2758, 1994.

[23] Harold P. Erickson. FtsZ, a prokaryotic homolog of tubulin? *Cell*, 80: 367-370, 1995.

[24] Piet de Boer, Robin Crossley, and Lawrence Rothfield. The essential bacterial cell-division protein is a GTPase. *Nature*, 359: 254-256, 1992.

[25] Debabrata RayChaudhuri and James T. Park. *Escherichia coli* cell-division gene *ftsZ* encodes a novel GTP-binding protein. *Nature*, 359: 251-254, 1992.

[26] William Margolin, Joseph C. Corbo, and Sharon R. Long. Cloning and characterization of a *Rhizobium meliloti* homolog of the *Escherichia coli* cell division gene *ftsZ*. *J. Bacteriol*., 173: 5822-5830, 1991.

[27] Erfei Bi and Joe Lutkenhaus. FtsZ regulates frequency of cell division in *Escherichia coli*. *J. Bacteriol*., 172: 2765-2768, 1990.

[28] Amit Mukherjee, Kang Dai, and Joe Lutkenhaus. *Escherichia coli* cell division protein FtsZ is a guanine nucleotide binding protein. *Proc. Natl. Acad. Sci. USA*, 90: 1053-1057, 1993.

[29] Kang Dai, Amit Mukherjee, Xifan Xu, and Joe Lutkenhaus. Mutations in *ftsZ* that confer resistance to SulA affect the interaction of FtsZ with GTP. *J. Bacteriol*., 176: 130-136, 1994.

[30] Jan Löwe and Linda A. Amos. Crystal structure of the bacterial cell-division protein FtsZ. *Nature*, 391: 203-206, 1998.

[31] Eva Nogales, Sharon G. Wolf, and Kenneth H. Downing. Structure of the αβ tubulin dimer by electron crystallography. *Nature*, 391: 199-203, 1998.

[32] Eva Nogales, Kenneth H. Downing, Linda A. Amos, Jan Löwe. Tubulin and FtsZ form a distinct family of GTPases. *Nat. Struct. Biol*., 5: 451-458, 1998.

[33] Harold P. Erickson. Atomic structures of tubulin and FtsZ [Review]. *Trends Cell Biol*., 8: 133-137, 1998.

[34] Arshad Desai and Timothy J. Mitchison. Microtubule polymerization dynamics [Review]. *Annu. Rev. Cell Dev*. 13:83-117, 1997.

[35] Sonia Huecas, Oscar Llorca, Jasminka Boskovic, Jamie Martín-Benito, and José María Valpuesta. Energetics and geometry of FtsZ polymers: nucleated self-assembly of single protofilaments. 94: 1796-1806, 2008.

[36] Yaodong Chen and Harold P. Erickson. FtsZ filament dynamics at steady state: subunit exchange with and without nucleotide hydrolysis. *Biochemistry* 48: 6664-6673, 2009.

[37] Amit Mukherjee, Chune Cao, and Joe Lutkenhaus. Inhibition of FtsZ polymerization by SulA, an inhibitor of septation in *Escherichia coli*. *Proc. Natl. Acad. Sci. USA* 95: 28885-2890, 1998.

[38] Chunlin Lu, Mary Reedy, and Harold P. Erickson. Straight and curved conformations of FtsZ are regulated by GTP hydrolysis. *J. Bacteriol*. 182: 164-170, 2000.

[39] Tushar K. Keuria, Shyan Sundar Krishnakumar, Saurabh Sahar, Neera Singh, Kamlesh Gupta, Mallika Meshram, and Dulal Panda. Glutamate-induced assembly of bacterial cell division protein FtsZ. *J. Biol. Chem.* 278:3735-3741, 2003.

[40] Harold P. Erickson, David E. Anderson, and Masaki Osawa. FtsZ in bacterial cytokinesis: cytoskeleton and force generator all in one [Review]. *Microbiol. Mol. Biol. Rev.* 74: 504-528, 2010.

[41] Sonia Huecas, Claudia Schaffner-Barbero, Wanius García, Hugo Yébenes, Juan Manuel Palacios, José Fernando Díaz, Margarita Menéndez, and José Manuel Andreu. The interactions of cell division protein FtsZ with guanine nucleotides. *J. Biol. Chem.* 282: 37515-37528, 2007.

[42] Amit Mukherjee and Joe Lutkenhaus. Dynamic assembly of FtsZ regulated by GTP hydrolysis. *EMBO J.* 17: 462-469, 1998.

[43] Yaodong Chen, Keith Bjornson, Sambra D. Redick, and Harold P. Erickson. A rapid fluorescence assay for FtsZ assembly indicates cooperative assembly with a dimer nucleus. *Biophys. J.* 88: 505-514, 2005.

[44] Alex Dajkovic, Amit Mukherjee, and Joe Lutkenhaus. Investigation of regulation of FtsZ assembly by SulA and development of a model for FtsZ polymerization. *J. Bacteriol.* 190: 2513-2526, 2008.

[45] Emily R. Miraldi, Peter J. Thomas, and Laura Romberg. Allosteric models for cooperative polymerization of linear polymers. *Biophys. J.* 95: 2470-2486, 2008.

[46] Nathaniel L. Elsen, Jun Lu, Gopal Parthasarathy, John C. Reid, Sujata Sharma, Stephen M. Soisson, and Kevin J. Lumb. Mechanism of action of the cell-division inhibitor PC190723: modulation of FtsZ assembly cooperativity. *J. Am. Chem. Soc.* 134: 12342-12345, 2012.

[47] Jesse Stricker, Paul Maddox, E. D. Salmon, and Harold P. Erickson. Rapid assembly dynamics of the *Escherichia coli* FtsZ-ring demonstrated by fluorescence recovery after photobleaching. *Proc. Natl. Acad. Sci. USA* 99: 3171-3175, 2002.

[48] David E. Anderson, Frederico J. Gueiros-Filho, and Harold P. Erickson. Assembly dynamics of FtsZ rings in *Bacillus subtilis* and *Escherichia coli* and effects of FtsZ-regulating proteins. *J. Bacteriol.* 186: 5775-5781, 2004.

[49] Brett Geissler, Daisuke Shiomi, and William Margolin. The *ftsA** gain-of-function allele of *Escherichia coli* and its effects on the stability and dynamics of the Z ring. *Microbiol.* 153: 814-825, 2007.

[50] Yaodong Chen and Harold P. Erickson. Rapid *in vitro* assembly dynamics and subunit turnover of FtsZ demonstrated by Fluorescence Resonance Energy Transfer. *J. Biol. Chem*. 280: 22549-22554, 2005.

[51] Qin Sun and William Margolin. FtsZ dynamics during the division cycle of live *Escherichia coli* cells. *J. Bacteriol*. 180: 2050-2056, 1998.

[52] Hao Yuan Kueh and Timothy J. Mitchison. Structural plasticity in actin and tubulin polymer dynamics [Review]. *Science* 325: 960-963, 2009.

[53] Sambra D. Redick, Jesse Stricker, Gina Briscoe, and Harold P. Erickson. Mutants of FtsZ targeting the protofilament interface: effects on cell division and GTPase activity. *J. Bacteriol*. 187: 2727-2736, 2005.

[54] Masaki Osawa, David E. Anderson, and Harold P. Erickson. Reconstitution of contractile FtsZ rings on Liposomes. *Science* 320: 792-794, 2008.

[55] Antonio Tormo and Miguel Vicente. The *ftsA* gene product participates in formation of the *Escherichia coli* septum structure. *J. Bacteriol*. 157: 779-784, 1984.

[56] Fusinita van den Ent and Jan Löwe. Crystal structure of the cell division protein FtsA from *Thermotoga maritima*. *EMBO J*. 19: 5300-5307, 2000.

[57] Lucía Yim, Guy Vandenbussche, Jesús Mingorance, Sonsoles Rueda, Mercedes Casanova, Jean-Marie Ruysschaert, and Miguel Vicente. Role of the carboxy terminus of *Escherichia coli* FtsA in self-interaction and cell division. *J. Bacteriol*. 182: 6366-6373, 2000.

[58] Andrea Feucht, Isabelle Lucet, Michael D. Yedkin, and Jeffery Errington. Cytological and biochemical characterization of the FtsA cell division protein of *Bacillus subtilis*. *Mol. Microbiol*. 40:115-125, 2001.

[59] Daisuke Shiomi and William Margolin. Dimerization or oligomerization of the actin-like FtsA protein enhances the integrity of the cytokinetic Z ring. *Mol. Microbiol*. 66: 1396-1415, 2007.

[60] Xunde Wang, Jian Huang, Amit Mukherjee, Chune Cao, and Joe Lutkenhaus. Analysis of the interaction of FtsZ with itself, GTP, and FtsA. *J. Bacteriol*. 179: 5551-5559, 1997.

[61] Xiaolan Ma and William Margolin. Genetic and functional analyses of the conserved C-terminal core domain of *Escherichia coli* FtsZ. *J. Bacteriol*. 181: 7531-7544, 1999.

[62] Ana Isabel Rico, Marta García-Ovalle, Jesús Mingorance, and Miguel Vicente. Role of two essential domains of *Escherichia coli* FtsA in localization and progression of the division ring. *Mol. Microbiol*. 53: 1359-1371, 2004.

[63] Sebastien Pichoff and Joe Lutkenhaus. Identification of a region of FtsA required for interaction with FtsZ. *Mol. Microbiol.* 64: 1129-1138, 2007.

[64] Brett Geissler, Dany Elraheb, and William Margolin. A gain-of-function mutation in *ftsA* bypasses the requirement for the essential cell division gene *zipA* in *Escherichia coli*. *Proc. Natl. Acad. Sci. USA* 100: 4197-4202, 2003.

[65] Sebastien Pichoff and Joe Lutkenhaus. Tethering the Z ring to the membrane through a conserved membrane targeting sequence in FtsA. *Mol. Microbiol.* 55:1722-1734, 2005.

[65] Cynthia A. Hale and Piet A. J. de Boer. Direct binding of FtsZ to ZipA, an essential component of the septal ring structure that mediates cell division in *E. coli*. *Cell* 88:175-185, 1997.

[66] Cynthia A. Hale, Amy C. Rhee, and Piet A. J. de Boer. ZipA-induced bundling of FtsZ polymers by an interaction between C-terminal domains. *J. Bacteriol.* 182: 5153-5166, 2000.

[67] Zhan Liu, Amit Mukherjee, and Joe Lutkenhaus. Recruitment of ZipA to the division site by interaction with FtsZ. *Mol. Microbiol.* 31: 1853-1861, 1999.

[68] Lidia Mosyak, Yan Zhang, Elizabeth Glasfeld, Steve Haney, Mark Stahl, Jasbir Seehra, and William S. Somers. The bacterial cell-division protein ZipA and its interaction with an FtsZ fragment revealed by X-ray crystallography. *EMBO J.* 19: 3179-3191, 2000.

[69] Piet A. J. de Boer. Advances in understanding *E. coli* cell fission [Review]. *Curr. Opin. Microbiol.* 13: 730-737, 2010.

[70] Sebastien Pichoff and Joe Lutkenhaus. Unique and overlapping roles for ZipA and FtsA in septal ring assembly in *Escherichia coli*. *EMBO J.* 21: 685-693, 2002.

[71] Leendert W. Hamoen, Jean-Christophe Meile, Wouter de Jong, Philippe Noirot, and Jeff Errington. SepF, a novel FtsZ-interacting protein required for a late step in cell division. *Mol. Microbiol.* 59: 989-999, 2006.

[72] Jay Kumar Singh, Ravindra D. Makde, Vinay Kumar, and Dulal Panda. SepF increases the assembly and bundling of FtsZ polymers and stabilizes FtsZ protofilaments by binding along its length. *J. Biol. Chem.* 283: 45: 31116-31124, 2008.

[73] Muhammet E. Gündoğdu, Yoshikazu Kawai, Nada Pavlendova, Naotake Ogasawara, Jeff Errington, Dirk-Jan Scheffers and Leendert W. Hamoen. Large ring polymers align FtsZ polymers for normal septum formation. *EMBO J.* 30: 617-626, 2011.

[74] Petra Anne Levin, Iren G. Kurtser, and Alan D. Grossman. Identification and characterization of a negative regulator of FtsZ ring formation in *Bacillus subtilis*. *Proc. Natl. Acad. Sci. USA* 96: 9642-9647, 1999.

[75] Daniel P. Haeusser, Rachel L. Schwartz, Alison M. Smith, Michelle Erin Oates, and Petra Anne Levin. EzrA prevents aberrant cell division by modulating assembly of the cytoskeletal protein FtsZ. *Mol. Microbiol.* 52: 801-814, 2004.

[76] Dennis Claessen, Robyn Emmins, Leendert W. Hamoen, Richard A. Daniel, Jeff Errington, and David H. Edwards. Control of the cell elongation-division cycle by shuttling of PBP1 protein in *Bacillus subtilis*. *Mol. Microbiol.* 68: 1029-1046, 2008.

[77] Lotte B. Pedersen, Esther R. Angert, and Peter Setlow. Septal localization of Penicillin-binding Protein 1 in *Bacillus subtilis*. *J. Bacteriol.* 181: 3201-3211, 1999.

[78] Frederico J. Gueiros-Filho and Richard Losick. A widely conserved bacterial cell division protein that promotes assembly of the tubulin-like protein FtsZ. *Genes Dev.* 16: 2544-2556, 2002.

[79] Gitte Ebersbach, Elisa Galli, Jakob Møller-Jensen, Jan Löwe, and Kenn Gerdes. Novel coiled-coil cell division factor ZapB stimulates Z ring assembly and cell division. *Mol. Microbiol.* 68: 720-735, 2008.

[80] Elisa Galli and Ken Gerdes. Spatial resolution of two bacterial cell division proteins: ZapA recruits ZapB to the inner face of the Z-ring. *Mol. Microbiol.* 76: 1514-1526, 2010.

[81] Cynthia A. Hale, Diasuke Shiomi, Bing Liu, Thomas G. Bernhardt, William Margolin, Hironori Niki, and Piet A. J. de Boer. Identification of *Escherichia coli* ZapC (YcbW) as a component of the division apparatus that binds and bundles FtsZ polymers. *J. Bacteriol.* 193: 93-1404, 2011.

[82] Klas Flärdh, Teresa Garrido, and Miguel Vicente. Contribution of individual promoters in the *ddlB-ftsZ* region to the transcription of the essential cell-division gene *ftsZ* in *Escherichia coli*. *Mol. Microbiol.* 24: 927-936, 1997.

[83] M. Vicente, M. J. Gomez, and J. A. Ayala. Regulation of transcription of cell division genes in the *Escherichia coli dcw* cluster [Review]. *Cell. Mol. Life Sci.* 54: 317-324, 1998.

[84] Aline Robin, Danièle Joseleau-Petit, and Richard d'Ari. Transcription of the *ftsZ* gene and cell division in *Escherichia coli*. *J. Bacteriol.* 172: 1392-1399, 1990.

[85] Teresa Garrido, Manuel Sánchez, Pilar Palacios, Martí Aldea, and Miguel Vicente. Transcription of *ftsZ* oscillates during the cell cycle of *Escherichia coli*. *EMBO J.* 12: 3957-3965, 1993.

[86] Ping Zhou and Charles E. Helmstetter. Relationship between *ftsZ* gene expression and chromosome replication in *Escherichia coli*. *J. Bacteriol.* 176: 6100-6106, 1994.

[87] Martí Aldea, Teresa Garriod, Jesús Pla, and Miguel Vicente. Division genes in *Escherichia coli* are expressed coordinately to cell septum requirements by gearbox promoters. *EMBO J*. 9: 3787-3794, 1990.

[88] Richard W. P. Smith, Millicent Masters, and William D. Donachie. Cell division and transcription of *ftsZ*. *J. Bacteriol*. 175: 2788-2791, 1993.

[89] Xunde Wang, Piet A. J. de Boer, and Lawrence I. Rothfield. A factor that positively regulates cell division by activating transcription of the major cluster of essential division genes of *Escherichia coli*. *EMBO J*. 10: 3363-3372, 1991.

[90] Dmitry M. Sitnikov, Jeffrey B. Schineller, and Thomas O. Baldwin. Control of cell division in *Escherichia coli*: regulation of transcription of *ftsQA* involves both *rpoS* and SdiA-mediated autoinduction. *Proc. Natl. Acad. Sci. USA* 93: 336-341, 1996.

[91] J. García-Lara, L. H. Shang, and L. I. Rothfield. An extracellular factor regulates expression of *sdiA*, a transcriptional activator of cell division genes in *Escherichia coli*. *J. Bacteriol*. 178: 2742-2748, 1996.

[92] François G. Gervais, Pauline Phoenix, and Gabriel R. Drapeau. The *rcsB* gene, a positive regulator of colonic acid biosynthesis in *Escherichia coli*, is also an activator of *ftsZ* expression. *J. Bacteriol*. 174: 3964-3971, 1992.

[93] Bradford S. Powell and Donald L. Court. Control of *ftsZ* expression, cell division, and glutamine metabolism in Luria-Bertani medium by the alarmone ppGpp in *Escherichia coli*. *J. Bacteriol*. 180: 1053-1062.

[94] Geneviève Gonzy-Tréboul, Céline Karmazyn-Campelli, and Patrick Stragier. Developmental regulation of transcription of the *Bacillus subtilis ftsAZ* operon. *J. Mol. Biol*. 224: 967-979, 1992.

[95] Ahmad Gholamhoseinian, Zhu Shen, Jiunn-Jong Wu, and Patrick Piggot. Regulation of Transcription of the cell division gene *ftsA* during sporulation of *Bacillus subtilis*. *J. Bacteriol*. 174: 4647-4656, 1992.

[96] Virginie Molle, Masaya Fujita, Shane T. Jensen, Patrick Eichenberger, José E. González-Pastor, Jun S. Liu, and Richard Losick. The Spo0A regulon of *Bacillus subtilis*. *Mol. Microbiol*. 50: 1683-1701, 2003.

[97] Petra Anne Levin and Richard Losick. Transcription factor Spo0A switches the localization of the cell division protein FtsZ from a medial to bipolar pattern in *Bacillus subtilis*. *Genes Dev*. 10: 478-488, 1996.

[98] Sigal Ben-Yehuda and Richard Losick. Asymmetric cell division in *B. subtilis* involves a spiral-like intermediate of the cytokinetic protein FtsZ. *Cell* 109: 257-266, 2002.

[99] Petra Anne Levin, Richard Losick, Patrick Stragier, and Fabrizio Arigoni. Localization of the sporulation protein SpoIIE in *Bacillus subtilis* is dependent upon the cell division protein FtsZ. *Mol. Microbiol.* 25: 839-846, 1997.

[100] Anastasia Khvorova, Ling Zhang, Michael L. Higgins, and Patrick Piggot. The *spoIIE* locus is involved in the Spo0A-dependent switch in the location of FtsZ rings in *Bacillus subtilis*. *J. Bacteriol.* 180: 1256-1260, 1998.

[101] Isabelle Lucet, Andrea Feucht, Michael D. Yudkin, and Jeffery Errington. Direct interaction between the cell division protein FtsZ and the cell differentiation protein SpoIIE. *EMBO J.* 19: 1467-1475, 2000.

[102] Joe Pogliano, Nick Osborne, Marc D. Sharp, Angelica Abanes-De Mello, Ana Perez, Ya-Lin Sun and Kit Pogliano. A vial stain for studying membrane dynamics in bacteria: a novel mechanism controlling septation during *Bacillus subtilis* sporulation. *Mol. Microbiol.* 31: 1149-1159, 1999.

[103] Klas Flärdh, Emmanuelle Leibovitz, Mark J. Buttner, and Keith F. Chater. Generation of a non-sporulating strain of *Streptomyces coelicolor* A3(2) by the manipulation of a developmentally controlled *ftsZ* promoter. *Mol. Microbiol.* 38: 737-749, 2000.

[104] Isabelle Kuhn, Ling Peng, Sylvie Bedu, and Cheng-Cai Zhang. Developmental regulation of the cell division protein FtsZ in *Anabaena* sp. strain PCC 7120, a cyanobacterium capable of terminal differentiation. *J. Bacteriol.* 182: 4640-4643, 2000.

[105] Sandra Ramirez-Arcos, Hossein Salimnia, Isabelle Bergevin, Madeleine Paradis, and Jo-Anne R. Dillon. Expression of *Neisseria gonorrhoeae* cell division genes *ftsZ*, *ftsE*, and *minD*, is influenced by environmental conditions. *Res. Microbiol.* 152: 781-791, 2001.

[106] Jangyul Kwak, Amitha J. Dharmatilake, Hao Jiang, and Kathleen E. Kendrick. Differential Regulation of *ftsZ* transcription during septation of *Streptomyces griseus*. *J. Bacteriol.* 183: 5092-5101, 2001.

[107] Iulia-Andra Anca, Erica Lumini, Stefano Ghignone, Alessandra Salvioli, Valeria Bianciotto, and Paula Bonfante. The *ftsZ* gene of the endocellular bacterium *Candidatus* Glomeribacter gigasporarum is preferentially expressed during the symbiotic phases of its host mycorrhizal fungus. *Mol. Plant Microbe Interact.* 22: 302-310, 2009.

[108] Sougata Roy, Deepak Anand, Srinivasan Vijay, Prabuddha Gupta, and Parthasarathi Ajitkumar. The *ftsZ* gene of *Mycobacterium smegmatis* is expressed through multiple transcripts. *Open Microbiol.* 5: 43-53, 2011.

[109] H. I. Adler, W. D. Fisher, A. Cohen, and Alice A. Hardigree. Miniature *Escherichia coli* cells deficient in DNA. *Proc. Natl. Acad. Sci. USA* 57: 321-326, 1967.

[110] R. M. Teather, J. F. Collins, and W. D. Donachie. Quantal behavior of a diffusible factor which initiates septum formation at potential division sites in *Escherichia coli*. *J. Bacteriol*. 118: 407-413, 1974.

[111] Piet A. J. de Boer, Robin E. Crossley, and Lawrence I. Rothfield. Isolation and properties of *minB*, a complex genetic locus involved in correct placement of the division site in *Escherichia coli*. *J. Bacteriol*. 170: 2106-2112, 1988.

[112] Piet A, J. de Boer, Robin E. Crossley, and Lawrence I. Rothfield. A division inhibitor and a topological specificity factor coded for by the minicell locus determine proper placement of the division septum in *E. coli*. *Cell* 56: 641-649, 1989.

[113] Petra Anne Levin, Peter S. Margolis, Peter Setlow, Richard Losick, and Dongxu Sun. Identification of *Bacillus subtilis* genes for septum placement and shape determination. *J. Bacteriol*. 6717-6728, 1992.

[114] A. W. Varley and George C. Stewart. The *divIVB* region of the *Bacillus subtilis* chromosome encodes homologs of *Escherichia coli* septum placement (MinCD) and cell shape (MreBCD) determinants. *J. Bacteriol*. 174: 6729-6742, 1992.

[115] Piet A. J. de Boer, Robin E. Crossley, and Lawrence I. Rothfield. Roles of MinC and MinD in the site-specific septation block mediated by the MinCDE system of *Escherichia coli*. *J. Bacteriol*. 174: 63-70, 1992.

[116] Piet A. J. de Boer, Robin E. Crossley, and Lawrence I. Rothfield. Central role for the *Escherichia coli minC* gene product in two different cell division-inhibition systems. *Proc. Natl. Acad. Sci. USA* 87: 1129-1133, 1990.

[117] Erfei Bi and Joe Lutkenhaus. Interaction between the *min* Locus and *ftsZ*. *J. Bacteriol*. 172: 5610-5616, 1990.

[118] Zonglin Hu, Amit Mukherjee, Sebastien Pichoff, and Joe Lutkenhaus. The MinC component of the division site selection system in *Escherichia coli* interacts with FtsZ to prevent polymerization. *Proc. Natl. Acad. Sci. USA* 96: 14819-14824, 1999.

[119] Zonglin Hu and Joe Lutkenhaus. Analysis of MinC reveals two independent domains involved in interaction with MinD and FtsZ. *J. Bacteriol*. 182: 3965-3971, 2000.

[120] Suzanne C. Cordell, Rebecca E. Anderson, and Jan Löwe. Crystal structure of the bacterial cell division inhibitor MinC. *EMBO J*. 20: 2454-2461, 2001.

[121] Andrea Feucht and Jeffery Errington. *ftsZ* mutations affecting cell division frequency, placement, and morphology in *Bacillus subtilis*. *Microbiol*. 151: 2053-2064, 2005.

[122] Bang Shen and Joe Lutkenhaus. The conserved C-terminal tail of FtsZ is required for the septal localization and division inhibitory activity of $MinC^{C}$/MinD. *Mol. Microbiol.* 72: 410-424, 2009.

[123] Bang Shen and Joe Lutkenhaus. Examination of the interaction between FtsZ and $MinC^{N}$ in *E. coli* suggests how MinC disrupts Z rings. *Mol. Microbiol.* 75: 1285-1298, 2010.

[124] Valdir Blasios, Alexandre W. Bisson-Filho, Patricia Castellen, Maria Luiza C. Nogueira, Jefferson Bettini, Rodrigo V. Portugal, Ana Carolina M. Zeri, and Frederico J. Gueiros-Filho. Genetic and Biochemical Characterization of the MinC-FtsZ interaction in *Bacillus subtilis*. *PLoS One* 8: e60690, 2013.

[125] Suey van Baarle and Marc Bramkamp. The MinCDJ system in *Bacillus subtilis* prevents minicell formation by promoting divisome disassembly. *PLoS One* 5: e9850, 2010.

[126] Victor M. Hernández-Rocamora, Concepción García-Montañés, Belén Reija, Begoña Monterroso, William Margolin, Carlos Alfonso, Silvia Zorrilla, and Germán Rivas. MinC protein shortens FtsZ protofilaments by preferentially interacting with GDP-bound subunits. *J. Biol. Chem.* 288: 24625-24635, 2013.

[127] Piet A. J. de Boer, Robin E. Crossley, Arthur R. Hand, and Lawrence I. Rothfield. The MinD protein is a membrane ATPase required for the correct placement of the *Escherichia coli* division site. *EMBO J.* 10: 4371-4380, 1991.

[128] Zonglin Hu, Edward P. Gogol, and Joe Lutkenhaus. Dynamic assembly of MinD of phospholipid vesicles regulated by ATP and MinE. *Proc. Natl. Acad. Sci. USA* 99: 6761-6766, 2002.

[129] Zonglin Hu and Joe Lutkenhaus. A conserved sequence at the C-terminus of MinD is required for binding to the membrane and targeting of MinC to the septum. *Mol. Microbiol.* 47: 345-355, 2003.

[130] Zonglin Hu, Cristian Saez, and Joe Lutkenhaus. Recruitment of MinC, an inhibitor of Z-ring formation, to the membrane in *Escherichia coli*: Role of MinD and MinE. *J. Bacteriol.* 185: 196-203, 2003.

[131] Laura L. Lackner, David M. Raskin, and Piet A. J. de Boer. ATP-dependent interactions between *Escherichia coli* Min proteins and the phospholipid membrane *in vitro*. *J. Bacteriol.* 185: 735-749, 2003.

[132] Sébastien Pichoff, Benedikt Vollrath, Christian Touriol, Jean-Pierre Bouché. Deletion analysis of gene *minE* which encodes the topological specificity factor of cell division in *Escherichia coli*. *Mol. Microbiol.* 18: 321-329, 1995.

[133] Zonglin Hu and Joe Lutkenhaus. Topological regulation of cell division in *E. coli*: spatiotemporal oscillation of MinD requires stimulation of its ATPase by MinE and phospholipid. *Mol. Cell* 7:1337-1343, 2001.

[134] Jian Huang, Chune Cao, and Joe Lutkenhaus. Interaction between FtsZ and inhibitors of cell division. *J. Bacteriol.* 178: 5080-5085, 1996.

[135] David M. Raskin and Piet A. J. de Boer. The MinE ring: an FtsZ-independent cell structure required for selection of the correct division site in *E. coli*. *Cell* 91: 685-694, 1997.

[136] David M. Raskin and Piet A. J. de Boer. MinDE-dependent pole-to-pole oscillation of division inhibitor MinC in *Escherichia coli*. *J. Bacteriol.* 181: 6419-6424, 1999.

[137] David M. Raskin and Piet A. J. de Boer. Rapid pole-to-pole oscillation of a protein required for directing division to the middle of *Escherichia coli*. *Proc. Natl. Acad. Sci. USA* 96: 4971-4976, 1999.

[138] Xiaoli Fu, Yu-Ling Shih, Yan Zhang, and Lawrence I. Rothfield. The MinE ring required for proper placement of the division site is a mobile structure that changes its cellular location during the *Esherichia coli* division cycle. *Proc. Natl. Acad. Sci. USA* 98: 980-985, 2001.

[139] Adele L. Marston, Helena B. Thomaides, David H. Edwards, Michaela E. Sharpe, and Jeffery Errington. Polar localization of the MinD protein of *Bacillus subtilis* and its role in selection of the mid-cell division site. *Genes Dev.* 12: 3419-3430, 1998.

[140] Adele L. Marston and Jeffery Errington. Selection of the midcell division site in *Bacillus subtilis* through MinD-dependent polar localization and activation of MinC. *Mol. Microbiol.* 33: 84-96, 1999.

[141] Joyce E. Patrick and Daniel B. Kearns. MinJ (YvjD) is a topological determinant of cell division in *Bacillus subtilis*. *Mol. Microbiol.* 70: 1166-1179, 2008.

[142] Marc Bramkamp, Robyn Emmins, Louise Weston, Catriona Donovan, Richard A. Daniel, and Jeff Errington. A novel component of the division-site selection system of *Bacillus subtilis* and a new mode of action for the division inhibitor MinCD. *Mol. Microbiol.* 70: 1556-1569, 2008.

[143] David H. Edwards, Helena B. Thomaides, and Jeffery Errington. Promiscuous targeting of *Bacillus subtilis* cell division protein DivIVA to division sites in *Escherichia coli* and fission yeast. *EMBO J.* 19: 2719-2727, 2000.

[144] Elizabeth J. Harry and Peter J. Lewis. Early targeting of Min proteins to the cell poles in germinated spores of *Bacillus subtilis*: evidence for division apparatus-independent recruitment of Min proteins to the division site. *Mol. Microbiol.* 47: 37-48, 2003.

[145] Joe Lutkenhaus. Assembly dynamics of the bacterial MinCDE system and spatial regulation of the Z ring [Review]. *Annu. Rev. Biochem.* 76: 539-562, 2007.

[146] Egbert Mulder and Conrad L. Woldringh. Actively replicating nucleoids influence positioning of division sites in *Escherichia coli* filaments forming cells lacking DNA. *J. Bacteriol.* 171: 4303-4314, 1989.

[147] Qin Sun, Xuan-Chuan Yu, and Willian Margolin. Assembly of the FtsZ ring at the central division site in the absence of the chromosome. *Mol. Microbiol.* 29: 491-503, 1998.

[148] Xuan-Chuan Yu and William Margolin. FtsZ ring clusters in *min* and partition mutants: role of both the Min system and the nucleoid in regulating FtsZ ring localization. *Mol. Microbiol.* 32: 315-326, 1999.

[149] Jörg Sievers, Brian Raether, Marta Perego, and Jeff Errington. Characterization of the *parB*-like *yyaA* gene of *Bacillus subtilis*. *J. Bacteriol.* 184: 1101-1111, 2002.

[150] Ling Juan Wu and Jeff Errington. Coordination of cell division and chromosome segregation by a nucleoid occlusion protein in *Bacillus subtilis*. *Cell* 117: 915-925, 2004.

[151] Ling Juan Wu, Shu Ishikawa, Yoshikazu Kawai, Taku Oshima, Naotake Ogasawara, and Jeff Errington. Noc protein binds to specific DNA sequences to coordinate cell division with chromosome segregation. *EMBO J.* 28: 1940-1952, 2009.

[152] Thomas G. Bernhardt and Piet A. J. de Boer. SlmA, a nucleoid-associated, FtsZ binding protein required for blocking septal ring assembly over chromosomes in *E. coli*. *Mol. Cell* 18: 555-564, 2005.

[153] Nam Ky Tonthat, Stefan T. Arold, Brian F. Pickering, Michael W. Van Dyke, Shoudan Liang, Yue Lu, Tushar K Beuria, William Margolin, and Maria A. Schumacher. Molecular mechanism by which the nucleoid occlusion factor, SlmA, keeps cytokinesis in check. *EMBO J.* 30: 154-164, 2011.

[154] Nam K. Tomthat, Sara L. Milam, Nagababu Chinnam, Travis Whitfill, William Margolin, and Maria A. Schumacher. SlmA forms a higher-order structure on DNA that inhibits cytokinetic Z-ring formation over the nucleoid. *Proc. Natl. Acad. Sci. USA* 110: 10586-10591, 2013.

[155] Hongbaek Cho, Heather R. McManus, Simon L. Dove, and Thomas G. Bernhardt. Nucleoid occlusion factor SlmA is a DNA-activated FtsZ polymerization antagonist. *Proc. Natl. Acad. Sci. USA* 108: 3773-3778, 2011.

[156] Hongbaek Cho and Thomas G. Bernhardt. Identification of the SlmA active site responsible for blocking bacterial cytokinetic ring assembly over the chromosome. *PLoS Genet*. 9: e1003304, 2013.

[157] Ling Juan Wu and Jeff Errington. Nucleoid occlusion and bacterial cell division [Review]. *Nat. Rev. Microbiol*. 10: 8-12, 2011.

[158] Takumi Koyama, Masao Yamada, and Michio Matsuhashi. Formation of regular packets of *Staphylococcus aureus* cells. *J. Bacteriol*. 129: 1518-1523, 1977.

[159] Helena Veiga, Ana M. Jorge, and Mariana G. Pinho. Absence of nucleoid occlusion effector Noc impairs formation of orthogonal FtsZ rings during *Staphylococcus aureus* cell division. *Mol. Microbiol*. 80: 1366-1380, 2011.

[160] Graham C. Walker. SOS-regulated proteins in translesion DNA synthesis and mutagenesis [Review]. *Trends Biochem. Sci*. 20: 416-20, 1995.

[161] Bradley T. Smith and Graham C. Walker. Mutagenesis and more: *umuDC* and the *Escherichia coli* response [Review]. *Genetics* 148: 1599-610, 1998.

[162] Randall C. Gayda, Leslie T. Yamamoto, and Alvin Markovitz. Second-site mutation in *capR*(*lon*) strains of *Escherichia coli* K-12 that prevent radiation sensitivity and allow bacteriophage lambda to lysogenize. *J. Bacteriol*. 127: 1208-1216, 1976.

[163] Olivier Huisman, Richard D'Ari, and Susan Gottesman. Cell-division control in *Escherichia coli*: specific induction of the SOS function SfiA protein is sufficient to block septation. *Proc. Natl. Acad. Sci. USA* 81: 4490-4494, 1984.

[164] Joyce M. Schoemaker, Randall C. Gayda, and Alvin Markovitz. Regulation of cell division in *Escherichia coli*: SOS induction and cellular location of the SulA protein, a key to *lon*-associated filamentation and death. *J. Bacteriol*. 158: 551-561, 1985.

[165] Chris Jones and I. Barry Holland. Role of the SulB (FtsZ) protein in division inhibition during the SOS response in *Escherichia coli*: FtsZ stabilizes the inhibitor SulA in maxicells. *Proc. Natl. Acad. Sci. USA* 82: 6045-6049, 1985.

[166] Erfei Bi and Joe Lutkenhaus. Analysis of *ftsZ* mutations that confer resistance to the cell division inhibitor SulA (SfiA). *J. Bacteriol*. 172: 5602-5609, 1990.

[167] Erfei Bi and Joe Lutkenhaus. Cell division inhibitors SulA and MinCD prevent formation of the FtsZ ring. *J. Bacteriol*. 175: 1118-1125, 1993.

[168] Atsushi Higashitani, Nahoko Higashitani, and Kensuke Horiuchi. A cell division inhibitor SulA of *Escherichia coli* directly interacts with FtsZ through GTP hydrolysis. *Biochem. Biophys. Res. Commun*. 209: 198-204, 1995.

[169] Dorina Trusca, Solomon Scott, Chris Thompson, and David Bramhill. Bacterial SOS checkpoint protein SulA inhibits polymerization of purified FtsZ cell division protein. *J. Bacteriol*. 180: 3946-3853, 1998.

[170] Suzanne C. Cordell, Elva J. H. Robinson, and Jan Löwe. Crystal structure of the SOS cell division inhibitor SulA and in complex with FtsZ. *Proc. Natl. Acad. Sci. USA* 100: 7889-7894, 2003.

[171] Yaodong Chen, Sara L. Milam, and Harold P. Erickson. SulA inhibits assembly of FtsZ by a simple sequestration mechanism. *Biochemistry* 51: 3100-3109, 2012.

[172] Yoshikazu Kawai, Shigeki Moriya, and Naotake Ogasawara. Identification of a protein, YneA, responsible for cell division suppression during the SOS response in *Bacillus subtilis*. *Mol. Microbiol*. 47: 113-1122, 2003.

[173] Allison H. Mo and William F. Burkholder. YneA, an SOS-induced inhibitor of cell division in *Bacillus subtilis*, is regulated posttranslationally and requires the transmembrane region for activity. *J. Bacteriol*. 192: 3159-3173, 2010.

[174] Ashwini Chauhan, Hava Lofton, Erin Maloney, Jacob Moore, Marek Fol, Murty V. V. S. Madiraju, and Malini Rajagopalan. Interference of *Mycobacterium tuberculosis* cell division by Rv2719c, a cell wall hydrolase. *Mol. Microbiol*. 62: 132-147, 2006.

[175] Hidetaka Ogino, Haruhiko Teramoto, Masayuki Inui, and Hideaki Yukawa. *DivS*, a novel SOS-inducible cell-division suppressor in *Corynebacterium glutamicum*. *Mol. Microbiol*. 67: 597-608, 2008.

[176] Wayne L. Nicholson, Nobuo Munakata, Gerda Hornneck, Henry J. Melosh, and Peter Setlow. Resistance of *Bacillus* endospores to extreme terrestrial and extraterrestrial environments [Review]. *Microbiol. Mol. Biol. Rev*. 64:548-572, 2000.

[177] Peter Setlow. Spore germination [Review]. *Curr. Opin. Microbiol*. 6: 550-556, 2003.

[178] Patrick J. Piggot and David W. Hilbert. Sporulation of *Bacillus subtilis* [Review]. *Curr. Opin. Microbiol*. 7: 579-586, 2004.

[179] Aaron A. Handler, Joo Eun Lim, and Richard Losick. Peptide inhibitor of cytokinesis during sporulation in *Bacillus subtilis*. *Mol. Microbiol*. 68: 588-599, 2008.

[180] Shashikant Ray, Ashutosh Kumar, and Dulal Panda. GTP regulates the interaction between MciZ and FtsZ: a possible role of MciZ in bacterial cell division. *Biochemistry* 52: 392-401, 2013.

[181] Joseph R. McCormick, Edwin P. Su, Adam Driks, and Richard Losick. Growth and viability of *Streptomyces coelicolor* mutant for the cell division gene *ftsZ*. *Mol. Microbiol*. 14: 243-254, 1994.

[182] Joost Willemse, Jan Willem Borst, Ellen de Waal, Ton Bisseling, and Gilles P. van Wezel. Positive control of cell division: FtsZ is recruited by SsgB during sporulation of *Streptomyces*. *Genes Dev*. 25: 89-99, 2011.

[183] M. Schaecter, O. Maaløe, and N. O. Kjeldgaard. Dependency on medium and temperature of cell size and chemical composition during balanced growth of *Salmonella typhimurium*. *J. Gen. Microbiol*. 19: 592-606, 1958.

[184] Michael G. Sargent. Control of cell length in *Bacillus subtilis*. *J. Bacteriol*. 123: 7-19, 1975.

[185] W. D. Donachie, K. J. Begg, and M. Vicente. Cell length, cell growth, and cell division. *Nature* 264: 328-333, 1976.

[186] Richard B. Weart and Petra Anne Levin. Growth rate-dependant regulation of medial FtsZ ring formation. *J. Bacteriol*. 185: 2826-2834, 2003.

[187] Richard B. Weart, Amy H. Lee, An-Chun Chien, Daniel P. Haeusser, Norbert S. Hill, and Petra Anne Levin. A Metabolic Sensor Governing Cell Size in Bacteria. *Cell* 130: 335-347, 2007.

[188] An-Chun Chien, Shannon Kian Gharabiklou Zareh, Yan Mei Wang, and Petra Anne Levin. Changes in the oligomerization potential of the division inhibitor UgtP co-ordinate *Bacillus subtilis* cell size with nutrient availability. *Mol. Microbiol*. 86: 594-610, 2012.

[189] Norbert S. Hill, Paul J. Buske, Yue Shi, and Petra Anne Levin. A moonlighting enzyme links *Escherichia coli* cell size with central metabolism. *PLoS Genet*. 9: e1003663, 2013.

[190] Hélène Barreteau, Andreja Kovač, Audry Boniface, Matej Sova, Stanislav Gobec, and Didier Blanot. Cytoplasmic steps of peptidoglycan biosynthesis [Review]. *FEMS Microbiol. Rev*. 32: 168-207, 2008.

[191] Deo Prakash Pandey and Kenn Gerdes. Toxin-antitoxin loci are highly abundant in free-living but lost from host-associated prokaryotes [Review]. *Nucl. Acids Res*. 33: 966-976, 2005.

[192] Yoshihiro Yamaguchi, Jung-Ho Park, and Masayori Inouye. Toxin-antitoxin systems in bacteria and archaea [Review]. *Annu. Rev. Genet*. 45: 61-79, 2011.

[193] Qian Tan, Naoki Awano, and Masayori Inouye. YeeV is an *Escherichia coli* toxin that inhibits cell division by targeting the cytoskeleton proteins, FtsZ and MreB. *Mol. Microbiol*. 79: 109-118, 2011.

[194] Hisako Masuda, Qian Tan, Naoki Awano, Kuen-Phon Wu, and Masayori Inouye. YeeU enhances the bundling of cytoskeletal polymers of MreB and FtsZ, antagonizing the CbtA (YeeV) toxicity in *Escherichia coli*. *Mol. Microbiol.* 84: 979-989, 2012.

[195] Richard B. Weart, Shunji Nakano, Brooke E. Lane, Peter Zuber, and Petra Anne Levin. The ClpX chaperone modulates assembly of the tubulin-like protein FtsZ. *Mol. Microbiol.* 57: 238-249, 2005.

[196] Daniel P. Haeusser, Amy H. Lee, Richard B. Weart, and Petra Anne Levin. ClpX inhibits FtsZ assembly in a manner that does not require its ATP hydrolysis-dependent chaperone activity. *J. Bacteriol.* 191: 1986-1991, 2009.

[197] Renata Dziedzic, Manjot Kiran, Przemyslaw Plocinski, Malgorzata Ziolkiewicz, Anna Brzostek, Meredith Moomey, Indumati S. Vadrevu, Jaroslaw Dziadek, Murty Madiraju, and Malini Rajagopalan. *Mycobacterium tuberculosis* ClpX interacts with FtsZ and interferes with FtsZ assembly. *PLoS One* 5: e11058, 2010.

[198] Shinya Sugimoto, Kunitoshi Yamanaka, Shingo Nishikori, Atsushi Miyagi, Toshio Ando, and Teru Ogura. AAA^+ chaperone ClpX regulates dynamics of prokaryotic cytoskeletal protein FtsZ. *J. Biol. Chem.* 285: 6648-6657, 2010.

[199] Jodi L. Camberg, Joel R. Hoskins, and Sue Wickner. ClpXP protease degrades the cytoskeletal protein, FtsZ, and modulates FtsZ polymer dynamics. *Proc. Natl. Acad. Sci. USA* 106: 10614-10619, 2009.

[200] Jodi L. Camberg, Joel R. Hoskins, and Sue Wickner. The interplay of ClpXP with the cell division machinery in *Escherichia coli*. *J. Bacteriol.* 193: 1911-1918, 2011.

[201] Robert T. Sauer and Tania A. Baker. AAA+ proteases: ATP-fueled machines of protein destruction. *Annu. Rev. Biochem.* 80: 587-612, 2011.

[202] Christopher D. A. Rodrigues and Elizabeth J. Harry. The Min system and nucleoid occlusion are not required for identifying the division sit in *Bacillus subtilis* but ensure its efficient utilization. *PLoS Genet.* 8: e1002561, 2012.

[203] Remi Bernard, Kathleen A. Marquis, and David Z. Rudner. Nucleoid occlusion prevents cell division during replication fork arrest in *Bacillus subtilis*. *Mol. Microbiol.* 78: 866-882, 2010.

[204] S. Moriya, R. A. Rashid, C. D. Andrade Rodrigues, and E. J. Harry. Influence of the nucleoid and the early stages of DNA replication on positioning the division site in *Bacillus subtilis*. *Mol. Microbiol.* 76: 634-647, 2010.

[205] Joshua Cambridge, Alexandra Blinkova, David Magnan, David Bates, and James R. Walker. A replication-inhibited unsegregated nucleoid at mid-cell blocks Z-ring

formation and cell division independently of SOS and the SlmA nucleoid occlusion protein in *Escherichia coli*. *J. Bacteriol*. 196: 36-49, 2014.

[206] Katrina Surdova, Pamela Gamba, Dennis Claessen, Tjalling Siersma, Martijs J. Jonker, Jeff Errington, and Leendert W. Hamoen. The conserved DNA-binding protein WhiA is involved in cell division in *Bacillus subtilis*. *J. Bacteriol*. 195: 5450-5460, 2013.

[207] Michal Letek, María Fiuza, Efrén Ordóñez, Almudena F. Villadangos, Astrid Ramos, Luís M. Mateos, and José A. Gil. Cell growth and cell division in the rod-shaped actinomycete *Corynebacterium glutamicum*. *Antonie Van Leeuwenhoek* 94: 99-109, 2008.

[208] Catriona Donovan, Astrid Schwaiger, Reinhard Krämer, and Marc Bramkamp. Subcellular localization and characterization of the ParAB system from *Corynebacterium glutamicum*. *J. Bacteriol*. 192: 3441-3451, 2010.

[209] Catriona Donovan, Astrid Schauss, Reinhard Krämer, and Marc Bramkamp. Chromosome segregation impacts on cell growth and division site selection in *Corynebacterium glutamicum*. *PLoS One* 8: e55078, 2013.

[210] J. L. Stove and R. Y. Stanier. Cellular differentiation in stalked bacteria. *Nature* 196: 1189-1192, 1962.

[211] Jeanne Stove Poindexter. Biological properties and classification of the *Caulobacter* group [Review]. *Bacteriol. Rev*. 28: 231-295, 1964.

[212] J. S. Poindexter and J. G. Hagenzieker. Constriction and septation during cell division in caulobacters. *Can. J. Microbiol*. 27: 704-19, 1981.

[213] Marian Evinger and Nina Agabian. Envelope-Associated Nucleoid from *Caulobacter crescentus* stalked and swarmer cells. *J. Bacteriol*. 132: 294-301, 1977.

[214] Ellen Quardokus, Neena Din, and Yves V. Brun. Cell cycle regulation and cell type-specific localization of the FtsZ division initiation protein in *Caulobacter*. *Proc. Natl. Acad. Sci. USA* 93: 6314-6319, 1996.

[215] Yan Wang, Benjamin D. Jones, and Yves V. Brun. A set of *ftsZ* mutants blocked at different stages of cell division in *Caulobacter*. *Mol. Microbiol*. 40: 347-360, 2001.

[216] Neena Din, Ellen M. Quardokus, Marcella J. Sackett, and Yves S. Brun. Dominant C-terminal deletions of FtsZ that affect its ability to localize in *Caulobacter* and its interaction with FtsA. *Mol. Microbiol*. 27: 1051-1063, 1998.

[217] Kiani A. J. Arkus Gardner, Desmond A. Moore, and Harold P. Erickson. The C-terminal linker of *Escherichia coli* FtsZ functions as an intrinsically disordered peptide. *Mol. Microbiol*. 89: 264-275, 2013.

[218] Sara L. Milam and Harold P. Erickson. Rapid *in vitro* assembly of *Caulobacter crescentus* FtsZ protein at pH 6.5 and 7.2. *J. Biol. Chem.* 288: 23675-23679, 2013.

[219] Aaron J. Kelly, Marcella J. Sackett, Neena Din, Ellen Quardokus, and Yves V. Brun. Cell cycle-dependent transcriptional and proteolytic regulation of FtsZ in *Caulobacter*. *Genes Dev.* 12: 880-893, 1998.

[220] Dane A. Mohl, Jesse Easter Jr., and James W. Gober. The chromosome partitioning protein, ParB, is required for cytokinesis in *Caulobacter crescentus*. *Mol. Microbiol.* 42: 741-755, 2001.

[221] Erin D. Goley, Yi-Chun Yeh, Sun-Hae Hong, Michael J. Fero, Eduardo Abeliuk, Harley H. McAdams, and Lucy Shapiro. Assembly of the *Caulobacter* cell division machine. *Mol. Microbiol.* 80: 1680-1698, 2011.

[222] Zhuo Li, Michael J. Trimble, Yves V. Brun, and Grant J. Jensen. The structure of FtsZ filaments *in vivo* suggests a force-generating role in cell division. *EMBO J.* 26: 4694-4708, 2007.

[223] Julie S. Biteen, Erin D. Goley, Lucy Shapiro, and W. E. Moerner. Three-dimensional super-resolution imaging of the midplane protein FtsZ in live *Caulobacter crescentus* cells using astigmatism. *Chem. Phys. Chem.* 13: 1007-1012, 2012.

[224] Ellen M. Quardokus, Neena Din, and Yves V. Brun. Cell cycle and positional constraints on FtsZ localization and the initiation of cell division in *Caulobacter crescentus*. *Mol. Microbiol.* 39: 949-959, 2001.

[225] Urs Jenal and Thomas Fuchs. An essential protease involved in bacterial cell-cycle control. *EMBO J.* 17: 5658-5669, 1998.

[226] Ibrahim J. Domian, Kim C. Quon, and Lucy Shapiro. Cell type-specific phosphorylation and proteolysis of a transcriptional regulator controls the G1-to-S transition in a bacterial cell cycle. *Cell* 90: 415-424, 1997.

[227] Ellen M. Quardokus and Yves V. Brun. DNA replication initiation is required for mid-cell positioning of FtsZ rings in *Caulobacter crescentus*. *Mol. Microbiol.* 45: 605-616, 2002.

[228] Rasmus B. Jensen and Lucy Shapiro. The *Caulobacter crescentus smc* gene is required for cell cycle progression and chromosome segregation. *Proc. Natl. Acad. Sci. USA* 96: 10661-10666, 1999.

[229] Erin D. Goley, Natalie A. Dye, John N. Werner, Zemer Gitai, and Lucy Shapiro. Imaging-based identification of a critical regulator of FtsZ protofilament curvature in *Caulobacter*. *Mol. Cell* 39: 975-987, 2010.

[230] Sunish Kumar Radhakrishnan, Sean Pritchard, and Patrick H. Viollier. Coupling prokaryotic cell fate and division control with a bifunctional and oscillating oxidoreductase homolog. *Dev. Cell* 18: 90-101, 2010.

[231] Gregory B. Hecht, Todd lane, Noriko Ohta, Jürg M. Sommer, and Austin Newton. An essential single domain response regulator required for normal cell division and differentiation in *Caulobacter crescentus*. *EMBO J*. 14: 3915-3924, 1995.

[232] Jianguo Wu, Noriko Ohta, and Austin Newton. An essential, multicomponent signal transduction pathway for cell cycle regulation in *Caulobacter*. *Proc. Natl. Acad. Sci. USA* 95: 1443-1448, 1998.

[233] Sunish Kumar Radhakrishnan, Martin Thanbichler, and Patrick H. Viollier. The dynamic interplay between a cell fate determinant and a lysozyme homolog drives the asymmetric division cycle of *Caulobacter crescentus*. *Genes Dev*. 22: 212-215, 2008.

[234] Martin Thanbichler and Lucy Shapiro. MipZ, a spatial regulator coordinating chromosome segregation with cell division in *Caulobacter*. *Cell* 126: 147-162, 2006.

[235] Daniela Kiekebusch, Katharine A. Michie, Lars-Oliver Essen, Jan Löwe, and Martin Thanbichler. Localized dimerization and nucleoid binding drive gradient formation by the bacterial cell division inhibitor MipZ. *Mol. Cell* 46: 245-259, 2012.

[236] Marcella J. Sackett, Aaron J Kelly, and Yves V. Brun. Ordered expression of *ftsQA* and *ftsZ* during the *Caulobacter* cell cycle. *Mol. Microbiol*. 28: 421-434, 1998.

CHAPTER 2

The Chromosome Partitioning System of *Caulobacter crescentus*

The *Caulobacter crescentus* chromosome and partitioning system.

The chromosome of *Caulobacter crescentus* is approximately 4 Mbp and circular [1, 2]. Under normal growth conditions the cell contains a single chromosome, which is highly organized within the cytosol [3, 4]. In *Caulobacter crescentus*, chromosome segregation is mediated by the essential ParAB/*parS* system, homologous to *Bacillus subtilis* Soj/Spo0J system involved in sporulation and chromosome segregation [5-7, 21, 24, 27]. This system was first identified in phage plasmid partitioning systems, and is essential for plasmid propagation and stability [8-10]. The system is comprised of a small region of centromere like DNA encoded proximally to the operon, *parS*, which is bound specifically by the ParB protein (Spo0J in *B. subtilis*) [6, 11, 12, 21, 23]. The operon also encodes the ParA protein, which is a member of a large family of ATPases with diverse biological functions [13-15, 23, 24]. Transcription of the operon is autoregulated by binding of ParB to the *parS* sequences [16-18, 24]. ParB and ParA interact, regulating the function of both proteins [18, 19, 23, 24]. This system is essential in *Caulobacter crescentus*, where it not only operates in chromosome segregation, but also likely plays an additional role in the coordination of cell division by regulating the cytokinetic protein, FtsZ [21, 22, 24, 27, 35, 40].

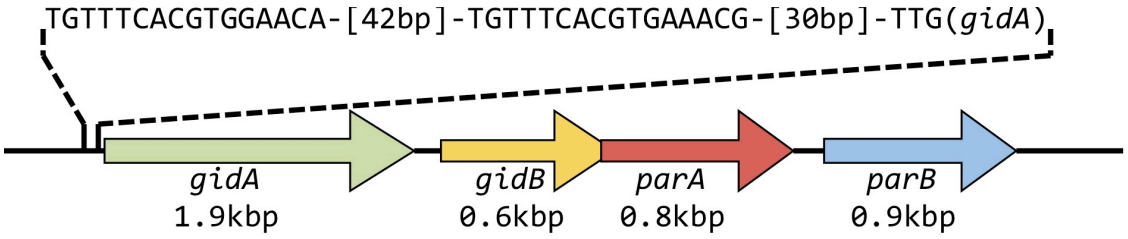

Figure 2.1: Organization of the *gidABparAB* operon of *Caulobacter crescentus*.
The genes encoding ParA and ParB are found in an operon with *gidA* and *gidB (*Glucose Inhibited Division protein A and B). The operon is encoded on the reverse strand of the chromosome, approximately 10,000bp away from the origin of replication. Two *parS* consensus sequences found just upstream of the operon are indicated, with the number of bases between regions indicated in brackets. Sequences, locations, and gene sizes in this figure are based off the CB15-strain sequence [1].

The ParA and ParB proteins in the *Caulobacter crescentus* cell cycle.

Transcription of the *parAB* genes is controlled by an upstream promoter and is coordinated with the development of the cell. A LacZ fusion to ParA, under control of the endogenous promoter, has been used to monitor transcription in synchronized *C. crescentus* cultures. Transcription is not apparent in the swarmer cell, and does not become detectable until after differentiation into a stalked and replicative cell. Transcription remains low through most of the cell cycle, but noticeably peaks prior to cytokinesis, declining following cytokinesis [21]. Direct immunoblotting of ParA and ParB show that protein levels remain constant through the cell cycle. This suggests that this transcriptional cycle serves to increase protein levels in coordination with the increasing size of the predivisional cell, maintaining constant protein levels through the cell cycle and for each daughter cell [21]. Transcription of the *gidABparAB* operon is also modulated by binding of ParB to *parS* sequences found upstream of the operon; a sequence that has been shown to play an essential role in chromosome segregation *in vivo* [23, 27]. During the progression of the *C. crescentus* cell cycle, ParB exists as discrete foci and exhibits a dynamic localization pattern. ParB starts in a single localized focus at the flagellated pole of swarmer cells; in stalked cells, ParB maintains the same localization pattern early in the cell cycle. After differentiation and the beginning of elongation, ParB foci split into two spots: one spot remains at the stalked pole while the second ParB focus quickly moves to the opposite end of the cell, where the flagellum will form in the nascent daughter cell [21, 22, 25, 26]. In contrast to ParB, the ParA protein seems to be localized in a more diffuse pattern that is not limited to discrete foci or cellular positions. While localization data of ParB is in agreement whether visualized using immunofluorescence microscopy [21, 22] or fluorescent fusions in live cells [25, 26], the same cannot be said of ParA. The first visualizations of ParA with fluorescently

labeled antibodies suggested a generally diffuse localization, roughly bipolar and diffusing toward the midcell [21]. More recent work utilizing fluorescent fusions to ParA have suggested a uni-polar density opposite the initial position of ParB that diffuses toward the midcell [26]. This localization pattern was also seen in another study using a different fusion construct, in addition to a single band of ParA localization parallel to the length of the cell, running from pole to pole [25]. Despite discrepancies in localization data for ParA, it is clear that the localization patterns observed for ParA do not directly mimic the pattern observed for ParB [21, 25].

The ParAB/*parS* system in chromosome partitioning

The basis of chromosome partitioning in *Caulobacter crescentus* is the *parS* sequence, a short inverted repeat sequence of approximately 16-bases (TGTTnCACGTGAAACA). This sequence is found at multiple sites within the chromosome, clustered near the origin of replication (unpublished observations). The ParB protein specifically binds the *parS* sequences as a dimer [24]. In gel-shift assays, random sequences of DNA were unable to compete with *parS* for binding by ParB, suggesting a highly specific and strong association [21]. Interaction with *parS* is mediated by both a C-terminal dimerization domain and a DNA binding region that comprises the internal domain of ParB; thus, dimerization is required for stable binding to *parS* [24]. Once the *parS* sequence has been duplicated following the onset of DNA replication, ParB•*parS* complexes move to the opposite poles of the cell [25, 27].

The binding of ParB to *parS* is modulated by the nucleotide bound state of the ParA protein. ParA bound to ATP is able to dissociate ParB from *parS* DNA *in vitro* as observed by Surface Plasmon Resonance experiments; in contrast, ParA•ADP is unable to cause a dissociation of the

complex [23]. The interaction between ParA and ParB is dependent upon the N-terminal domain of ParB: when deleted, ParB is able to bind *parS* as a dimer, but ParA•ATP stimulated dissociation does not occur [24]. The effect of ParA on the ParB•*parS* complex was also demonstrated *in vivo* through overexpression of ParA: when induced, there was a 5-fold increase in transcription of the *gidABparAB* operon as monitored by LacZ fusions; furthermore, ParA overexpression inhibited the formation of polar ParB foci as viewed by immunofluorescence microscopy [23]. The nucleotide bound state of ParA is not passively controlled by the relative concentration of nucleotides in the cell, but is directly modulated by both itself and ParB. ParA is an active ATPase, like its plasmid encoded and *Bacillus subtilis* homologues, though turnover is relatively slow, on the order of one hydrolysis per minute [13, 23, 28]. The interaction of ParA and ParB stimulates nucleotide exchange by ParA, resulting in a slight stimulation of the apparent hydrolysis rate of ATP and a mild reduction in the K_m for ATP from 60 to 48μM in the presence of ParB. However, since ATP hydrolysis by ParA does not appear to be required for nucleotide exchange, it was proposed that these *in vitro* observations were reflective of an increased rate of nucleotide release and ATP binding, rather than an increase in the hydrolysis rate itself [23]. Since cells generally have a higher ATP than ADP content, it is likely that the ParB-induced exchange favors the ParA•ATP form *in vivo* [29, 30]. This would suggest that ParB affects its own ability to bind *parS* by favoring ParA•ATP, which would in turn dissociate ParB from *parS*. The ParA protein has a second distinct function when bound to ADP, which enables the binding of single-stranded DNA in a non-specific manner, suggesting that ParA•ADP may also play an essential role in transcription or DNA replication processes [24].

Recent work has suggested that ParA•ATP is capable of forming filaments, and that destabilization of these structures upon interaction with ParB provides the energetic means to segregate the chromosomes, similar to certain plasmid systems [25, 31-33]. In *Caulobacter crescentus*, fluorescent fusions to ParA formed a linear focal pattern down the long axis of the cell, which retreated toward the flagellated pole as the cell cycle progressed [25]. ParA was shown to polymerize *in vitro*, in an ATP dependent manner, as observed by 90°-angle light scattering and electron microscopy. Fluorescent fusions to ParA mutants deficient in ATP binding were diffuse throughout the cell, while mutants deficient in ATP hydrolysis showed multiple punctate foci, suggesting a critical concentration of ParA•ATP necessary for proper segregation [25]. This work also presented limited *in vitro* evidence that ParA•ATP is capable of binding double-stranded DNA non-specifically, similar to DNA binding dimers formed Soj and certain plasmid encoded ParA proteins [25, 31, 34]. It was also observed that ParA•ATP interacts with the polarity protein TipN, and cells lacking TipN showed defects in segregation of ParB•*parS* complexes and a reduced shrinking of ParA localizations [25, 35]. Recent work has suggested a role for ParA in the recruitment of the PopZ polarity protein to the nascent flagellar pole in late-predivisional cells using cytological experiments [36]. This work showed that N-terminally truncated PopZ fluorescent fusions, unable to interact with ParA remained at only the stalked pole. Furthermore, ParA fusions to DivIVA polarity factor were capable of localizing PopZ to cell poles in *B. subtilis* [36]. Taken together, the authors propose that a nucleoprotein filament of ParA•ATP and chromosome exists that extends across the cell, anchored by TipN at the nascent swarmer pole. Interaction with ParB•*parS* dissociates ParA from DNA and the filament, causing a retraction of the nucleoprotein filament toward the TipN pole. As ParA

accumulates at the TipN pole, PopZ is recruited and TipN disperses, leading to the formation of a new PopZ network capable of binding the incoming ParB•*parS* complex [25, 35, 26].

The ParAB proteins in cytokinesis.

The ParAB system of *Caulobacter crescentus* likely plays an essential role in the regulation of cytokinesis as well as a conserved role in chromosome segregation. Linking of these two events is common among bacterial species, and often involves a chromosomally associated inhibitor of the cytokinetic tubulin homologue, FtsZ [37-39]. One known link between FtsZ and ParB occurs via the protein MipZ [40]. MipZ is an ATPase protein capable of dimerization, and dimerized MipZ is a direct inhibitor of FtsZ assembly; alternatively, monomeric MipZ interacts with ParB [41]. It is proposed that ParB acts to arrange a polar gradient of MipZ, with the highest concentrations near ParB•*parS* complexes; as ParB•*parS* translocates in coordination with chromosome segregation, monomeric MipZ is dragged along behind. The higher concentrations of MipZ in these regions favor dimerization; therefore, FtsZ assembly is inhibited near the ParB•*parS* complexes, but favored in the midcell far from the segregated ParB proteins where MipZ concentrations are low [40, 41].

In *C. crescentus*, changes to the normal protein levels of either ParA or ParB causes a sudden arrest of cell division and affects the localization of FtsZ [21, 22, 27]. Overexpression of ParA or ParB leads to the filamentation of *C. crescentus* as well as the formation of anucleate minicells. Depletion of ParB from *C. crescentus* inhibits the formation of FtsZ rings and leads to smooth filamentous cells, and an overall increase in cell length [22]. Interestingly, overexpression of both ParA and ParB reduced the filamentation, though minicell formation still occurred; in these

cells, FtsZ ring structures were capable of forming, but appeared at aberrant sites [21, 22]. Expression of N-terminally truncated ParB, which is unable to interact with ParA and therefore is roughly equivalent to depleting ParB protein, produced a dominant-negative filamentous phenotype similar to that of ParA overexpression [24]. In both overexpression of ParA, and the expression of the N-terminally truncated ParB, the ratio of ParA•ATP to ParA•ADP was shifted toward the ADP bound form, as opposed to an abundance of ATP bound ParA in wild-type cells [23, 24]. This suggests that changes in ParA or ParB levels, which lead to a shift toward ParA•ADP, directly inhibit FtsZ ring formation.

The action of MipZ alone does not seem sufficient to explain all of these observations, and thus other effectors of FtsZ likely exist; we propose that ParA itself plays a direct role in FtsZ regulation. In *C. crescentus*, a burst of FtsZ assembly is seen at the functionalized pole at the onset of cell differentiation [42]. At this time, transcription from the FtsZ promoter is still relatively weak, and total FtsZ protein levels are low [43, 44]. Finally, the concentration of MipZ is at the highest near the poles due to the retention of one of the segregating ParB•*parS* complexes at this position [21, 40]. The relatively low levels of FtsZ protein, and high levels of MipZ inhibitor suggest that an effector protein capable of stimulating FtsZ assembly is likely necessary at the pole at this moment in the cell cycle. The critical role of this polar assembly of FtsZ is confirmed by the multiple stalks and bifurcated stalk structures observed when FtsZ is overexpressed [43]. Additionally, it has been observed that the depletion of ParB leads to filamentation of cells and inhibition of FtsZ ring formation. The dispersal of MipZ throughout the cell has been proposed as the likely cause of this pheontype the cell [22, 40]. However, clear inhibition of FtsZ requires relatively high concentrations of MipZ, as well as MipZ dimerization,

furthermore, analysis suggests that FtsZ and MipZ are maintained at similar protein levels in the cell [40, 41]. If MipZ alone were responsible for FtsZ regulation, the dispersal of MipZ due to ParB depletion would likely lower the localized MipZ concentration below the threshold for efficient dimerization and FtsZ assembly inhibition. Therefore, one might expect to see an increase in aberrant division sites, not the smooth filaments normally observed [22]. Indeed, depletion of MipZ directly results in such aberrant division sites and minicell formation early as the initial phenotype upon switch to non-permissive growth conditions [40]. In this dissertation, work is presented which proposes a direct role for ParA in the regulation of FtsZ assembly. This system likely acts in concert with the MipZ protein to modulate inhibition and stimulation of FtsZ assembly so that the cell cycle can proceed efficiently.

A model of the cell cycle of *Caulobacter crescentus* and the roles of ParA and ParB.

In the *Caulobacter* swarmer cell, DNA duplication is arrested through a CtrA mediated block of DnaA binding to the origin of replication (*Cori*). ParB is bound to *parS* sites near *Cori*, and both the origin of replication and the ParB•*parS* are located at the flagellated pole, held in place by ParB interactions with the PopZ polarity protein [4, 21, 24, 45, 46]. At the opposite pole are both the TipN polarity protein and the terminus region of the circular chromosome of *Caulobacter crescentus* [4, 47, 48]. At the onset of cell differentiation, CtrA is degraded via the ClpXP protease system and DNA replication begins at the previously flagellated pole [49, 50]. At this time in the cell cycle, a short burst of FtsZ localization occurs at the functionalized pole, suggesting a role for FtsZ in the formation of the stalk structure [42, 43]. Following replication of *parS* sequences, two distinct ParB foci appear and begin to segregate. One ParB•*parS* complex remains at the original PopZ-containing pole, while the other ParB•*parS* complex

moves toward the opposite pole of the elongating cell [21, 25]. It is proposed that this movement is mediated by interactions with nucleoprotein polymers of ParA•ATP, which extend out from TipN at the far side of the cell [25, 35]. As ParA and ParB interact, the polymer destabilizes shrinks back toward the pole by releasing ParA monomers, bringing with it ParB•*parS* complexes [25, 33]. This interaction also dissociates ParB from *parS* and favors the formation of ParA•ADP that can bind single-stranded DNA non-specifically, though the exact role of these processes is in cell division is not fully clear [23]. It is possible that this serves to modulate chromosome segregation by inhibiting ParB•*parS* formation or DNA replication as part of a checkpoint mechanism, since ParA binding to single stranded DNA could inhibit the replication fork. Concurrent with ParB•*parS* segregation, the FtsZ assembly inhibitor MipZ begins to segregate into two foci due to a direct interaction with ParB [40]. The DNA replication machinery slowly follows the distal ParB•*parS* complex and moves to the mid-cell in a likely passive manner; thus when DNA duplication is completed, the two nascent *ter* regions will be at the pole opposite the stalk or flagellum in both cells [4, 51]. As the segregating ParB•*parS* approaches the pole, TipN dissociates from the nascent flagellated pole, and new PopZ protein begins to accumulate in its place [35, 36]. FtsZ assembly commences in the mid-cell, farthest from the two ParB•*parS* complexes at either pole where the concentration of MipZ is lowest [22, 40]. Observations that the ParA protein is often localized near the midcell after ParB•*parS* bipolar localization could suggest a role for ParA in regulating medial FtsZ assembly [21, 25]. Coincident with the invagination of the membrane and the formation of the larger divisome complex, TipN localizes to the division plane [47]. In the stalked cell compartment, CtrA is preferentially degraded so that the stalked cell may immediately recommence DNA segregation and cell division; CtrA remains active in the nascent swarmer cell compartment, suppressing

progression of the cell cycle [49]. Thus, following complete cytokinesis, both daughter cells have chromosome and polarity arrangements that are identical despite having different developmental programs: PopZ, ParB•*parS,* and *Cori* are at the functionalized cell pole (either flagellated or stalked, dependent on cell type); TipN and *ter* are at the fore-pole, which represents the most recent site of cytokinesis.

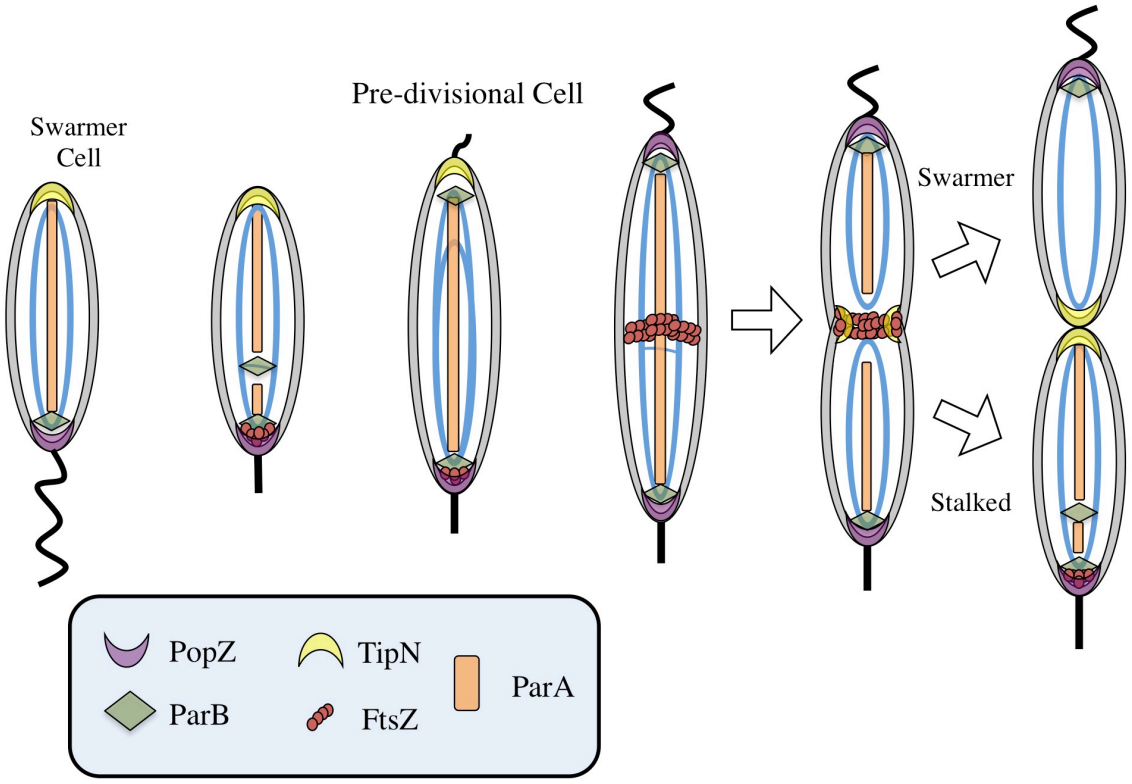

Figure 2.2: Polarity and Division in the Cell Cycle of *Caulobacter crescentus*.
This figure is an expanded version of that presented in Chapter 1 (Fig. 1.4); and a schematic representation of the events described in the most recent section of this Chapter. Polarity determinants PopZ and TipN are shown in purple and yellow, respectively; ParB is shown as a green diamond. ParA localization follows that proposed by Ptacin, *et al*. [25]. Blue lines represent the chromosomal DNA and red circles indicate assembled FtsZ, as in Figure 1.4.

References

[1] William C. Nierman, Tamara V. Feldblyum, Michael T. Laub, Ian T. Paulsen, Karen E. Nelson, Jonathan Eisen, John F. Heidelberg, M. R. K. Alley, Noriko Ohta, Janine R. Maddock, Isabel Potocka, William C. Nelson, Austin Newton, Craig Stephens, Nikhil D. Phadke, Bert Ely, Robert T. DeBoy, Robert J. Dodson, A. Scott Durkin, Michelle L. Gwinn, Daniel H. Haft, James F. Kolonay, John Smit, M. B. Craven, Hoda Khouri, Jyoti Shetty, Kriti Berry, Teresa Utterback, Kevin Tran, Alex Wolf, Jessica Vamathevan, Maria Ermolaeva, Owen White, Steven L. Salzberg, J. Craig Venter, Lucy Shapiro, and Claire M. Fraser. Complete genome sequence of *Caulobacter crescentus*. *Proc. Natl. Acad. Sci. USA* 98: 4136-4141, 2001.

[2] Bert Ely, Tracey W. Ely, Connie J. Gerardot, and Andrew Dingwall. Circularity of the *Caulobacter crescentus* chromosome determined by Pulsed-Field gel electrophoresis. *J. Bacteriol*. 172: 1262-1266, 1990.

[3] Patrick H. Viollier, Martin Thanbichler, Patrick T. McGrath, Lisandra West, Maliwan Meewan, Harley H. McAdams, and Lucy Shapiro. Rapid and sequential movement of individual chromosomal loci to specific subcellular locations during bacterial DNA replication. *Proc. Natl. Acad. Sci. USA* 101: 9257-9262, 2004.

[4] Rasmus B. Jensen. Coordination between chromosome replication, segregation and cell division in *Caulobacter crescentus*. *J. Bacteriol*. 188: 2244-2253, 2006.

[5] Keith Ireton, Nereus W. Gunther IV, and Alan D. Grossman. *spo0J* is required for normal chromosome segregation as well as the initiation of sporulation in *Bacillus subtilis*. *J. Bacteriol* 176: 5320-5329, 1994.

[6] Michaela E. Sharpe and Jeffery Errington. The *Bacillus subtilis soj-spo0J* locus is required for a centromere-like function involved in prespore chromosome partitioning. *Mol. Microbiol*. 21: 501-509, 1996.

[7] Daniel Chi-Hong Lin, Petra Anne Levin, and Alan D. Grossman. Bipolar localization of a chromosome partition protein in *Bacillus subtilis*. *Proc. Natl. Acad. Sci. USA* 94: 4721-4726, 1997.

[8] Teru Ogura and Sota Hiraga. Partition mechanism of F plasmid: two plasmid gene-encoded products and a cis-acting region are involved in partition. *Cell* 32: 351-360, 1983.

[9] Kathy A. Martin, Stanley A. Friedman, and Stuart J. Austin. Partition site of the P1 plasmid. *Proc. Natl. Acad. Sci. USA* 84: 8544-8547, 1987.

[10] Barbara E. Funnell. Mini-P1 plasmid partitioning: excess ParB protein destabilizes plasmids containing the centromere *parS*. *J. Bacteriol*. 170: 954-960, 1988.

[11] Daniel Chi-Hong Lin and Alan D. Grossman. Identification and characterization of a bacterial chromosome partitioning site. *Cell* 92: 675-685, 1998.

[12] M.A. Davis and S. J. Austin. Recognition of the P1 plasmid centromere analog involves binding of the ParB protein and is modified by a specific host factor. *EMBO J*. 7: 1881-1888, 1988.

[13] M. A. Davis, K. A. Martin, and S. J. Austin. Biochemical activities of the ParA partition protein of the P1 plasmid. *Mol. Microbiol*. 6: 1141-1147, 1992.

[14] Eugene V. Koonin. A superfamily of ATPases with diverse functions containing either classical or deviant ATP-binding motif. *J. Mol. Biol*. 229: 1165-1174, 1993.

[15] Christina M. Hester and Joe Lutkenhaus. Soj (ParA) DNA binding is mediated by conserved arginines and is essential for plasmid segregation. *Proc. Natl. Acad. Sci. USA* 104: 20326-20331, 2007.

[16] Stanley A. Friedman and Stuart J. Austin. The P1 plasmid-partition system synthesizes two essential proteins from an autoregulated operon. *Plasmid* 19: 103-112, 1988.

[17] M. Hirano, H. Mori, T. Onogi, M. Yamazoe, H. Niki, T. Ogura, and S. Hiraga. Autoregulation of the partition genes of the mini-F plasmid and the intracellular localization of their products in *Escherichia coli*. *Mol. Gen. Genet*. 257: 392-403, 1998.

[18] Jean Yves-Bouet and Barbara E. Funnell. P1 ParA interacts with the P1 partition complex at *parS* and an ATP-ADP switch controls ParA activities. *EMBO J*. 18: 1415-1424, 1999.

[19] Megan J. Davey and Barbara E. Funnell. Modulation of the P1 plasmid partition protein ParA by ATP, ADP, and P1 ParB. *J. Biol. Chem*. 272: 15286-15292, 1997.

[20] Emma Fung, Jean-Yves Bouet, and Barbara E. Funnell. Probing the ATP-binding site of P1 ParA: partition and repression have different requirements for ATP binding and hydrolysis. *EMBO J*. 20: 4901-4911, 2001.

[21] Dane A. Mohl and James W. Gober. Cell cycle-dependent polar localization of chromosome partitioning proteins in *Caulobacter crescentus*. *Cell* 88: 675-684, 1997.

[22] Dane A. Mohl, Jesse Easter, Jr., and James W. Gober. The chromosome partitioning protein, ParB, is required for cytokinesis in *Caulobacter crescentus*. *Mol. Microbiol*. 42: 741-755, 2001.

[23] Jesse Easter, Jr. and James W. Gober. ParB-stimulated nucleotide exchange regulates a switch in functionally distinct ParA activities. *Mol. Cell* 10:427-434, 2002.

[24] Rainer M. Figge, Jesse Easter, Jr., and James W. Gober. Productive interaction between the chromosome partitioning proteins, ParA and ParB, is required for the progression of the cell cycle *Caulobacter crescentus*. *Mol. Microbiol.* 47: 1225-1237, 2003.

[25] Jerod L. Ptacin, Steven F. Lee, Ethan C. Garner, Esteban Toro, Michael Eckart, Luis R. Comolli, W. E. Moerner, and Lucy Shapiro. A spindle-like apparatus guides bacterial chromosome segregation. *Nat. Cell Biol.* 12: 791-798, 2010.

[26] Conrad W. Shebelut, Jonathan M. Guberman, Sven van Teeffelen, Anastasiya A. Yakhnina, and Zemer Gitai. *Caulobacter* chromosome segregation is an ordered multistep process. *Proc. Natl. Acad. Sci. USA* 107: 14194-14198, 2010.

[27] Esteban Toro, Sun-Hae Hong, Harley H. Mcadams, and Lucy Shapiro. *Caulobacter* requires a dedicated mechanism to initiate chromosome segregation. *Proc. Natl. Acad. Sci. USA* 40: 15435-15440, 2008.

[28] Graham Scholefield, Rachel Whiting, Jeff Errington, and Heath Murray. Spo0J regulates the oligomeric state of Soj to trigger its switch from an activator to an inhibitor of DNA replication initiation. *Mol. Microbiol.* 79: 1089-1100, 2011.

[29] Heather A. Cole, J. W. T. Wimpenny, and D. E. Hughes. The ATP Pool in *Escherichia coli* I. Measurement of the pool using a modified luciferase assay. *Biochim. Biophys. Acta* 45:445-453, 1967.

[30] Quang Hon Tran and Gottfried Unden. Changes in the proton potential and the cellular energetics of *Escherichia coli* during growth by aerobic and anaerobic respiration or by fermentation. *Eur. J. Biochem.* 251: 538-543, 1998.

[31] Simon Ringgaard, Jeroen van Zon, Martin Howard, and Kenn Gerdes. Movement and equipositioning of plasmids by ParA filament disassembly. *Proc. Natl. Acad. Sci. USA* 106: 19369-19374, 2009.

[32] Edward J. Banigan, Michael A. Gelbert, Zemer Gitai, Ned S. Wingreen, and Andrea J. Liu. Filament depolymerization can explain chromosome pulling during bacterial mitosis. *PLoS Comput. Biol.* 7: e1002145, 2011.

[33] Blerta Shtylla and James P. Keener. A mathematical model of ParA filament-mediated chromosome movement in *Caulobacter crescentus*. *J. Theor. Biol.* 307: 82-95, 2012.

[34] Thomas A Leonard, P. Jonathan Butler, and Jan Löwe. Bacterial chromosome segregation: structure and DNA binding of the Soj dimer – a conserved biological switch. *EMBO J.* 24: 270-282, 2005.

[35] Whitman B. Schofield, Hoong Chuin Lim, and Christine Jacobs-Wagner. Cell cycle coordination and regulation of bacterial chromosome segregation dynamics by polarly localized proteins. *EMBO J.* 29: 3068-3081, 2010.

[36] Géraldine Laloux and Christine Jacobs-Wagner. Spatiotemporal control of PopZ localization through cell cycle-coupled multimerization. *J. Cell Biol.* 201: 827-841, 2013.

[37] Eva Nogales, Kenneth H. Downing, Linda A. Amos, and Jan Löwe. Tubulin and FtsZ form a distinct family of GTPases. *Nat. Struct. Biol.*, 5: 451-458, 1998.

[38] Ling Juan Wu and Jeff Errington. Coordination of cell division and chromosome segregation by a nucleoid occlusion protein in *Bacillus subtilis*. *Cell* 117: 915-925, 2004.

[39] Thomas G. Bernhardt and Piet A. J. de Boer. SlmA, a nucleoid-associated, FtsZ binding protein required for blocking septal ring assembly over chromosomes in *E. coli*. *Mol. Cell* 18: 555-564, 2005.

[40] Martin Thanbichler and Lucy Shapiro. MipZ, a spatial regulator coordinating chromosome segregation with cell division in *Caulobacter*. *Cell* 126: 147-162, 2006.

[41] Daniela Kiekebusch, Katharine A. Michie, Lars-Oliver Essen, Jan Löwe, and Martin Thanbichler. Localized dimerization and nucleoid binding drive gradient formation by the bacterial cell division inhibitor MipZ. *Mol. Cell* 46: 245-259, 2012.

[42] Ellen M. Quardokus, Neena Din, and Yves V. Brun. Cell cycle and positional constraints on FtsZ localization and the initiation of cell division in *Caulobacter crescentus*. *Mol. Microbiol.* 39: 949-959, 2001.

[43] Ellen Quardokus, Neena Din, and Yves V. Brun. Cell cycle regulation and cell type-specific localization of the FtsZ division initiation protein in *Caulobacter*. *Proc. Natl. Acad. Sci. USA* 93: 6314-6319, 1996.

[44] Aaron J. Kelly, Marcella J. Sackett, Neena Din, Ellen Quardokus, and Yves V. Brun. Cell cycle-dependent transcriptional and proteolytic regulation of FtsZ in *Caulobacter*. *Genes Dev.* 12: 880-893, 1998.

[45] Grant R. Bowman, Luis R. Comolli, Jian Zhu, Michael Eckart, Marcell Koenig, Kenneth H. Downing, W. E. Moerner, Thomas Earnest, and Lucy Shapiro. A polymeric protein anchors the chromosomal origin/ParB complex at a bacterial cell pole. *Cell* 134: 945-955, 2008.

[46] Gitte Ebersbach, Ariane Briegel, Grant J. Jensen, and Christine Jacobs-Wagner. A self-associating protein critical for chromosome attachment, division, and polar organization in *Caulobacter*. *Cell* 134: 956-968, 2008.

[47] Edgar Huitema, Sean Pritchard, David Matteson, Sunish Kumar Radhakrishnan, and Patrick H. Viollier. Bacterial birth scar proteins mark future flagellum assembly site. *Cell* 124: 1025-1037, 2006.

[48] Hubert Lam, Whitman B. Schofield, and Christine Jacobs-Wagner. A landmark protein essential for establishing and perpetuating the polarity of a bacterial cell. *Cell* 124: 1011-1023, 2006.

[49] Ibrahim J. Domian, Kim C. Quon, and Lucy Shapiro. Cell type-specific phosphorylation and proteolysis of a transcriptional regulator controls the G1-to-S transition in a bacterial cell cycle. *Cell* 90: 415-424, 1997.

[50] Urs Jenal and Thomas Fuchs. An essential protease involved in bacterial cell-cycle control. *EMBO J*. 17: 5658-5669, 1998.

[51] Rasmus B. Jensen, Sherry C. Wang, and Lucy Shapiro. A moving DNA replication factory in *Caulobacter crescentus*. *EMBO J*. 20: 4952-4963, 2001.

CHAPTER 3

Stimulation of the Assembly of the Cytokinetic Protein FtsZ by the Chromosome Partitioning System Protein ParA

Abstract

The *parAB*/*parS* chromosome partitioning system of *Caulobacter crescentus* is essential to the viability of the cell and is responsible for the earliest stages of chromosome segregation to opposing poles of a growing and dividing cell. Bi-polar segregation of ParB foci always precedes the mid-cell localization of FtsZ and onset of cell division [1, 2]. Previous work has shown that changes in the expression levels of either ParA or ParB results in severe cell division defects and misplacement of FtsZ rings within the cell [1, 3]. The ParB protein indirectly controls FtsZ localization through its interaction with an FtsZ inhibitor, MipZ [4, 5]. Additionally, ParB acts as a nucleotide exchange factor for ParA, which exists either bound to ATP or ADP with distinct functions depending on the bound nucleotide [6]. When conditions are present that would favor the ADP bound form, either depletion of ParB or over-expression of ParA, the cells exhibit a filamentous phenotype and reduced FtsZ ring formation [1, 3, 7]. We have hypothesized that the ATP-bound form of ParA plays a direct role in the control of cell division by regulating the assembly of FtsZ necessary for cell division. Biochemical assays using purified components were selected as the ideal means by which to test this theory, due to the essential nature of the chromosome partitioning system. Additionally, the role of ParB in the regulation of the FtsZ inhibitor MipZ could lead to phenotypically ambiguous results in cytological and genetic studies. Using four different and previously used *in vitro* assays, we have shown that ParA is a potent activator of FtsZ assembly. Furthermore, activation of FtsZ assembly requires the presence of both ATP and ParB, the nucleotide exchange factor for ParA. We propose that these experiments implicate the partitioning system of *Caulobacter crescentus*, specifically the ATP-bound form of ParA, as playing an essential role in cell division regulation.

Section 1: Purification of FtsZ, ParB, and ParA

1.1 Protein Expression in *Escherichia coli*

Caulobacter crescentus FtsZ was expressed from a pET-21a vector, provided by M. Thanbichler [4]. ParA and ParB were independently expressed as Histidine-tagged proteins from the pTrcHisB vector (Invitrogen), created by J. Easter [6]. Constructs were expressed in the *E. coli* Rosetta 2 (DE3) strain from Novagen encoding seven rare tRNA sequences [genotype: F^- *ompT* *hsdS*$_B$($r_B^-m_B^-$) *gal dcm* (DE3) pRARE2(Cam^R)]. Expression strains were grown in Luria-Bertani media, supplemented with 20 μg/mL Chloramphenicol and 50 μg/mL Ampicillin, at 37°C with 250rpm of orbital shaking. Cultures were induced during mid-log phase growth (OD_{600} = 0.5 ± 0.1) with isopropyl β-D-1-thiogalactopyranoside (IPTG) to a concentration of 500μM, and allowed to grow under the same conditions of temperature and shaking for an additional 4 hours. Induced cultures were cooled in an ice bath for 15 minutes and harvested by centrifugation at ~7000 x g, at 4°C for 15 minutes (Sorvall GS3 rotor, Sorvall RC5B centrifuge, 6,500 rpm). Induced cell pellets were homogenized and washed with the primary purification buffer (see below), and harvested again as before; at this point, cell pellets were stored at -80°C if necessary.

1.2 Purification of FtsZ

Induced, washed, and harvested Rosetta 2 (DE3) cells were suspended in the primary purification buffer supplemented with freshly added 1mM phenylmethylsulfonyl fluoride (PMSF). The primary purification buffer for FtsZ, Buffer Z1, is 25mM TRIS, 10mM $MgCl_2$, 50mM KCl, 1mM β-mercaptoethanol [β-ME], and 10% (w/v) glycerol at pH 7.9. Cells were lysed via two passages through a cooled microfluidizer (Microfluidics Corp., Model M110P-20) at 17,500 psi of applied pressure. Lysates were centrifuged at ~32,500 x g, at 4°C for 45 minutes

(Sorvall SS-34 rotor, Sorvall RC5B centrifuge, 16,500 rpm), and the supernatant was collected for subsequent work. Saturated ammonium sulfate was added to a final concentration of 27.5% (w/v) while the supernatant was slowly stirred over ice. The slurry was spun as previously done to clear lysates (~32,50 0x g, 4°C for 45 minutes), and supernatants were discarded. Precipitated FtsZ was reconstituted in a small volume of Buffer Z1 with mild rocking at 4°C, overnight, then dialyzed extensively against Buffer Z1 at 4°C. FtsZ was then loaded onto a DEAE-Sepharose column pre-equilibrated with Buffer Z1 and eluted with a gradient to 500mM KCl (Buffer Z2: 25mM TRIS, 10mM $MgCl_2$, 500mM KCl, 1mM β-ME, 10% (w/v) glycerol at pH 7.9); peak elution of FtsZ occurred at about 250mM KCl. FtsZ containing fractions were pooled, concentrated, and dialyzed heavily against FtsZ polymerization buffer ('HMK Buffer': 50mM HEPES, 10mM $MgCl_2$, 50mM KCl, 1mM β-ME, 10% (w/v) glycerol at pH 7.5). FtsZ was further purified via size exclusion chromatography using a HiLoad 16/60 column with Superdex S-200 resin (Pharmacia Biotech) in 1.5mL loads at a total protein concentration of approximately 5mg/mL, as determined by Bradford colorimetric protein assays using a bovine serum albumin (BSA) standard from Promega Life Sciences. The column was equilibrated and run with HMK Buffer at 0.5mL/min with 0.5mL fractions collected. Peak FtsZ containing fractions were pooled and concentrated. FtsZ concentration was monitored by Bradford Assay with BSA standards until it reached above 1.0mg/mL. FtsZ was adjusted to 1.0mg/mL with HMK buffer, distributed into 250μL aliquots, and snap frozen in liquid Nitrogen for storage at -80°C.

1.3 Purification of ParB

Induced, washed, and harvested Rosetta 2 (DE3) cells were suspended in the primary purification buffer supplemented with freshly added 1mM PMSF. The primary purification

buffer for ParB, Buffer B1, is 25mM TRIS, 500mM NaCl, 5mM Imidazole, 1mM β-ME, 10% (w/v) glycerol at pH 7.5. Cells were lysed via microfluidizer, and the lysates cleared by centrifugation, using identical parameters to those described for FtsZ purification. Cleared lysate was loaded onto a Ni(II)-chelated NTA-Agarose column (Qiagen) equilibrated with Buffer B1. ParB-TrcHis was purified step-wise with Buffer B2 (25mM TRIS, 500mM NaCl, 500mM Imidazole, 1mM β-ME, 10% (w/v) glycerol at pH 7.5): with major impurities eluting at 15% Buffer B2 (79mM Imidazole), and ParB-TrcHis eluted with 100% Buffer B2 (500mM Imidazole). Peak fractions were pooled, concentrated and dialyzed heavily against HMK Buffer (see FtsZ purification). Further purification was achieved by gel filtration with Superdex S-200 pre-equilibrated with HMK buffer, as described for FtsZ. Peak fractions were pooled and concentrated to around 1.0 mg/mL, monitored by Bradford Assay using BSA standards. ParB-TrcHis concentration was adjusted to 1.0mg/mL with HMK buffer, distributed into 250μL aliquots, and snap frozen in liquid Nitrogen for storage at -80°C.

1.4 Purification of ParA

Induced, washed, and harvested Rosetta 2 (DE3) cells were suspended in the primary purification buffer supplemented with freshly added 1mM PMSF. The primary purification buffer for ParA, Buffer A1, is 25mM TRIS, 500mM NaCl, 5mM Imidazole, 30μM ATP, 1mM β-ME, 10% (w/v) glycerol at pH 7.5. The presence of ATP in these buffers is in accordance with previous purifications of ParA [6]. Cells were lysed via microfluidizer, and the lysates cleared by centrifugation, using identical parameters to those described for FtsZ purification. Cleared lysate was loaded onto a Ni(II)-chelated NTA-Agarose column equilibrated with Buffer A1. ParA-TrcHis was purified in a step-wise manner with Buffer A2: 25mM TRIS, 500mM NaCl, 500mM

Imidazole, 30μM ATP, 1mM β-ME, 10% (w/v) glycerol at pH 7.5. Major impurities were eluted with 25% Buffer A2 (129 mM Imidazole), and ParA-TrcHis eluted with 100% Buffer A2 (500mM Imidazole). ParA-TrcHis was found to be extremely unstable once eluted from the Ni(II) column, with agitation, air-bubbles, time, and increased concentration causing the formation of precipitates or aggregates. The presence of imidazole had a stabilizing effect on ParA-TrcHis, extending the time before spontaneous formation of precipitates occurred, thus reducing protein loss. Therefore, ParA-TrcHis was diazlyzed heavily into a derivative of HMK buffer, HMK-I (50mM HEPES, 10mM $MgCl_2$, 50mM KCl, 200mM Imidazole, 1mM β-ME, 10% (w/v) glycerol at pH 7.5). ParA-TrcHis was further purified with size-exclusion chromatography as was described for ParB on an identical column equilibrated and run with HMK-I buffer; though a load of 0.5mL was used and total protein concentration was nearer to 500μg/mL. Peak fractions were pooled and concentrated to about 500μg/mL, as monitored by Bradford protein assay with BSA standards, the maximum apparent concentration under these conditions without precipitation and protein loss. ParA-TrcHis was distributed into 250μL aliquots, and snap frozen in liquid Nitrogen for storage at -80°C.

Section 2: Monitoring FtsZ Assembly using Light Scattering

2.1 Background

The use of monochromatic light scattering to monitor the assembly of cytoskeletal elements is a well-established technique, first employed to study the polymerization of tubulin [8, 9]. This technique has also been successfully employed in the study of FtsZ assembly in *Bacillus subtilis, Escherichia coli*, and *Caulobacter crescentus*; furthermore, many of these studies used this technique to assess the action of inhibitors and activators of FtsZ assembly [4, 10-14]. In this assay, the turbidity of the solution is measured utilizing a detector arranged at a 90°-angle from the incident light, relative to the sample being measured. The detector is tuned to the same wavelength as the incident light, so that only light scattering from assembled protein is measured. The wavelength of 350nm is utilized as this is sufficiently small to give a strong signal but not so low that fluorescent effects of protein residues would become an issue (also note that scattering intensity at any angle is inversely proportional to the wavelength of incident light) [8]. Furthermore, because polymerized protein is so much larger than the wavelength of light, turbidity is roughly proportional to the size and concentration of the rod-like polymers, and not influenced by the scattering properties related to the size and shape of protein monomers [8].

2.2 Materials and Methods

90°-angle light scattering was measured on a Fluorolog-2 Spectrofluorimeter (Photon Technologies International; London, Ontario); incident light was produced using a 75 Watt Xenon-Arc Lamp. The sample chamber was a rectangular Quartz cuvette with an internal spacing of 10mm (Starna Cells; Atascadero, CA). Scattering data was recorded every 4 seconds for 12 minutes with both Excitation and Emission set to 350nm with a 2nm bandwidth. Purified

protein components (see Section 1) were premixed to achieve a final concentration of 1μM each in a final reaction volume of 200μL, with or without the addition of 1mM ATP. ATP was added from a 100mM stock in HMK buffer (ATP powder: MP Biomedicals, Cat. #150226). The pre-mixing procedure was stepwise as follows, with 198μL as the initial volume: HMK buffer, FtsZ in HMK buffer, ParB in HMK buffer, ParA in HMK-I buffer, 2μL 100mM ATP or HMK buffer. For assays controls in which FtsZ or ParB were omitted, an appropriate amount of HMK buffer was substituted; for omissions of ParA, HMK-I buffer was substituted to control for any effects from imidazole on the experimental results. Premixed components were allowed to incubate at room temperature for 3 minutes, and then transferred to the cuvette. Background counts were recorded for 30 seconds to establish a scattering baseline. The cuvette was removed from the system and 2μL of 100mM GTP in HMK buffer was added to initiate FtsZ assembly and bring the reaction to the 200μL final volume (GTP powder: Acros Organics, Cat # 226250010); alternatively, HMK buffer was added for controls in which GTP was omitted. After this final addition, the system was gently mixed by pipetting for 5 seconds and immediately returned to the system to initiate data collection. Between assays, the cuvette was cleaned by gentle scrubbing of the insides with a cotton tipped applicator and 0.1% SDS (w/v) in water, followed by extensive water rinsing and drying with ethanol.

2.3 Results of 90°-angle Light Scattering experiments

The full set of scattering data is presented in Figure 3.1; Figure 3.2 presents just the control experiments to highlight differences discussed herein. For all presented data, the 30 seconds of background counts were averaged and subtracted from all subsequent data points for each run. Each condition presented is the averaged result of four independent experiments, normalized

with the background subtraction method prior to averaging. The normalization procedure was necessary due to the variability in initial scattering, likely due to mixing issues or the presence of particulate or air bubbles. To preserve the net changes in counts for each trial, all averages were left at the normalized value, even when less than zero. A similar graph to Figure 3.1 using averaged, but not normalized data, is presented in the Appendix of this work. All data processing and the graphical representation of data were performed with Microsoft Excel.

A clear stimulation of FtsZ assembly was observed solely in the presence of both ParA and ParB, dependent on the presence of ATP (Fig. 3.1: ◆). Under all other tested conditions FtsZ was unable to undergo GTP-stimulated assembly. No stimulation was seen in the presence of ParA and ParB proteins alone, suggesting that the stimulation of FtsZ assembly is ATP dependent and not due to molecular crowding effects (Fig. 3.1, 3.2: +, ▲). The small increase in scattering seen for ParA and ParB in the presence of ATP is likely indicative of the association involved in the ParB stimulated nucleotide exchange of ParA (Fig. 3.1, 3.2: ●). While it is possible that the large increase in scattering observed for FtsZ•GTP with ParB/ParA•ATP is due to stimulation by FtsZ of a ParA-ParB association, assay controls suggest that this is not the case. The increase in scattering observed for ParAB•ATP with FtsZ alone is comparable to scattering for ParB/ParA•ATP without FtsZ, suggesting FtsZ itself does not stimulate this association (Fig. 3.1, 3.2: ●, ×). ParA and ParB in the presence of FtsZ•GTP also shows a comparable change in scattering, suggesting that FtsZ bound to GTP does not stimulate ParA and ParB association (Fig. 3.1, 3.2: ▲).

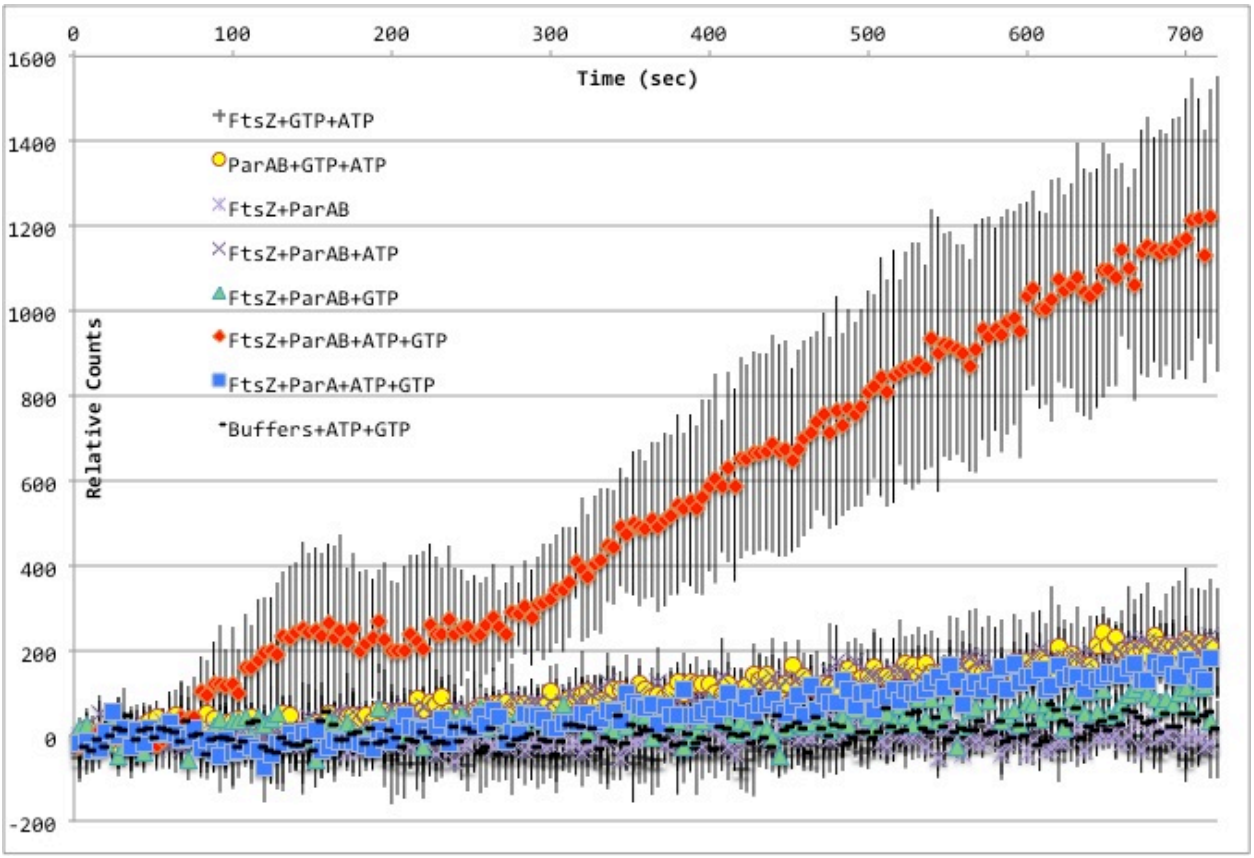

Figure 3.1: 90°-angle Light Scattering of FtsZ.
The light scattering of FtsZ under various conditions was recorded at 350nm, as measured by the relative counts of scattered light over time (X-axis, seconds). All protein components were at 1μM, ATP and GTP were at 1mM; ParAB indicates the presence of both ParA and its nucleotide exchange factor, ParB. Data and standard deviations bars shown are the result of four independent trials for each condition. Red diamonds (◆) indicate the scattering from GTP-induced FtsZ assembly in the presence of ParB/ParA•ATP. Notable controls are: GTP-induced assembly of FtsZ in the presence of ParA+ATP, without nucleotide exchange factor, ParB, thus ParA•ADP (■); GTP-induced FtsZ assembly in the presence of ParB and ParA without ATP, thus, ParA•ADP (▲); ParA-ParB nucleotide exchange of ATP [ParB/ParA•ATP] without FtsZ (●); ParA-ParB nucleotide exchange of ATP [ParB/ParA•ATP] in the presence of FtsZ (×).

It is important to note that the addition of ATP should not be required for association of ParA and ParB. Previous work has demonstrated that ParB can interact with ParA•ATP and ParA•ADP equally, acting as a nucleotide exchange factor [6]. Since ParA was purified in the presence of ATP, it is expected that all ParA is nucleotide bound when added to the assay from stocks; it is likely bound to ADP due to the intrinsic ATPase activity of the ParA protein [6].

Finally, ParA with ATP and FtsZ•GTP shows a similar change in counts to other controls over the course of the experiment (Fig. 3.1, 3.2: ■), demonstrating that activation of FtsZ assembly requires ParB to maintain ParA in the ATP bound form. Furthermore, this also suggests that FtsZ does not stimulate ParA self-association or polymerization, as might be suggested by data proposing ParA assembly [15]. Taken together, these light scattering assays clearly demonstrate that GTP induced FtsZ assembly is stimulated by the presence of ParA in the ATP-bound form (ParA•ATP).

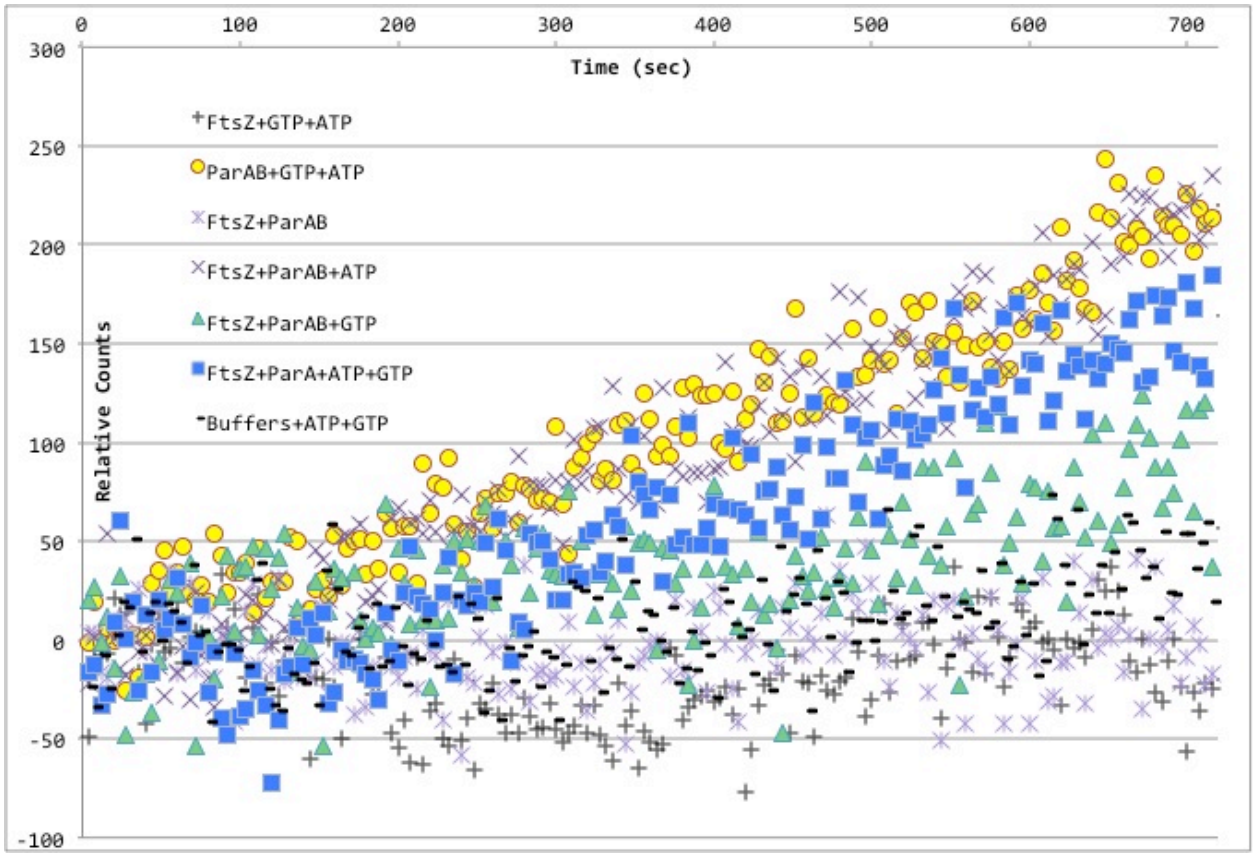

Figure 3.2: 90°-angle Light Scattering of FtsZ.
Presented here are the light scattering data from the various control experiments discussed above. These data are exactly the same as that presented in Figure 3.1. The condition of FtsZ•GTP with ParB/ParA•ATP has been omitted, and the Y-axis scale has been adjusted accordingly. For clarity, standard deviation bars shown in Figure 3.1 have been removed, due to the denseness of the data and high signal variability over this small range of counts.

Section 3: Sedimentation of Assembled FtsZ

3.1 Background

We sought to confirm and extend the results 90°-angle Light Scattering experiments following the observation that ParA in the ATP-bound form is a positive factor for assembly of FtsZ. High-speed centrifugation is another well-established technique used to monitor assembly of FtsZ. In sedimentation experiments, after a certain lag-time to allow for protein assembly following induction, protein samples are centrifuged at high speeds to separate large assembled proteins from monomers. This technique has been used to establish the critical concentration of FtsZ required for polymerization, and also to assay the effect of FtsZ assembly factors [4, 16-18]. If the scattering signal previously observed was indeed due to FtsZ•GTP assembly stimulated by ParB/ParA•ATP, then FtsZ polymers should specifically sediment. This assay is also advantageous, as it would confirm whether ParA and/or ParB assemblies induced scattering, as these would of a size that would sediment as well. Finally, using sedimentation assays, concentration dependence activation of FtsZ assembly could be established for ParB/ParA•ATP. Such a concentration dependence on activity is common among regulators of FtsZ assembly [4, 12, 17, 23].

3.2 Materials & Methods

Sedimentation assay components were premixed in polycarbonate centrifuge tubes to a final assay volume of 100μL, at the protein concentrations described for each condition below; GTP and ATP were added to 1mM final concentration when included. In controls, omitted components were substituted with their corresponding buffer, namely, HMK-I buffer in the place of ParA. Assay components were added step-wise in the same order as described for 90°-angle

light scattering experiments to an initial volume of 99μL, then allowed to incubate at room temperature for 3 minutes. After addition of 1μL of 100mM GTP or HMK buffer, samples were allowed to incubate at room temperature for 15 minutes; samples were then transferred to a pre-cooled rotor for centrifugation for 15 minutes at 4°C and ~278,000 x g (Beckmann-Coulter Optima TLX centrifuge, Beckmann-Coulter TLA-100 rotor, 80,000 rpm). Supernatants were removed and saved; 100μL of HMK buffer was added to each tube and gently mixed by pipetting to preserve the pelleted proteins. Reserved supernatants and pelleted samples were mixed with 4X-loading dye containing 200μg/mL lysozyme (USB Corp., Cleveland, OH Cat. #9001-63-2), which served as a loading control [19]. Samples were run on a denaturing 12%-acrylamide gel at 120V in tris-glycine buffer [19]. Following electrophoresis, gels were stained overnight in 1:5000 Sypro Orange (Invitrogen, Cat. # S-6650) in 7.5%(v/v) acetic acid in water, and scanned on a Pharos FX Plus imager (BioRad: Hercules, CA) with 488nm/530nm Ex/Em. FtsZ and lysozyme bands were quantified with QuantityOne software (BioRad: Hercules, CA) using identically sized rectangles. Quantification of SyproOrange stained gels was used to determine the relative concentration of FtsZ in supernatants and collected pellets. All quantifications were calculated as a relative unit of the fluorescence intensity of the FtsZ band normalized to the intensity of the corresponding loading lysozyme loading control band. This method of quantification was employed to normalize for differences in SyproOrange staining intensities between different gels. A standard curve of Lysozyme-normalized SyproOrange staining was created using known concentrations of FtsZ from six independent runs, ranging from 0-250μg/mL ($R^2 = 0.98469$, see Appendix).

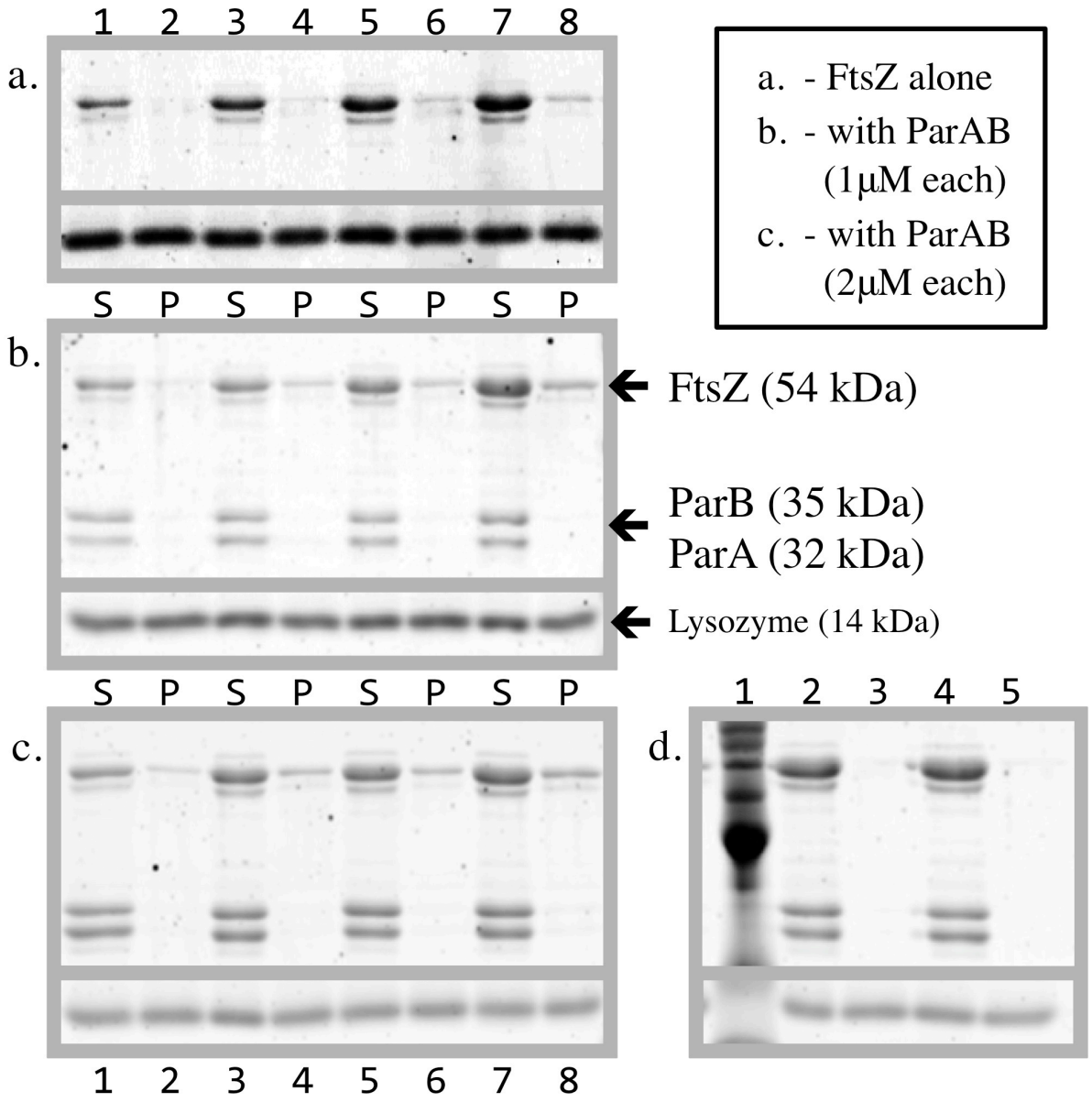

Figure 3.3: Sedimentation of FtsZ under different conditions.
Representative polyacrylamide gels from a single run of FtsZ sedimentation experiments are shown above: FtsZ alone (a), FtsZ with ParA and ParB at 1μM each, ATP at 1mM (b), FtsZ with ParA and ParB at 2μM each, ATP at 1mM (c). Supernantants and pellets from each condition are grouped and marked with S or P, respectively. Initial FtsZ concentrations are identical in gels a-c, with GTP added at 1mM to each: 50μg/mL, Lanes 1&2; 75μg/mL, Lanes 3&4; 100μg/mL, Lanes 5&6; 125μg/mL, Lanes 7&8.
(d) Gel of Control sedimentations: Initial FtsZ concentration was 125μg/mL in both conditions, ParA and ParB were at 2μM each. Lane 2&3: ATP only at 1mM. Lane 4&5: GTP only at 1mM. Lane 1 contains a protein-standard (Invitrogen, Cat # 10747).

3.3: Results of Sedimentation Assays

Sedimentation assays of pure FtsZ in the presence of GTP were used to determine the baseline of assembled FtsZ at increasing initial concentrations. A marked increase in the amount of pelleted FtsZ did not occur until the initial concentrations reached 100µg/mL (Fig. 3.3: a). Quantifications suggested that some FtsZ was collected in the pellet at lower concentrations, however, the collected FtsZ similar to the amount collected in control assays where no GTP was added (Fig. 3.3: d) suggesting that this pelleted FtsZ is representative of unfolded FtsZ or simply an artifact of the analysis.

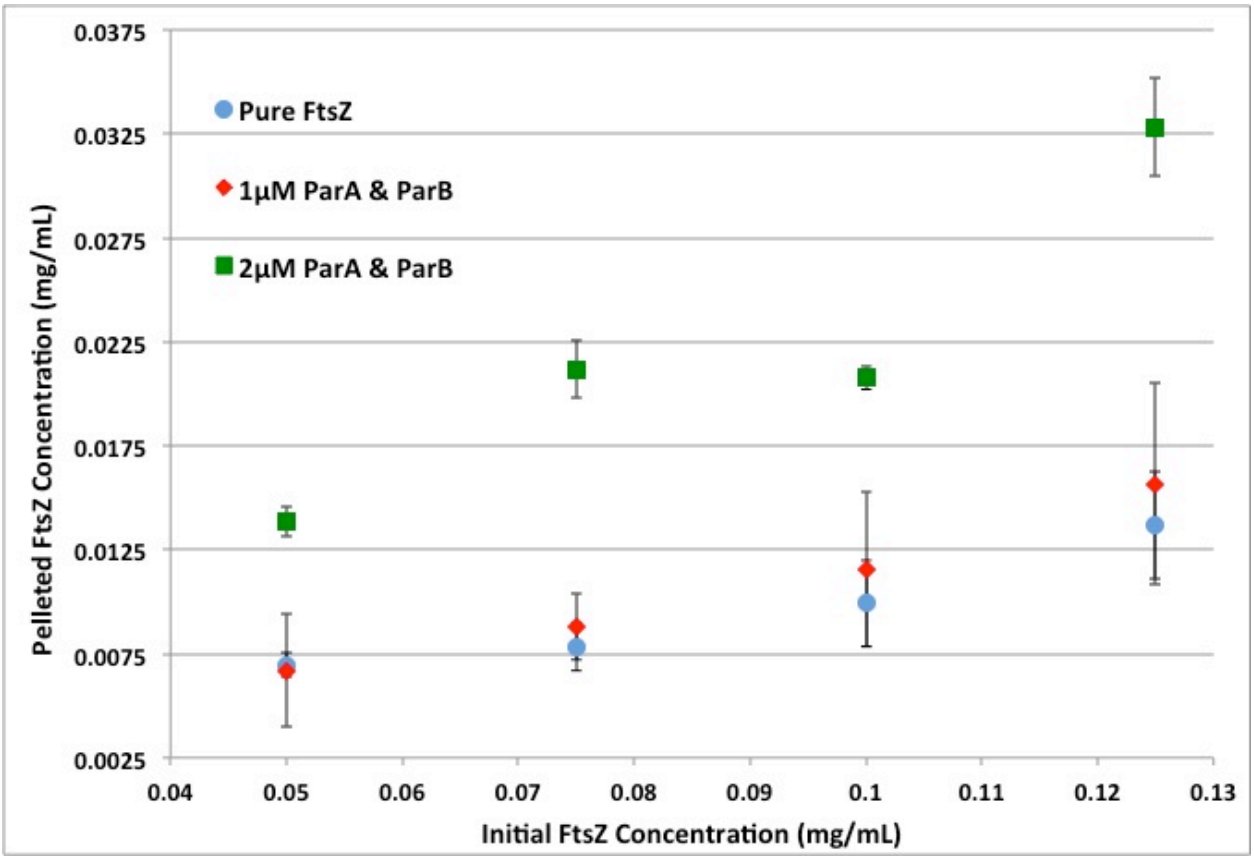

Figure 3.4: Quanitified FtsZ concentration in pellets under different conditions.
Gels were quantified by normalizing the fluorescence intensity of the FtsZ band to the intensity of the corresponding lysozyme band. Using a standard curve of FtsZ concentrations normalized in a similar manner, the amount of FtsZ collected in the pellet was determined. Data and standard deviations are the product of three trials for each condition.

In the presence of ParA, ParB, and ATP, sedimentation assays of FtsZ show a clear increase in the amount of pelleted FtsZ. Furthermore, FtsZ is observable in pellets at initial FtsZ concentrations below 100μg/mL (Fig. 3.3: b). Doubling of the ParAB-ATP concentration from 1μM to 2μM further increased the amount of FtsZ in the pellet at all initial concentrations of FtsZ (Fig. 3.3: c). Notably, ParA and ParB were not observed in the pellets suggesting that no co-sedimentation occurs between FtsZ and the ParAB proteins. This analysis is further supported by control sedimentations lacking GTP, which showed no observable FtsZ in the pellet. Finally, an additional control lacking ATP showed very little FtsZ in the pellet (Fig. 3.3: d), suggesting that increased sedimentation is nucleotide dependent and not a by product of molecular crowding effects due to the presence of additional protein species, namely ParA and ParB [20]. These results demonstrate that ParA and ParB stimulates GTP-induced FtsZ assembly, in an ATP dependent manner. Quantified amounts of FtsZ collected in the pellet are presented in Figure 3.4, produced from a minimum of three trials. This analysis demonstrates a significant increase in the quantity of pelleted FtsZ in the presence of ParA and ParB, in an ATP-dependent manner. Furthermore, these experiments show that this effect is also concentration dependent on ParA and ParB, as an increase in their concentration yielded increases in collected FtsZ. Thus, these sedimentation assays are taken as a confirmation of the initial findings of 90°-angle light scattering experiments: that ParA and ParB in the presence of ATP has a stimulatory effect on the assembly of FtsZ filaments.

Section 4: A Coupled and Continuous GTPase Assay of FtsZ

4.1 Background

Having confirmed that FtsZ assembly is stimulated in the presence of ATP-bound ParA (ParB/ParA•ATP) by two independent biochemical assays, a more mechanistic study of this interaction was sought. Sedimentation assays did not reliably quantify the lowering of the critical concentration for FtsZ assembly by ParA•ATP due to errors in the quantification method; though an increase in pelleted FtsZ at all initial concentrations was consistently observed. A GTPase assay would be an ideal experiment for such a determination as it provides quantified data that directly relates to the assembly state of FtsZ. Since the GTPase domain of FtsZ is split into two parts on a single FtsZ molecule, at minimum, a dimerization of FtsZ is required for GTP hydrolysis [21, 22]. Because our experimental system includes ParA, which has weak ATPase activity [6], an assay that quantified inorganic phosphate would be more difficult to interpret since both FtsZ and ParA activity could produce a positive signal.

A GTPase assay using the reduction of NADH as an output signal source has been used in the past to study the assembly of FtsZ [23]. In this assay, GDP produced by the GTPase activity is taken up by a two-component enzymatic system resulting in the regeneration of GTP allowing for a continuous assay, and a terminal reduction of NADH cofactor, which allows for a spectrophotometric based read-out of the rate of GDP production, and therefore, GTPase activity. The two-component system is comprised of pyruvate kinase (PK) and lactate dehydrogenase (LDH) enzymes. The pyruvate kinase reaction takes up GDP produced by the action of FtsZ, and along with phosphoenolpyruvate (PEP) supplied to the system, producing GTP and pyruvate.

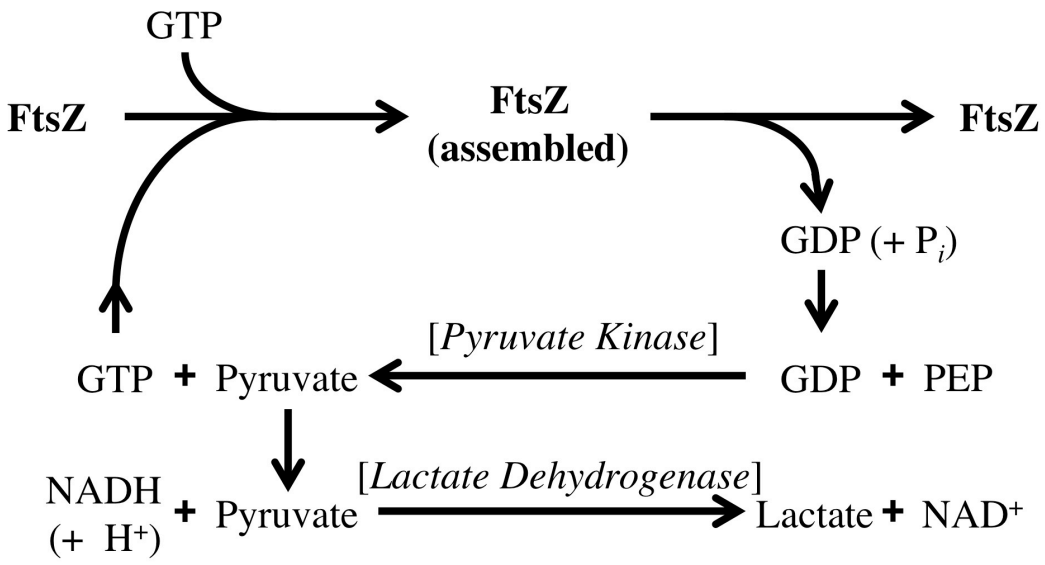

$$(n{+}1)\ \text{FtsZ} + n\ \text{GTP} \rightarrow [\text{FtsZ} \bullet \text{GTP}]_{poly} \rightarrow (n{+}1)\ \text{FtsZ} + n\ \text{GDP} + n\ P_i$$

$$n\ \text{GDP} + n\ \text{PEP} \rightarrow n\ \text{Pyruvate} + n\ \text{GTP}$$

$$n\ \text{Pyruvate} + n\ (\text{NADH} + H^+) \rightarrow n\ \text{Lactate} + n\ NAD^+$$

$$n\ \text{PEP} + n\ (\text{NADH} + H^+) \rightarrow n\ \text{Lactate} + n\ NAD^+ + n\ P_i$$

Figure 3.5: Reactions of a Coupled and Regenerative GTPase Assay.
A schematic of the three reactions comprising the GTPase assay are shown above. The stimulation of FtsZ assembly by GTP results in the hydrolysis of GTP to GDP and inorganic phosphate. GDP is consumed by pyruvate kinase and regenerated to GTP using phosphoenolpyruvate (PEP) as a phosphate donor. This GTP product is free to re-enter the polymerization and hydrolysis cycle of FtsZ assembly. The pyruvate product of the GTP-regenerative reaction is reduced to lactate using an NADH cofactor by lactate dehydrogenase. The oxidation NADH by this reaction results in a decrease in absorbance at 340nm, since the reduced form absorbs at this wavelength while the oxidized form (NAD^+) does not. Below the schematic are the chemical equations of all the components of the system. The "*n*" term is used to define stoichiometric ratios of the individual components; $[\text{FtsZ}\bullet\text{GTP}]_{poly}$ denotes assembled FtsZ polymers. Because the GTPase domain of FtsZ is divided into two parts, one additional FtsZ molecule is required for every GTPase reaction. Each released GDP is regenerated to GTP at the expense of a single PEP, resulting in a single pyruvate. This is irreversibly reduced to lactate at the expense of a single NADH. Thus, each GTPase event ultimately results in the oxidation of a singe NADH cofactor. The balanced equation of the system shows that only PEP and NADH are consumed, all other cofactors are either regenerated (GTP) or exist only as intermediates (GDP / pyruvate); therefore, PEP and NADH are the limiting reagents for this assay. The inorganic phosphate product is a result of GTP hydrolysis by FtsZ, since GTP regeneration by pyruvate kinase uses PEP as the phosphate donor.

The newly synthesized GTP molecule regenerates the initial pool so that it is not a limiting substrate in this system. The pyruvate product of the PK enzyme reaction is readily converted by lactate dehydrogenase to lactate; this conversion requires the oxidation of an NADH cofactor also supplied to the system (Fig. 3.5). The activity of this system is easily monitored by measuring absorbance since reduced NADH absorbs light at 340nm, while the oxidized form does not at this wavelength. Thus, a reduction in light absorbance at 340nm is indicative of a reduction of NADH that is stoichiometrically equivalent to GTP hydrolysis; thus, the rate of signal reduction at 340nm directly correlates to the rate of GDP production by FtsZ.

4.2 Materials & Methods

Regenerative GTPase assays were conducted in 96-well plates (Corning: flat, transparent, polypropylene; Cat #25861) with a reaction volume of 150μL, adapted from previously published methods [24]. Samples were read on a Tecan Infinite M1000 plate reader (Tecan Systems: San Jose, CA) at 340nm with absorbance readings taken every 15 seconds for 10 minutes at 25°C. Two concurrent assays were performed for each tested condition, additionally repeated three more times. A Master-Mix of all components, except FtsZ, ParA, and ParB, was prepared and distributed to two aliquots. ParA and ParB were then added to each aliquot followed by FtsZ, resulting in a final reaction volume of 200μL. From each of these reactions, 150μL was immediately removed, placed into a multi-well plate, and read as described above.

A Master-Mix (enough for two reactions) was prepared using HMK buffer, 10X pyruvate kinase (Roche, Cat # 10128155001), 10X lactate dehydrogenase (Roche, Cat # 10127876001), 40X PEP dissolved in HMK buffer (MP Biomedicals, Cat #151872), 40X NADH dissolved in HMK

buffer (MP Biomedicals, Cat# 101167), and 100X GTP and 100X ATP (same source as previous experiments). After distribution of this mix into aliquots, the 5X mixture of ParA and ParB was added to each tube, and allowed to incubate at room temperature for 5 minutes. This incubation was done to allow nucleotide exchange by ParA/ParB to form ParA•ATP. Furthermore, this incubation allowed for any ADP released by ParA or spontaneously formed GDP to be converted to GTP and ATP by pyruvate kinase. This was important since any GDP or ADP present in solution at the start of the assay could be used by pyruvate kinase, leading to a reduction in absorbance at 340nm independent of GTPase activity from FtsZ. After initial incubations, 10X FtsZ was added to each reaction aliquot, mixed briefly, and then measured as described above. Final reaction concentrations of all components were as follows: GTP and ATP at 1mM, NADH at 600μM, PEP at 1mM, pyruvate kinase at 20U/mL, and lactate dehydrogenase at 20U/mL; the concentration of FtsZ, ParA, and ParB were variable and are defined in presented data. Pyruvate kinase and lactate dehydrogenase assay amounts were calculated using manufacturer's data on activity per mg of protein (U/mg) at 25°C. These enzymes were purchased as a slurry in 3.2M ammonium sulfate, thus each reaction had a small amount of ammonium sulfate present (~64mM in final reaction); however, since this amount roughly corresponds to 0.8% (w/v) ammonium sulfate, it is not expected that this would have a significant effect on the assay system.

4.3 Results GTPase assay

As measured in this continuous GTPase assay, FtsZ assembly at 1μM in the presence of saturating GTP (1mM) lowers the absorbance at 340nm by NADH at a rate of approximately 0.0011 (AU/min). Using relationship defined by the Beer-Lambert Law (A=bεC), we can convert the rate of absorbance change directly into the rate of NADH concentration change. Using the extinction coefficient of NADH (ε = 6220 $M^{-1}cm^{-1}$), and previously described methods [24], the height of the sample solution in the multi-well plates was determined to be 0.38cm; this value corresponds to the path-length (b) in the Beer-Lambert law. Because the production of GDP by FtsZ leads to a stoichiometrically equivalent consumption of NADH, we can directly correlate the rate of NADH consumption to the rate of GDP production by FtsZ. Using these methods, the rate of GDP production by FtsZ alone at 1μM is roughly 0.47μmols/min.

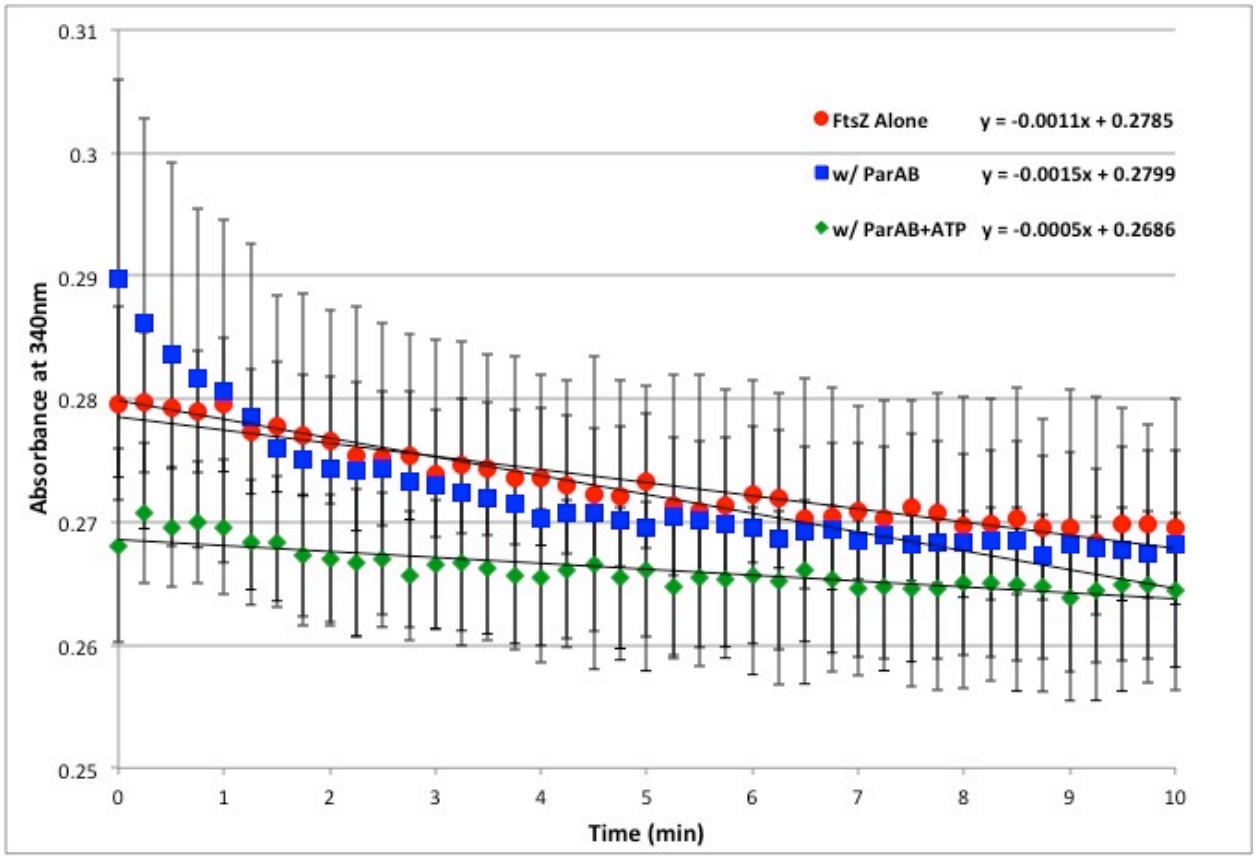

Figure 3.6 [Previous Page]: Absorbance Decrease at 340nm Under Different Conditions. Absorbance reading taken over a 10 minute period (with data acquisition every 15 seconds) is graphed for FtsZ assembly under three different conditions. The average data and standard deviations presented for each condition is the product of eight readings: two samples measured concurrently for four independent runs. Red circles represent FtsZ at 1μM in the presence of 1mM GTP. Blue squares represent FtsZ at 1μM in the presence of ParA and ParB at 1μM each, with only 1mM GTP. Green diamonds represent FtsZ at 1μM in the presence of ParA and ParB at 1μM each, with both GTP and ATP at 1mM. Linear trendlines were fit to the data using Microsoft Excel; the corresponding linear equations are shown next to the appropriate condition as part of the symbol legend in the top-right of the graph.

Surprisingly, in the presence of ATP-bound ParA (ParB/ParA•ATP), the rate of GDP production was not significantly altered. Based on our previous findings that ParA•ATP stimulated FtsZ assembly, we assumed that the likely outcome of these experiments would be an increase in the rate of GDP production by FtsZ. Since increasing FtsZ assembly should bring together more FtsZ monomers, the extent of GTP hydrolysis should increase as well. Strictly speaking, an increase in the rate of GTP hydrolysis may still be occurring in the presence of ParA•ATP. This assay relies on the release of GDP in order to initiate the metabolic cascade that results in the reduction of NADH, which ultimately produces the output signal of the assay. While it is assumed that the rate of NADH consumption is directly correlated to the GTPase rate of FtsZ, a more accurate description of the relationship would be that the rate of NADH consumption is directly correlated to the rate of GDP turnover. Thus, if the process of nucleotide exchange (GDP for GTP) by FtsZ were hindered by ParA•ATP, then the rate of NADH consumption would be slowed, independent of any changes to the rate of GTP hydrolysis by FtsZ. One possibility is that ParA•ATP is acting to stabilize FtsZ filaments or perhaps creating a nucleation complex. Both of these scenarios would increase filament formation, consistent with the results of light scattering and sedimentation assays; furthermore, either stabilized filaments or the formation of a nucleation complex would result in an apparent decrease in the GTPase rate by this assay

because filaments would be less able to break apart into monomers, allowing for GDP release. A similar decrease in the rate of GTP hydrolysis by FtsZ has been observed in the presence of filament stabilizing factors SepF, and FzlA [12, 14].

Finally, it is important to note that the conclusions that can be drawn from this assay are somewhat limited. A clear issue with this assay as performed is the very small rates of change in absorbance as well as the relatively high variability in initial absorbance values as well as variablility in readings throughout the assay time course. The result of this, coupled with variability in readings throughout the time course, is a rather large standard deviation of values that spans absorbance readings of all 3 tested conditions. In the appendix of this work, individual rate graphs of the three tested conditions are provided showing the average readings of each trial pair, as well as the average absorbance of all eight readings shown in Figure 3.6. These graphs show that all three conditions had an equivalent range of initial absorbance values; therefore this issue is likely intrinsic to the assay as performed and not a result of mechanistically important events. Figure 3.7 shows the average rate of change in absorbance for all three conditions. The average was obtained by applying a linear regression to all eight individual absorbance runs for each condition using the Microsoft Excel program; the individual rates were then used to produce the average rate and standard deviation for each condition shown in the figure. Though variability is still clearly an issue, it does not span the range of values to the same extent as is seen for the data presented in Figure 3.6. The advantage of this analysis is that it does not incorporate the variability in initial absorbance as it only looks at the rate of change for each run.

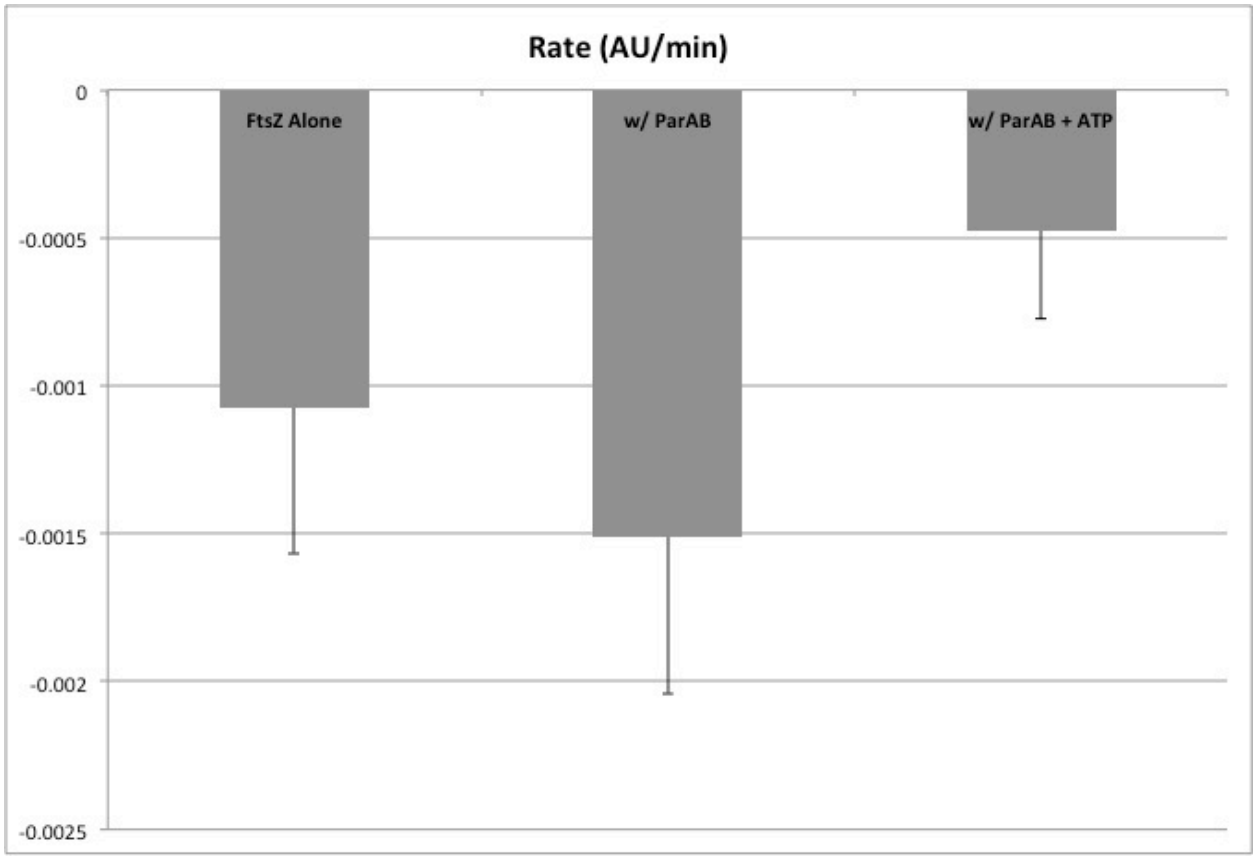

Figure 3.7: Average Rate of Change in Absorbance at 340nm.
Raw absorbance data collected for each individual run (four independent trials for each condition, two runs for each trial) was graphed over time and a linear trendline applied using Microsoft Excel. The individual rates for each run were then averaged, and a standard deviation calculated, for each condition. The average rate and standard deviation of the eight runs for each condition tested are presented in the bar graph above.

Further work with GTPase assays is clearly still required in order to get a clear picture of the mechanism of ParA•ATP stimulation of FtsZ assembly. This continuous and coupled assay may yet provide interesting answers, but must be approached differently in order to achieve significant results. One course of action would be to preform all assays individually in a single cuvette spectrophotometer. This would be advantageous as absorbance readings could be measured before the addition of FtsZ, which would allow for normalization of all data to initial absorbance readings for each run. Additionally, higher concentrations of FtsZ could be used to increase the rate of GDP production and NADH consumption. If ParA•ATP does in fact slow the

rate of GDP production as proposed here, then such an effect should still be apparent at higher concentrations of FtsZ as well. Alternatively, other GTPase assay could be employed. Analysis of the GTPase rate of FtsZ using radiolabelled GTP is a well-established technique, and would provide data independent of GDP release or nucleotide exchange, or any ATPase activity of ParA. Additionally, the rate of nucleotide exchange could be directly measured using fluorescent analogs of GTP such as mant-GTP; such experiments have been previously used to understand exchange dynamics in FtsZ from *M. jaanaschii* and have shown that FtsZ-bound nucleotide is stabilized against exchange with free nucleotide when FtsZ is assembled [25].

Section 5: Visualization of FtsZ filaments via Transmission Electron Microscopy

5.1: Background

Following the surprising results of the GTPase assay, suggesting that ATP-bound ParA has little effect on the production of GDP by FtsZ, we decided that it was necessary to directly visualize the formation of FtsZ filaments. If ParA•ATP indeed stimulates FtsZ assembly, then filaments should be seen at very low concentrations of FtsZ only in the presence of ParB/ParA•ATP. This would serve to confirm the conclusions drawn from the results of light scattering and sedimentation assays. Furthermore, by visualizing FtsZ filaments at higher concentrations, with and without ParB/ParA•ATP, it might be possible to discern some mechanism of ParA•ATP action. If ATP-bound ParA acts as a nucleator of assembly, it would be likely that more filaments of shorter length would be observed due to an increase in the number of nucleating FtsZ dimers, as proposed by Erickson *et al*. [23]. Alternatively, if ParA•ATP serves to stabilize filaments from breakdown into monomers, then we might expect to see an increase in the number and length of assembled FtsZ structures. A third possibility, consistent with previous data, is that ParA•ATP bundles assembled FtsZ; this too would be observable as there should be an increase in grouped and clumped filaments in the presence of ParB/ParA•ATP. Transmission electron microscopy (TEM) has a long history of success in visualizing fine structures, and has been regularly used to observe filament formation of FtsZ from a number of bacterial species, including *Caulobacter crescentus* [4, 26, 27]. Furthermore, transmission electron microscopy has been previously used to observe the effects of apparent stimulators of FtsZ assembly, making it an ideal and proven technique for our purposes [12, 14].

5.2: Materials & Methods

Prior to protein sample preparation, copper transmission electron microscope grids with a 300 mesh (Cat # IGC300: Ted Pella, Inc., Redding, CA) were coated with parlodion, followed by a coating of graphite. Coated grids were then subjected to ionizing radiation to create a hydrophilic surface. Samples of FtsZ at different concentrations in the presence or absence of ParA and ParB with ATP were prepared in 100μL reaction volumes. Components were added step-wise in the following order from sources previously described: buffer HMK, FtsZ, ParB, ParA, and ATP (to a total volume of 99μL). All protein component concentrations were variable and are listed with corresponding images below; ATP and GTP were present at a final concentration of 1mM each when added. In conditions where ParA was omitted, and equivalent volume of HMK-I buffer was added to account for any effects of imidazole. After all components were mixed, the samples were allowed to incubate at room temperature for 3 minutes to allow for nucleotide exchange by ParA. Following incubation, 1μL of 100mM GTP was added to the reaction to initiate FtsZ assembly and mixed gently by pipetting; samples were allowed to incubate for an additional 3 minutes at room temperature to allow for assembly. A small aliquot (10μL) was removed and placed onto pre-treated copper TEM grids and allowed incubate for 2 minutes. Buffer was wicked away and sample coated grids were stained with 4 rounds of 10μL additions of 1% (w/v) uranyl acetate in water; stained grids were dried in a sealed desiccator overnight. Grids were visualized using a Hitachi H-7000 electron microscope (Hitachi, Ltd.: Tokyo, Japan) at 50,000X magnification. Images were recorded with a 2.5 second exposure onto Kodak 4489 Electron Microscope film (Cat# 161 3108). Film was developed in Kodak D19 (Cat #146 4593) and standard fixer (Cat# 197 1746) according to manufacturers instructions. Developed films were scanned on an Epson Expression 1680 scanner. Brightness and contrast only were adjusted for

visability using Adobe Photoshop; resulting images were cropped and annotated with the same program.

5.3: Electron Microscopy of Assembled FtsZ

Micrographs taken from conditions where initial FtsZ concentration was held at 400nM, expected to be below the critical concentration for assembly, are nearly completely devoid of discernable structure (Fig. 3.8: A-D). Occasional filaments were observed, but these were in general short and straight (Fig. 3.8: D). By contrast, the introduction of ParA and ParB consistently shows FtsZ filaments (Fig. 3.8: E-H). A clear increase in the number of observable filaments can be seen in all the grid regions observed. In addition to an increase in number, many filaments are also of considerable length: sometimes surpassing 100nm (Fig. 3.8: F, H), which is near the average length for FtsZ filaments formed above the critical concentration [reviewed in 28]. It is also notable that the filaments observed with ParA and ParB present are rather curved compared to the occasional filament formed with FtsZ alone at these concentrations.

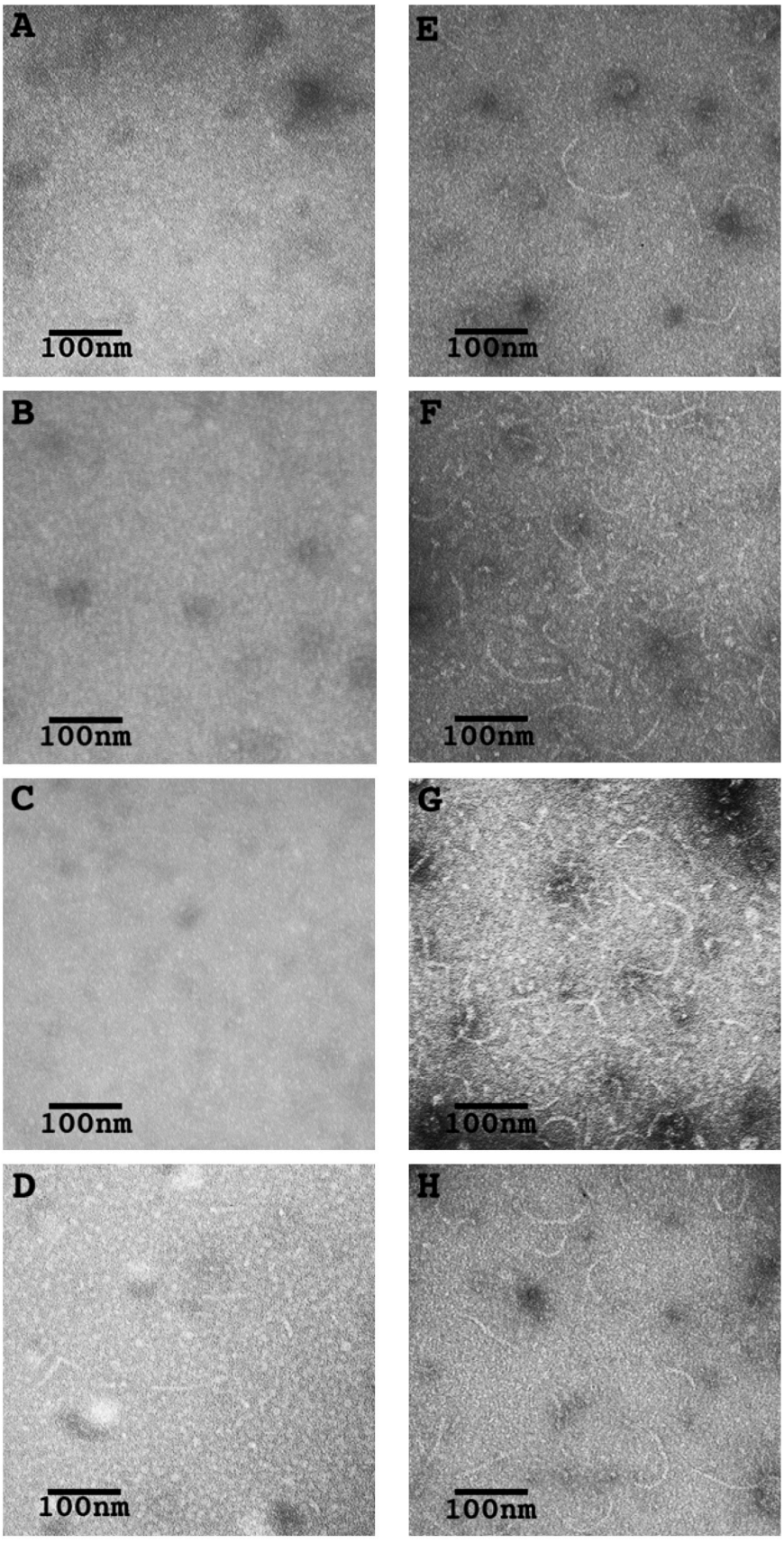
A
100nm
E
100nm
B
100nm
F
100nm
C
100nm
G
100nm
D
100nm
H
100nm

Figure 3.8 [Previous Page]: FtsZ Filaments Formed at 400nM.
Electron micrographs of assembled FtsZ alone (A-D) or in the presence of ParA and ParB with ATP (E-H). FtsZ was at 400nM; ParA and ParB were at 800nM each; ATP and GTP were added at 1mM each. Images were taken at 50,000X magnification, scale bars equivalent to 100nm are given for reference. Each image shown covers approximately 20% of the original electron micrograph; original images are provided in the appendix of this work.

FtsZ assembly was next monitored at 750nM, a concentration near the expected critical concentration for filamentation. FtsZ readily formed abundant filaments under the conditions used (Fig. 3.9: A-D). In general, these filaments appeared to be straight, with the occasional filaments showing slight curvatures. Filaments ranged in length from less than 20nm to the occasional filament in excess of 200nm. The average filament length was around 80nm, and the distribution of measured filaments can be seen in Figure 3.10. Overall, however, the majority of filaments appear to be in the range of 50-100nm, and are roughly straight. The introduction of ParA, ParB, and ATP had a surprising effect on the observed filaments. The number of observed filaments seemed to decrease in the presence of the ParAB proteins (Fig. 3.8: E-H). Despite an apparent decrease in the number of filaments, the overall length increased dramatically. The average length of quantified filaments increased to over 150nm, almost double the average length of pure FtsZ. The smallest observed filament was around 60nm in the presence of ParB/ParA•ATP, quite close to the average length of filaments observed when pure FtsZ was assembled; furthermore, a relatively large population of filaments are in excess of 200nm as compared to FtsZ assembly alone (Fig. 3.9). Another dramatic difference between the conditions is the extent of the filament curvature in the presence of ParB/ParA•ATP. The majority of filaments show some degree of curvature when ParB/ParA•ATP is present; occasionally, filaments seem to completely curve back onto themselves to form a circle, though the resolution is insufficient to determine if these filaments indeed form closed loops (Fig. 3.8: G, H).

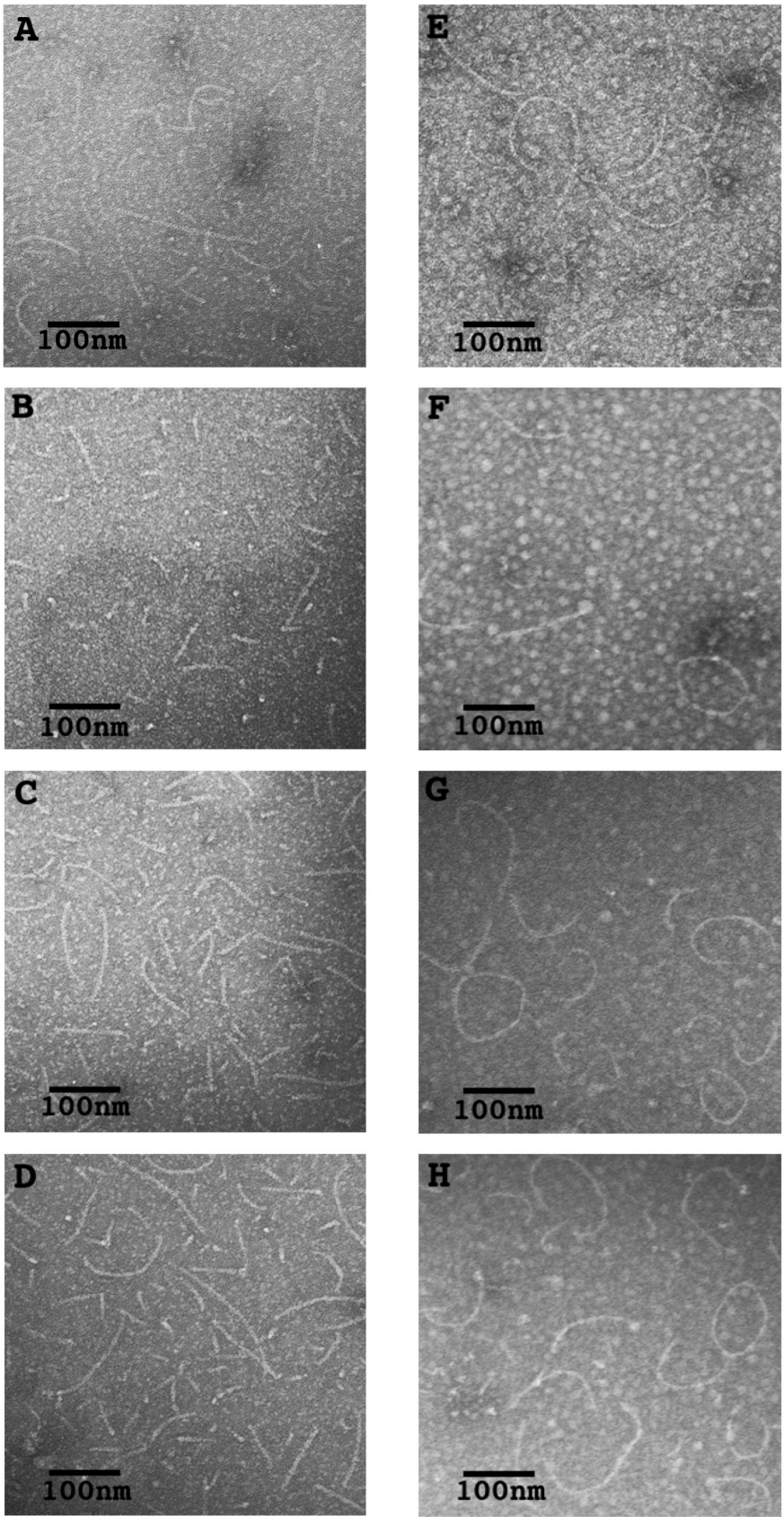
A
100nm
E
100nm
B
100nm
F
100nm
C
100nm
G
100nm
D
100nm
H
100nm

Figure 3.9 [Previous Page]: FtsZ Filaments Formed at 750nM.
Electron micrographs of assembled FtsZ alone (A-D) or in the presence of ParA and ParB with ATP (E-H). FtsZ was at 750nM; ParA and ParB were at 1.5μM each; ATP and GTP were added at 1mM each. Images were taken at 50,000X magnification, scale bars equivalent to 100nm are given for reference. Each image shown covers approximately 20% of the original electron micrograph; original images are provided in the appendix of this work.

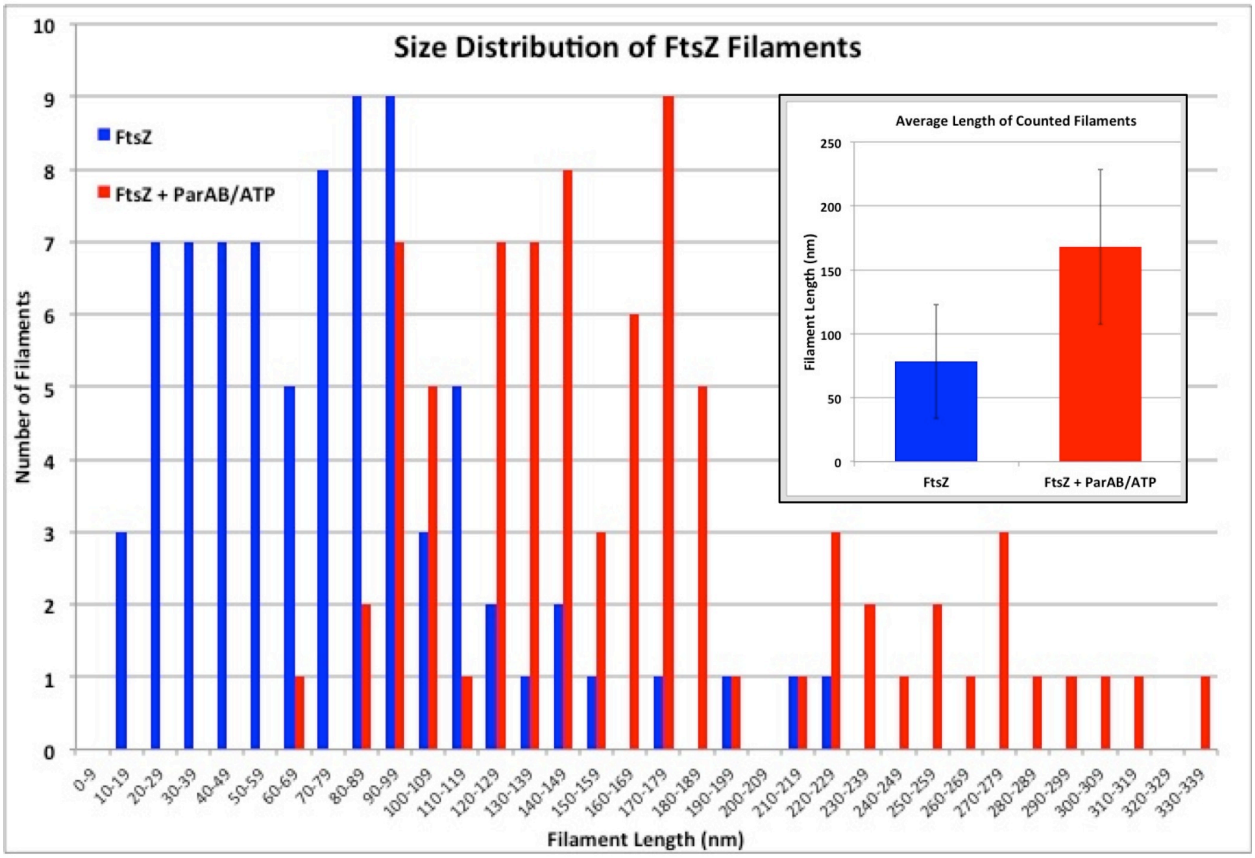

Figure 3.10: Quantification of FtsZ Filament Length.
Raw scanned images were used for quantifications (see appendix). Filaments were measured using the "Segmented Line" tool of ImageJ and subsequently converted to length in nanometers using the scanned picture resolution of 236.22 pixels/cm, and the picture scale of 100nm = 0.5cm. For each condition at total of 80 filaments were measured. The inset graph in the upper right corner shows the average length and standard deviation of all 80 measured filaments for both conditions.

ImageJ: Schneider , C.A., Rasband, W.S., and Eliceiri, K.W. NIH Image to ImageJ: 25 years of image analysis. *Nature Methods* 9: 671-675, 2012.

References

[1] Dane A. Mohl and James W. Gober. Cell cycle-dependent polar localization of chromosome partitioning proteins in *Caulobacter crescentus*. *Cell* 88: 675-684, 1997.

[2] Esteban Toro, Sun-Hae Hong, Harley H. Mcadams, and Lucy Shapiro. *Caulobacter* requires a dedicated mechanism to initiate chromosome segregation. *Proc. Natl. Acad. Sci. USA* 40: 15435-15440, 2008.

[3] Dane A. Mohl, Jesse Easter, Jr., and James W. Gober. The chromosome partitioning protein, ParB, is required for cytokinesis in *Caulobacter crescentus*. *Mol. Microbiol.* 42: 741-755, 2001.

[4] Martin Thanbichler and Lucy Shapiro. MipZ, a spatial regulator coordinating chromosome segregation with cell division in *Caulobacter*. *Cell* 126: 147-162, 2006.

[5] Daniela Kiekebusch, Katharine A. Michie, Lars-Oliver Essen, Jan Löwe, and Martin Thanbichler. Localized dimerization and nucleoid binding drive gradient formation by the bacterial cell division inhibitor MipZ. *Mol. Cell* 46: 245-259, 2012.

[6] Jesse Easter, Jr. and James W. Gober. ParB-stimulated nucleotide exchange regulates a switch in functionally distinct ParA activities. *Mol. Cell* 10: 427-434, 2002.

[7] Rainer M. Figge, Jesse Easter, Jr., and James W. Gober. Productive interaction between the chromosome partitioning proteins, ParA and ParB, is required for the progression of the cell cycle *Caulobacter crescentus*. *Mol. Microbiol.* 47: 1225-1237, 2003.

[8] Felicia Gaskin and Charles R. Cantor. Turbidimetric studies of the *in Vitro* assembly and disassembly of porcine neurotubules. *J. Mol. Biol.* 89: 737-758, 1974.

[9] Albrecht Wegner and Jeurgen Engel. Kinetics of the cooperative association of actin to actin filaments. *Biophys. Chem.* 3: 215-225, 1975.

[10] David Bramhill and Chris M. Thompson. GTP-dependent polymerization of *Escherichia coli* FtsZ protein to form tubules. *Proc. Natl. Acad. Sci. USA* 91: 5813-5817, 1994.

[11] Amit Mukherjee and Joe Lutkenhaus. Analysis of FtsZ assembly by light scattering and determination of the role of divalent metal cations. *J. Bacteriol.* 181: 823-832, 1999.

[12] Jay Kumar Singh, Ravindra D. Makde, Vinay Kumar, and Dulal Panda. SepF increases the assembly and bundling of FtsZ polymers and stabilizes FtsZ protofilaments by binding along its length. *J. Biol. Chem.* 283: 31116-31124, 2008.

[13] Laura B. Ruiz-Avila, Sonia Huecas, Marta Artola, Albert Vergoñós, Erney Ramírez-Aportela, Emilia Cercenado, Isabel Barasoain, Henar Vásquez-Villa, Mar Martín-Fontecha, Pablo Chacón, María L. López-Rodríguez, and José M. Andreu. Synthetic inhibitors of bacterial cell division targeting the GTP-binding site of FtsZ. *ACS Chem. Biol*. 8: 2072-2083, 2013.

[14] Erin D. Goley, Natalie A. Dye, John N. Werner, Zemer Gitai, and Lucy Shapiro. Imaging-based identification of a critical regulator of FtsZ protofilament curvature in *Caulobacter*. *Mol. Cell* 39: 975-987, 2010.

[15] Jerod L. Ptacin, Steven F. Lee, Ethan C. Garner, Esteban Toro, Michael Eckart, Luis R. Comolli, W. E. Moerner, and Lucy Shapiro. A spindle-like apparatus guides bacterial chromosome segregation. *Nat. Cell Biol*. 12: 791-798, 2010.

[16] Amit Mukherjee and Joe Lutkenhaus. Dynamic assembly of FtsZ regulated by GTP hydrolysis. *EMBO J*. 17: 462-469, 1998.

[17] Daniel P. Haeusser, Rachel L. Schwartz, Alison M. Smith, Michelle Erin Oates, and Petra Anne Levin. EzrA prevents aberrant cell division by modulating assembly of the cytoskeletal protein FtsZ. *Mol. Microbiol*. 52: 801-814, 2004.

[18] Cynthia A. Hale, Diasuke Shiomi, Bing Liu, Thomas G. Bernhardt, William Margolin, Hironori Niki, and Piet A. J. de Boer. Identification of *Escherichia coli* ZapC (YcbW) as a component of the division apparatus that binds and bundles FtsZ polymers. *J. Bacteriol*. 193: 93-1404, 2011.

[19] J. Sambrook, E. F. Fritsch, and T. Maniatis. Molecular cloning: a laboratory manual – 2nd Ed. *Cold Spring Harbor Laboratory Press*: Vol. 3: Chapter 18, 1989.

[20] Germán Rivas, Javier A. Fernández, and Allen P. Minton. Direct observation of the enhancement of noncooperative protein self-assembly by macromolecular crowding: indefinite linear self-association of bacterial cell division protein FtsZ. *Proc. Natl. Acad. Sci. USA* 98: 3150-3155, 2001.

[21] Jan Löwe and Linda A. Amos. Crystal structure of the bacterial cell-division protein FtsZ. *Nature* 391: 203-206, 1998.

[22] Yaodong Chen, Keith Bjornson, Sambra D. Redick, and Harold P. Erickson. A rapid fluorescence assay for FtsZ assembly indicates cooperative assembly with a dimer nucleus. *Biophys. J*. 88: 505-514, 2005.

[23] Yaodong Chen, Sara L. Milam, and Harold P. Erickson. SulA inhibits assembly of FtsZ by a simple sequestration mechanism. *Biochemistry* 51: 3100-3109, 2012.

[24] Elena Ingerman and Jodi Nunnari. A continuous, regenerative coupled GTPase assay for dynamin-related proteins. *Methods Enzymol*. 404: 611-619, 2005.

[25] Sonia Huecas, Claudia Schaffner-Barbero, Wanius García, Hugo Yébenes, Juan Manuel Palacios, José Fernando Díaz, Margarita Menéndez, and José Manuel Andreu. The interactions of cell division protein FtsZ with guanine nucleotides. *J. Biol. Chem.* 282: 37515-37528, 2007.

[26] Amit Mukherjee and Joe Lutkenhaus. Guanine nucleotide-dependant assembly of FtsZ into filaments. *J. Bacteriol.* 176: 2754-2758, 1994.

[27] Chunlin Lu, Mary Reedy, and Harold P. Erickson. Straight and curved conformations of FtsZ are regulated by GTP hydrolysis. *J. Bacteriol.* 182: 164-170, 2000.

[28] Harold P. Erickson, David E. Anderson, and Masaki Osawa. FtsZ in bacterial cytokinesis: cytoskeleton and force generator all in one [Review]. *Microbiol. Mol. Biol. Rev.* 74: 504-528, 2010.

CHAPTER 4

Concluding Remarks

Introduction

The coordination of cell division with the other core events of the cell cycle is essential to maintain the viability of a species. The oligotrophic and gram-negative α-proteobacteria, *Caulobacter crescentus*, is an ideal organism for the study of cell cycle linked events due to its biphasic life cycle and assymetric cell division. The primary engine of cytokinesis in bacteria is the highly conserved FtsZ protein, found to be essential in nearly every bacterial species studied to date. Like its eukaryotic homologue, tubulin, FtsZ monomers quickly assemble into linear filaments in the presence of GTP; assembly into filaments at the division plane is one of the first events of cell division and essential to the occurrence of any subsequent cell division processes. Bacteria have developed a diverse array of mechanisms that control FtsZ assembly spatially, temporally, and even in response to changing environmental conditions. The first chapter of this dissertation provides an in depth look at the FtsZ protein as well as a review of the many systems employed to regulate FtsZ assembly.

With this work, it is proposed that *Caulobacter crescentus* may employ proteins associated with chromosome partitioning as part of its regulation of FtsZ assembly. The chromosome partitioning system of *C. crescentus* is comprised of three core components, each essential to the viability of the cell. The first component is a small sequence chromosomally encoded of DNA, *parS*, found at multiple sites near the origin of replication; the *parS* sequence is specifically bound by the protein ParB. Binding of ParB to *parS* is regulated by the third conserved component, ParA, a weak ATPase protein with differing functions based on its nucleotide bound state. Previous work has shown that changes to the intracellular levels of either ParA or ParB results in an impairment of cell division, including the inhibition of FtsZ assembly at the mid-

cell. The second chapter of this dissertation reviews the ParAB/*parS* chromosome partitioning system of *C. crescentus* and the previous data that has connected this system to cytokinetic events.

In order to further study the link between chromosome partitioning and cell division, biochemical assays *in vitro* were used to directly analyze the effects of the partitioning proteins ParA and ParB on the assembly of FtsZ. The successful *in vitro* analysis of FtsZ assembly in the presence of effector proteins is well established in the literature. In the third chapter of this dissertation, data is presented showing that the ParA protein stimulates the assembly of FtsZ. Furthermore, this stimulation of assembly appears to require that ParA be bound to ATP, consistent with the previously demonstrated nucleotide-dependent multi-functionality of ParA.

Results

Using light scattering assays, ParA stimulation of FtsZ assembly was observed, dependent on both ATP and its nucleotide exchange factor, ParB. FtsZ assembly was monitored near its expected critical concentration of 1μM, and under the presented assay conditions, FtsZ alone with GTP produced little change in the scattering counts. There was no discernable increase in counts under any tested conditions except when ParA, ParB and, ATP were all supplied. This dependence on all three components suggests that ParA in the ATP-bound state (ParA•ATP) is responsible for this stimulatory effect. This proposal seems reasonable since ParA is purified in the ADP-bound form, and requires both an excess of ATP and the nucleotide exchange factor, ParB, for stimulation of assembly. Sedimentation by ultracentrifugation confirmed that FtsZ assembly was stimulated in the presence of ParA, ParB, and ATP. ParA•ATP was capable of

lowering the apparent critical concentration for assembly, showing increased pelleted FtsZ at all initial FtsZ concentrations. Furthermore, this assay showed that stimulation by ParA•ATP is concentration dependent, showing increased pelleted FtsZ at higher concentrations of ParA and ParB. Using these two well-established biochemical assays, it is clearly demonstrated that ParA in the ATP bound form behaves as an activator of FtsZ assembly: it stimulates formation of FtsZ filaments and lowers the apparent critical concentration for assembly.

Following these results, further quantification of the effect of ParA•ATP was sought by looking at the GTPase rate of assembled FtsZ. A continuous and regenerative GTPase assay was selected, that has been previously used to study the effect of the inhibitor, SulA, on FtsZ assembly. It was initially theorized that increased assembly should stimulate GTPase events by FtsZ, and therefore we should see an increase in activity in the presence of ParA, ParB, and ATP (ParA•ATP). Surprisingly, ParA•ATP seemed to have little effect on the GTPase rate of FtsZ. This is somewhat counterintuitive, since increased FtsZ assembly would increase the number of functional GTPase domains. This result may be a particular product of the assay employed, which requires the release of the GDP after hydrolysis in order to produce the assay signal. Thus, this assay is more accurately an assay of the rate of GDP production, which comprises both the rate of GTP hydrolysis and the rate of nucleotide exchange or release with the surrounding media. These results are still informative, however, since a reduced rate of GDP production could indicate the FtsZ filaments are not depolymerizing or exchanging hydrolysis products with the external pool of nucleotide. The differing effects of ParA and ParB with and without ATP is in keeping with the sedimentation and light scattering assays, and suggests that relevant effects maybe occurring, though not in statistically significant amount as measured.

Finally, direct visualization of FtsZ filaments was performed, with and without ParA•ATP, using transmission electron microscopy. Electron micrographs of FtsZ at a concentration expected to be well below the critical concentration for assembly (400nM) showed little discernable filament formation. However, in the presence of ParB/ParA•ATP, there was a dramatic increase in the number of observable filaments, confirming our other results showing that ParA•ATP stimulated FtsZ assembly. Additionally, we looked at FtsZ assembly at concentrations near the critical concentration to gain insight into the mechanism by which ParA•ATP stimulates assembly. It was expected that if ParA•ATP were acting as a nucleator of FtsZ filament formation an increase in the number of filaments, resulting from an increase in the number of filament starting points, would likely be observed. When polymerized alone at 750nM, FtsZ readily formed into filaments of about 85nm in length, on average. The majority of the filaments were essentially straight, occasionally showing some curvature. The filaments formed in the presence of ParA•ATP were extremely long and highly curved by contrast, with an average length of over 150nm. The curvature of these filaments was striking, with many looping so extensively that they appeared to form a full circle.

The Effect of ParA•ATP on FtsZ Assembly

The data presented in this work clearly shows that ParA, in the ATP-bound form, is a potent stimulator of FtsZ filamentation in vitro, and is capable of lowering the apparent critical concentration for assembly. Surprisingly, ParA•ATP does not seem to affect the rate of GTP hydrolysis despite increasing assembly, and therefore the number of complete GTPase domains. These effects on FtsZ assembly are reminiscent to those observed for other proteins generally

considered to be involved in the stabilization and organization of FtsZ filaments as part of divisome formation. The *Bacillus subtilis* protein, SepF, directly interacts with FtsZ and stimulates its assembly by reducing the apparent critical concentration and lowering the rate of GTP hydrolysis [1-4]. Additionally, the homologous proteins ZapA (*B. subtilis*) and YgfE (*E. coli*) have similar effects on the assembly dynamics of FtsZ *in vitro*, stimulating assembly while lowering the apparent rate of GTP hydrolysis [5-7]. Notably, *Caulobacter crescentus* also has a homologue of ZapA. Fluorescent fusions to ZapA localize to the division plane early in cytokinesis, though no biochemical studies have directly addressed the effects of ZapA on the assembly of *C. crescentus* FtsZ [8]. *Caulobacter crescentus* also encodes an essential protein, FzlA, which localizes to the midcell and directly interacts with FtsZ *in vitro*; like SepF and ZapA, FzlA increases FtsZ assembly in a concentration dependent manner and reduces the rate of GTP hydrolysis [9].

All of these activators of FtsZ assembly induce striking changes to the structures of filaments when viewed by electron microscopy (EM), with variable morphological changes. ZapA causes extensive bundling of FtsZ filaments, though the bundling pattern generally appears to be irregular [5-7]. SepF by contrast, induces the lateral bundling of FtsZ filaments into large tube-like structures, similar to the microtubules formed by tubulin. SepF alone forms ring structures with a diameter of about 50nm, suggesting that SepF provides a scaffold for the lateral association of FtsZ filaments to form a tube structure [4, 10]. Recent work has shown that SepF can associate with liposomes and may act as mediator of FtsZ contacts with the cell membrane; these findings coupled with the structures observed *in vitro* have implicated SepF as playing a role in membrane invagination in *Bacillus subtilis* [11]. The *C. crescentus* protein FzlA induces

the formation of circular FtsZ filaments and larger helical structures [9]. Though ParA•ATP clearly induced filamentation at low FtsZ concentrations, it did not appear to bundle filaments in any obvious way. The overall lengthening and induced curvature suggests that FtsZ filament reshaping of some sort may be occurring. It should be noted that the FtsZ concentration used in our EM studies was considerably lower than the others discussed here. It will be informative to continue on with these studies at still higher concentrations of proteins to see if regular filament patterns emerge.

ParA is a member of a large group of ATPase proteins that contain deviant Walker-A motifs. Notable members of this putative family of proteins are MinD (*E. coli*, *B. subtilis*) and MipZ (*C. crescentus*), both inhibitors of FtsZ assembly (indirectly and directly, respectively) as part of spatial regulation mechanisms [12-15]. Furthermore, localization of MipZ in *Caulobacter crescentus* is dependent on an interaction with ParB, the nucleotide exchange factor for ParA. This places ParA in a position to be a physiologically relevant activator of FtsZ assembly: it is functionally related to two established regulators of FtsZ, shares a binding partner with a known FtsZ regulator in *Caulobacter crescentus*, and *in vitro* it behaves like a stimulator of FtsZ assembly.

The Physiological Importance of ParA-Stimulated FtsZ Assembly

One crucial question remaining is when in the cell cycle of *Caulobacter crescentus* ParA induced FtsZ assembly is important, or the stabilization of filaments necessary. Previous localization studies have shown that ParA is certainly present throughout most of the cell, even if there is no clear agreement in localization among the methods used [16, 17]. However, neither ParA

localization study has shown anything mirroring the FtsZ ring at the midcell, arguing against the sustained stabilization of FtsZ filaments as part of divisome assembly. *C. crescentus* is already known to contain two stabilizers of FtsZ filaments structures, ZapA and FzlA, both of which co-localize with FtsZ at the midcell during cell division [8]. This could suggest that ParA activation is not necessary for normal midcell assembly of FtsZ, though the loss of these FtsZ rings under non-endogenous ParA and ParB expression levels suggests otherwise [18, 19]. Thus it is possible that ParA plays a very early and transient role in stimulation of FtsZ assembly. This would agree with our EM studies that showed clear FtsZ filament formation at very low concentrations, only in the presence of ParA•ATP, and explain why no obvious co-localization with divisome structure is observed. Toward this idea of a transient interaction, our sedimentation assays did not show significant ParA in the pellet despite a clear increase in the amount of pelleted FtsZ, as is the case for stabilizers such as SepF. Furthermore, a bacterial two-hybrid screen performed on many chromosomal segregation components and FtsZ has not shown an interaction between ParA and FtsZ. Notably, this screen did not show an interaction between ParA and ParB either, but was capable of identifying the interaction of ParB with itself (unpublished results). Thus, it is possible that the interaction of ParA with FtsZ is more equivalent to the interaction of ParA with its nucleotide exchange factor ParB than it is to more stably interacting proteins such as the ParB multimerization on *parS* sequences. Undoubtedly, protein interaction experiments are ongoing.

Early over-expression studies with *C. crescentus* FtsZ showed clear defects in the formation of stalks, leading to production of multiple stalks that were often bifurcated [20]. This is informative since it may suggest that another important event in the *Caulobacter* lifecycle, stalk biogenesis, is influenced by the actions of ParA. Early in the cell cycle a short burst of FtsZ

localization is observed at the stalked pole of the cell, notable since the levels of *ftsZ* transcription and FtsZ protein are relatively low early in the cell cycle [8, 20, 21]. Furthermore, localized peptidoglycan synthesis is observed at the stalked pole prior to the peptidoglycan synthesis associated with cell elongation and cell division. This short round of localized cell wall synthesis is abolished when FtsZ is depleted from the cell, and notably, stalks lack characteristic lateral bands under these conditions [22]. Thus, FtsZ assembly at this pole is important for this essential cell cycle event. Additionally, the MipZ inhibitory protein is localized to this pole at this time through its interaction with ParB, while the FtsZ stabilizers ZapA and FzlA are localized to the opposite pole and diffuse through the cell, respectively [8, 15]. Taken together, this suggests the need for an additional and potent activator of FtsZ assembly during this time: FtsZ protein levels are low, an assembly inhibitor is present, and identified assembly promoters are not in the vicinity. Thus, ParA could play an essential role in stalk biogenesis by stimulating the assembly of FtsZ; furthermore, the constant presence of ParB at this pole suggests that ParA in the ATP-bound state would be the predominant form, as is required for the activation of FtsZ assembly observed *in vitro*.

Future Directions

Continuing work with this system will proceed down two primary avenues. Biochemical results already obtained will be confirmed and extended, and through assay refinement more quantifiable changes to the GTPase rate and critical concentration of FtsZ in the presence and absence of ParA will be attempted. Electron Microscopy studies will focus on the identification of any FtsZ bundling activities by ParA at higher protein concentrations than previously employed. Additionally, ParA and FtsZ interaction studies will continue using traditional

methods such as co-immunoprecipitations or affinity-tag based pull-downs, as well as in vitro cross-linking with purified components. The strong curvature of FtsZ filaments induced by ParA•ATP when viewed by EM may also be of importance. Using reconstituted liposomes and fluorescent fusions to FtsZ, a system that has been previously used to study FtsZ dynamics [23, 24], real-time changes to the assembly and membrane reformation mediated by FtsZ will be monitored. If the observed curvature is of real significance, it should be obvious in the changes to the liposome shape that occur with and without the presence of ParA. Though not discussed in this work, experiments have begun addressing the effect of ParB on the assembly of FtsZ, following the observation that ParA and ParB without ATP slightly increased the production of GDP in our regenerative GTPase assay. Early sedimentation studies show a slight decrease in pelleted FtsZ at increasing concentrations of ParB, though insufficient work has been done to confirm these results. It will be interesting to see if this effect is enhanced by the presence of *parS* DNA; if so, this would be an indication of a direct nucleoid occlusion mechanism in *Caulobacter crescentus*, similar to Noc or SlmA in *B. subtilis* and *E. coli*. Finally, in the long term, it could prove insightful to compare the sequence of ParA with other known effectors of FtsZ assembly, and thereby identify residues or regions that should be mutagenized and studied with FtsZ. Comparisons with MipZ and MinD could highlight regions that mediate interactions between FtsZ and members of this family of deviant Walker-A ATPases. Additionally, comparisons to SepF, ZapA, and FzlA could identify regions that are responsible for the FtsZ filament-stabilizing effects of ParA observed *in vitro*.

The second focus of continuing work will be on the physiological importance of the activity of ParA in relation to FtsZ. An important starting point will be to address the discrepancy in ParA

localization data when visualized as a fluorescent fusion or by epitope tagged immunofluorescence. Clear localization data may help elucidate when and where ParA localization occurs in conjunction with FtsZ assemblies. Over-expression and rescue studies will also be used to confirm our *in vitro* results. Either over-expression of ParA or depletion of ParB will result in a shift toward ParA•ADP, as previously demonstrated [19, 25]. If over-expression of FtsZ is capable of suppressing the phenotype observed in a ParA•ADP dominant cell, then the *in vitro* results are very likely physiologically relevant. Additionally, using similar over-expression and depletion experiments, possible effects on stalk biogenesis can be monitored in ParA•ADP or ParA•ATP dominant-cells. If the proposed model is correct, then a ParA•ADP dominant cell should produce stalks that lack a banding pattern, as are observed in FtsZ depleted cells, while ParA•ATP dominant cells should produce multiple and bifurcated stalks, similar to FtsZ over-expression strains. It would also be interesting to see if FtsZ assembly and ring formation can be induced at aberrant sites through the forced relocation of ParA. This could be achieved through fusions to proteins not normally associated with the poles or division plane, such as the SMC protein, though many options exist [26, 27]. Additionally, the localization of ParB could be changed by inserting *parS* sequences into *terminus* proximal regions of the chromosome, which may induce ParA•ATP accumulation in regions where it would not normally occur. These experiments will be undoubtedly difficult since ParA plays an essential role in chromosome partitioning beyond any possible role in FtsZ regulation, thus phenotypes may be multifaceted and confusing; however, the possible information culled from such experiments make these approaches worth pursuing. Finally, if any residues or regions of interest are targeted for mutagenesis following sequence comparisons with FtsZ interacting proteins as described above, conditional expression strains will be created to monitor the effects of such

mutations *in vivo* in the absence of wild-type ParA. Another long-term goal for experiments with this system is to identify additional binding partners of ParA that may act as a nucleotide exchange factor. The ParB protein is discretely localized at the poles of the *Caulobacter* cell and only passes the midcell during its relatively rapid partitioning following the onset of DNA replication [16, 28]. Thus, if ParA•ATP is essential for the stimulation of FtsZ assembly at the midcell, it may be necessary to have an additional exchange factor to maintain the ATP-bound state. This search could be accomplished through a broad based tandem affinity purification of ParA followed by mass spectrometry, or through a more directed approach. The N-terminal portion of ParB has been shown to be essential for its interaction with ParA, and expression of truncated ParB produces similar FtsZ effects as a full depletion of ParB [19]. A search for uncharacterized proteins with similar motifs may yield a small subset of targets that could be further refined through other parameters, such as the presence of cell cycle dependent promoters for the particular identified genes. Identified targets would then be assayed for localization, and the effects of over-expression and depletion on the progression of the cell cycle and *Caulobacter crescentus* viability.

References

[1] Leendert W. Hamoen, Jean-Christophe Meile, Wouter de Jong, Philippe Noirot, and Jeff Errington. SepF, a novel FtsZ-interacting protein required for a late step in cell division. *Mol. Microbiol.* 59: 989-999, 2006.

[2] Shu Ishikawa, Yoshikazu Kawai, Konosuke Hiramatsu, Masayoshi Kuwano, and Naotake Ogasawara. A new FtsZ-interacting protein, YlmF, complements the activity of FtsZ during progression of cell division in *Bacillus subtilis*. *Mol. Microbiol.* 60: 1364-1380, 2006.

[3] Jay Kumar Singh, Ravindra D. Makde, Vinay Kumar, and Dulal Panda. SepF increases the assembly and bundling of FtsZ polymers and stabilizes FtsZ protofilaments by binding along its length. *J. Biol. Chem.* 283: 45: 31116-31124, 2008.

[4] Muhammet E. Gündoğdu, Yoshikazu Kawai, Nada Pavlendova, Naotake Ogasawara, Jeff Errington, Dirk-Jan Scheffers, and Leendert W. Hamoen. Large ring polymers align FtsZ polymers for normal septum formation. *EMBO J.* 30: 617-626, 2011.

[5] Frederico J. Gueiros-Filho and Richard Losick. A widely conserved bacterial cell division protein that promotes assembly of the tubulin-like protein FtsZ. *Genes Dev.* 16: 2544-2556, 2002.

[6] Elaine Small, Rachel Marrington, Alison Rodger, David J. Scott, Katherine Sloan, David Roper, Timothy R. Dafforn, and Stephen G. Addinall. FtsZ polymer-bundling by the *Escherichia coli* ZapA orthologue, YgfE, involves a conformational change in bound GTP. *J. Mol. Biol.* 369: 210-221, 2007.

[7] Tamimount Mohammadi, Ginette E. J. Ploeger, Jolanda Verheul, Anouskha D. Comvalius, Ariadna Martos, Carlos Alfonso, Jan van Marle, Germán Rivas, and Tanneke den Blaauwen. The GTPase activity of *Escherichia coli* FtsZ determines the magnitude of the FtsZ polymer bundling by ZapA *in vitro*. *Biochemistry* 48: 11056-11066, 2009.

[8] Erin D. Goley, Yi-Chun Yeh, Sun-Hae Hong, Michael J. Fero, Eduardo Abeliuk, Harley H. McAdams, and Lucy Shapiro. Assembly of the *Caulobacter* cell division machine. *Mol. Microbiol.* 80: 1680-1698, 2011.

[9] Erin D. Goley, Natalie A. Dye, John N. Werner, Zemer Gitai, and Lucy Shapiro. Imaging-based identification of a critical regulator of FtsZ protofilament curvature in *Caulobacter*. *Mol. Cell* 39: 975-987, 2010.

[10] Ewa Król, Sebastiaan P. van Kessel, Laura S. van Bezouwen, Neeraj Kumar, Egbert J. Boekema, and Dirk-Jan Scheffers. *Bacillus subtilis* SepF binds to the C-terminus of FtsZ. *PLoS One* 7: e43293, 2012.

[11] Ramona Duman, Shu Ishikawa, Ilkay Celik, Henrik Strahl, Naotake Ogasawara, Paulina Troc, Jan Löwe, and Leendert W. Hamoen. Structural and genetic analyses reveal the protein SepF as a new membrane anchor for the Z ring. *Proc. Natl. Acad. Sci. USA* 110: E4601-E4610, 2013.

[12] Eugene V. Koonin. A superfamily of ATPases with diverse functions containing either classical or deviant ATP-binding motif. *J. Mol. Biol.* 229: 1165-1174, 1993.

[13] Detlef D. Leipe, Yuri I. Wolf, Eugene V. Koonin, and L. Aravind. Classification and evolution of P-loop GTPases and related ATPases. *J. Mol. Biol.* 317: 41-72, 2002.

[14] Piet A. J. de Boer, Robin E. Crossley, and Lawrence I. Rothfield. Roles of MinC and MinD in the site-specific septation block mediated by the MinCDE system of *Escherichia coli*. *J. Bacteriol.* 174: 63-70, 1992.

[15] Martin Thanbichler and Lucy Shapiro. MipZ, a spatial regulator coordinating chromosome segregation with cell division in *Caulobacter*. *Cell* 126: 147-162, 2006.

[16] Dane A. Mohl and James W. Gober. Cell cycle-dependent polar localization of chromosome partitioning proteins in *Caulobacter crescentus*. *Cell* 88: 675-684, 1997.

[17] Jerod L. Ptacin, Steven F. Lee, Ethan C. Garner, Esteban Toro, Michael Eckart, Luis R. Comolli, W. E. Moerner, and Lucy Shapiro. A spindle-like apparatus guides bacterial chromosome segregation. *Nat. Cell Biol.* 12: 791-798, 2010.

[18] Dane A. Mohl, Jesse Easter, Jr., and James W. Gober. The chromosome partitioning protein, ParB, is required for cytokinesis in *Caulobacter crescentus*. *Mol. Microbiol.* 42: 741-755, 2001.

[19] Rainer M. Figge, Jesse Easter, Jr., and James W. Gober. Productive interaction between the chromosome partitioning proteins, ParA and ParB, is required for the progression of the cell cycle *Caulobacter crescentus*. *Mol. Microbiol.* 47: 1225-1237, 2003.

[20] Ellen Quardokus, Neena Din, and Yves V. Brun. Cell cycle regulation and cell type-specific localization of the FtsZ division initiation protein in *Caulobacter*. *Proc. Natl. Acad. Sci. USA* 93: 6314-6319, 1996.

[21] Aaron J. Kelly, Marcella J. Sackett, Neena Din, Ellen Quardokus, and Yves V. Brun. Cell cycle-dependent transcriptional and proteolytic regulation of FtsZ in *Caulobacter*. *Genes Dev.* 12: 880-893, 1998.

[22] Arun V. Divakaruni, Cyril Baida, Courtney L. White, and James W. Gober. The cell shape proteins MreB and MreC control cell morphogenesis by positioning the cell wall synthetic complexes. *Mol. Microbiol.* 66: 174-188, 2007.

[23] Masaki Osawa, David E. Anderson, and Harold P. Erickson. Reconstitution of contractile FtsZ rings on Liposomes. *Science* 320: 792-794, 2008.

[24] Masaki Osawa and Harold P. Erickson. Liposome division by a simple bacterial division machinery. *Proc. Natl. Acad. Sci. USA* 110: 11000-110004, 2013.

[25] Jesse Easter, Jr. and James W. Gober. ParB-stimulated nucleotide exchange regulates a switch in functionally distinct ParA activities. *Mol. Cell* 10: 427-434, 2002.

[26] Rasmus B. Jensen and Lucy Shapiro. Cell-cycle-regulated expression and subcellular localization of the *Caulobacter crescentus* SMC chromosome structural protein. *J. Bacteriol.* 185: 3068-3075, 2003.

[27] John N. Werner and Zemer Gitai. High-throughput screening of bacterial protein localization. *Methods Enzymol.* 471: 185-204, 2010.

[28] Esteban Toro, Sun-Hae Hong, Harley H. Mcadams, and Lucy Shapiro. *Caulobacter* requires a dedicated mechanism to initiate chromosome segregation. *Proc. Natl. Acad. Sci. USA* 40: 15435-15440, 2008.

APPENDIX I

Supplemental Data to Chapter 3

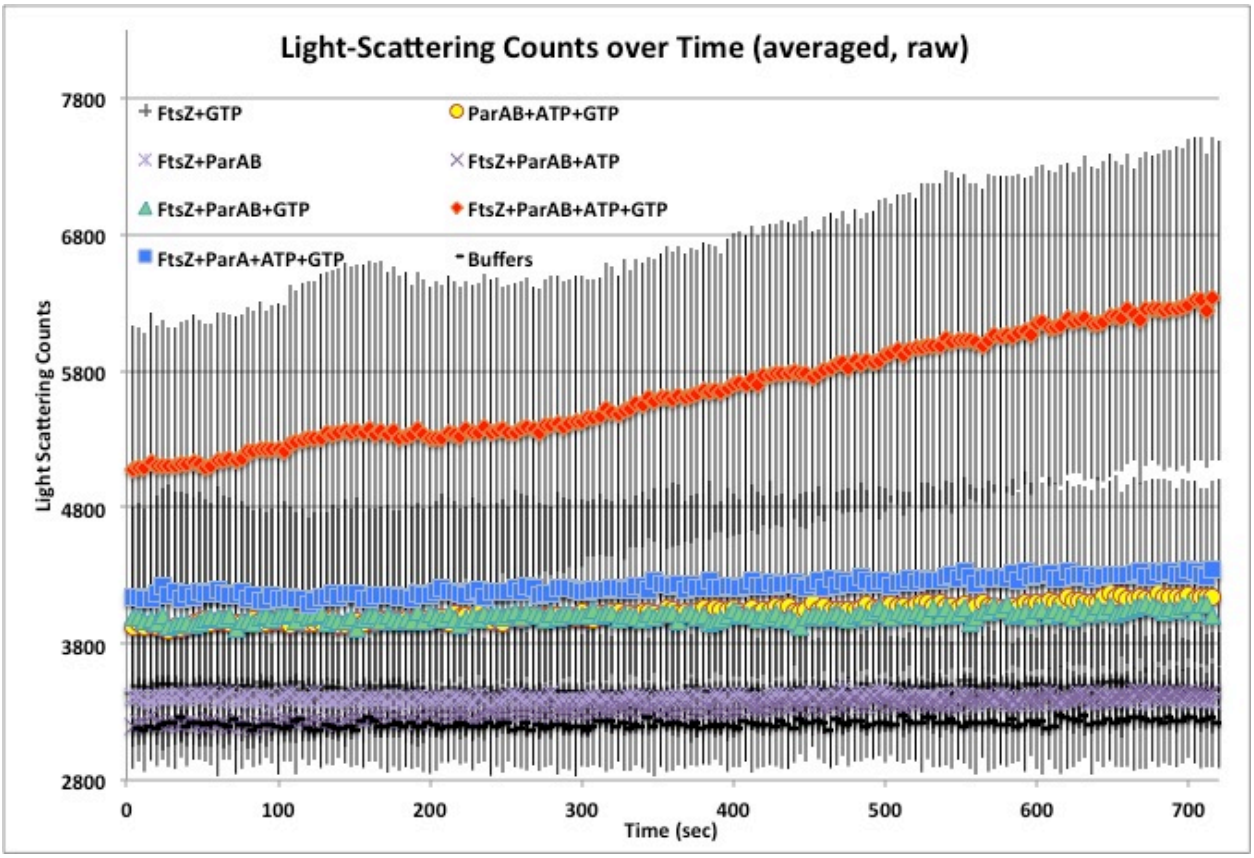

Figure S1: Averaged Raw Light Scattering Data (Chapter 3, Section 3).
Light scattering data from FtsZ assembly monitored under different conditions. This figure is identical to that presented in the main text, except that initial background counts have not been removed from the data prior to averaging. Recorded scattering data from the four trials for each condition was averaged and plotted versus time. The increase in the standard deviation of the averages versus that of the normalized data presented in the text is apparent. It should be noted that the increase in scattering observed in the presence of ParB/ParA•ATP still increases over the control conditions to a significant degree without the normalization of data.

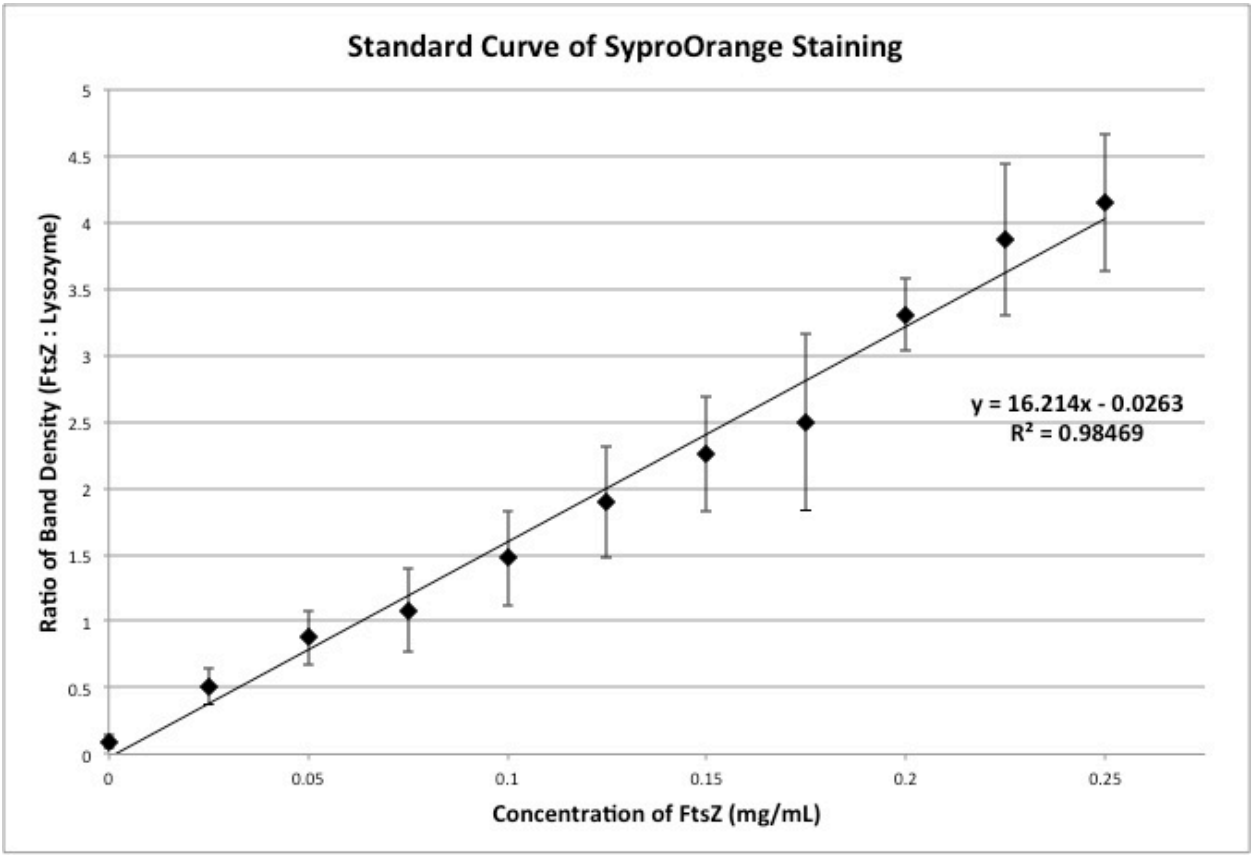

Figure S2: SyproOrange Standard Curve (Chapter 3, Section 3).
The standard curve of SyproOrange staining intensity of FtsZ, normalized to the staining intensity of a lysozyme loading band, is shown above produced from six protein gels using unique FtsZ preparations. FtsZ concentration was determined by Bradford assay using BSA as a standard. Band intensity was quantified using an identically sized box for all gels using the BioRad QuantityOne program. FtsZ concentration ranged from 0 to 250µg/mL in 25µg/mL increments. Graph, standard deviations, and linear trendline and equation were produced with Microsoft Excel.

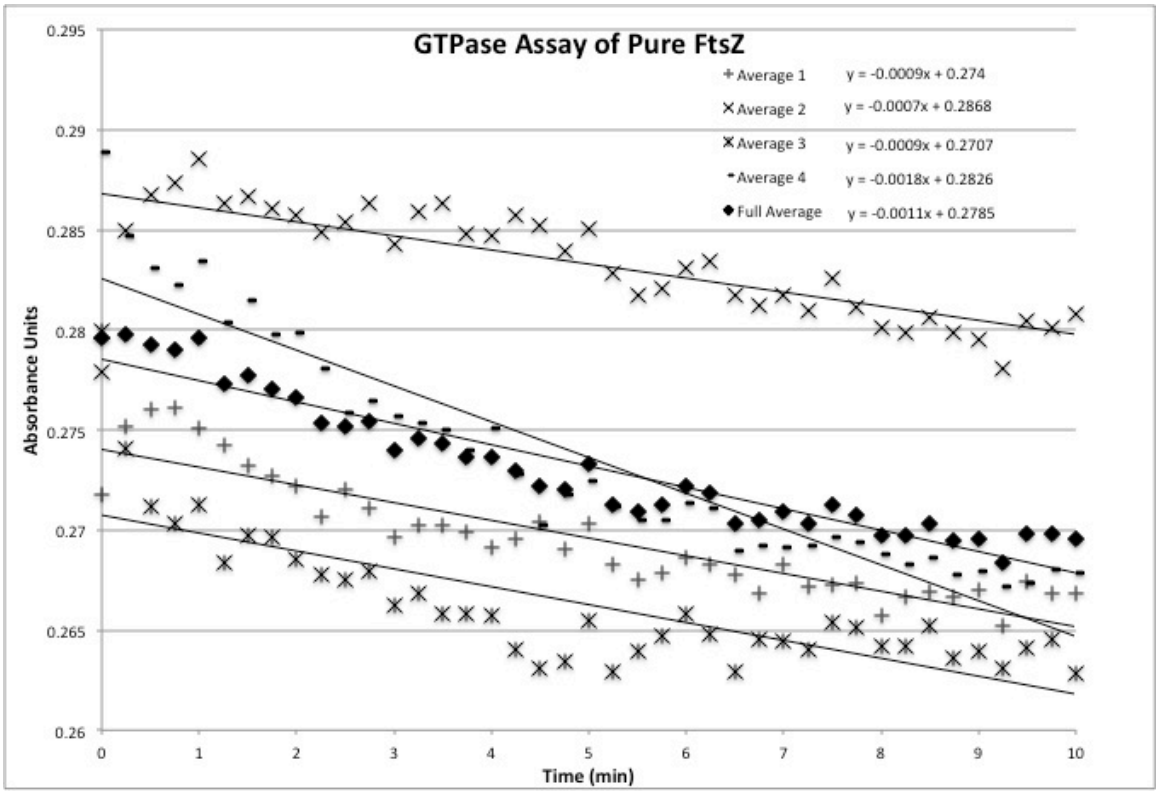

Figure S3: Absorbance data from individual runs of regenerative GTPase assay.
The averaged absorbance data from the two concurrent trials of each continuous and regenerative GTPase assay are shown. For each condition, four independent assays were performed, with each assay run in tandem. The averaged absorbance data duplicate sets are shown over time. The overall average rate, also shown in Figure 3.5 in the text, is presented with each condition for comparison. The equation of the applied linear trendline for each duplicate assay is presented next to the symbol legend. The first graph (above) shows data from the GTPase assay performed on pure FtsZ with GTP alone (at 1μM and 1mM, respectively). The subsequent graphs (following page) show data from the GTPase assay performed with FtsZ and GTP as before, with ParA and ParB (at 1μM each). The top graph presents data in the absence of ATP; the second graph in the presence of 1mM ATP.

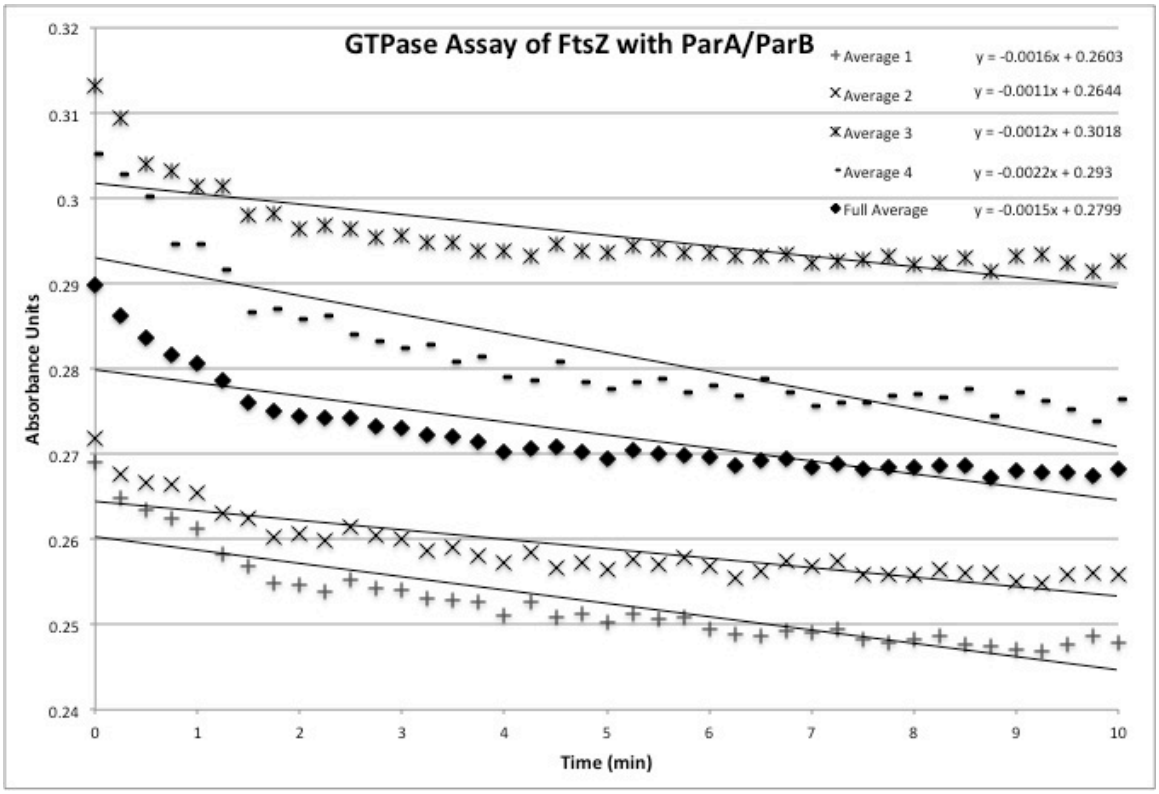
GTPase Assay of FtsZ with ParA/ParB
Average 1 y = -0.0016x + 0.2603
Average 2 y = -0.0011x + 0.2644
Average 3 y = -0.0012x + 0.3018
Average 4 y = -0.0022x + 0.293
Full Average y = -0.0015x + 0.2799
Absorbance Units
Time (min)

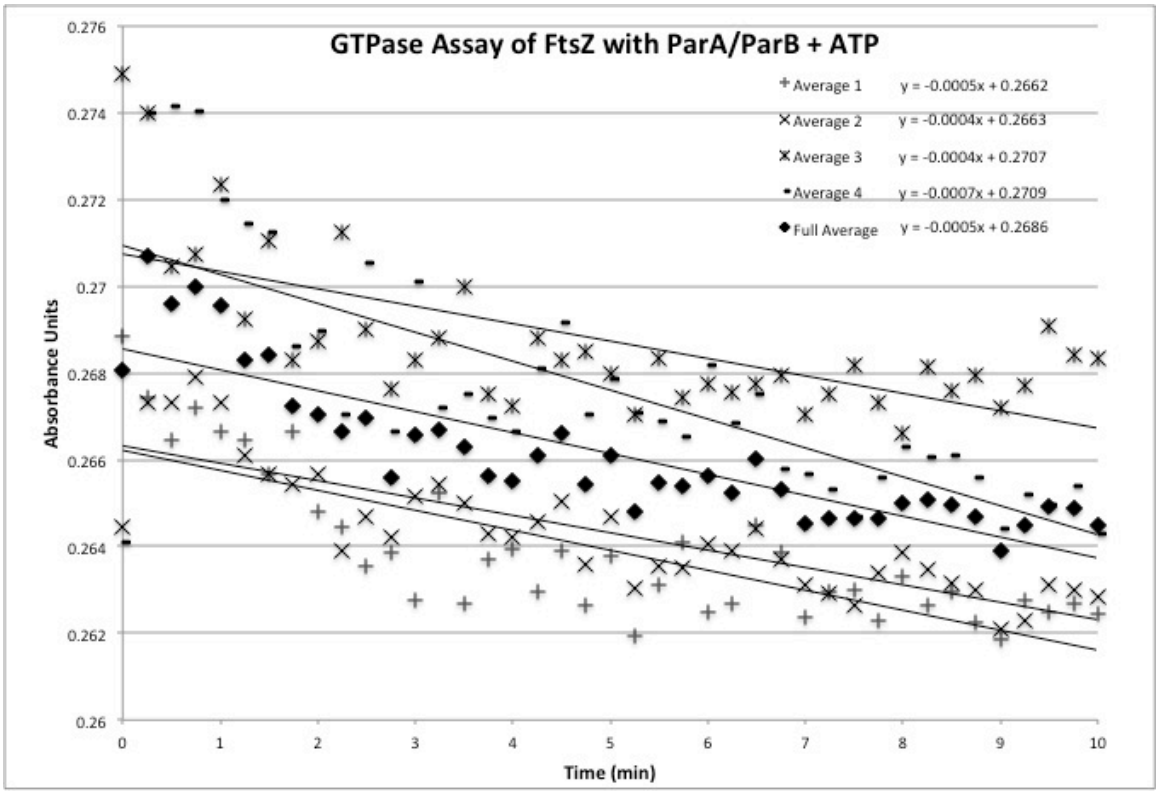
GTPase Assay of FtsZ with ParA/ParB + ATP
Average 1 y = -0.0005x + 0.2662
Average 2 y = -0.0004x + 0.2663
Average 3 y = -0.0004x + 0.2707
Average 4 y = -0.0007x + 0.2709
Full Average y = -0.0005x + 0.2686
Absorbance Units
Time (min)

Figure S4: Full Electron Micrographs of FtsZ Assembly Experiments.
Shown below are the full micrographs from experiments described in Chapter 3, Section 5. The white scale bar in the right corner corresponds to 100nm. Note: The long lines visible at the edge of some images are due to the glass support used during the scanning of micrograph negatives.

Images 1-4: FtsZ (400nM) + GTP (1mM)

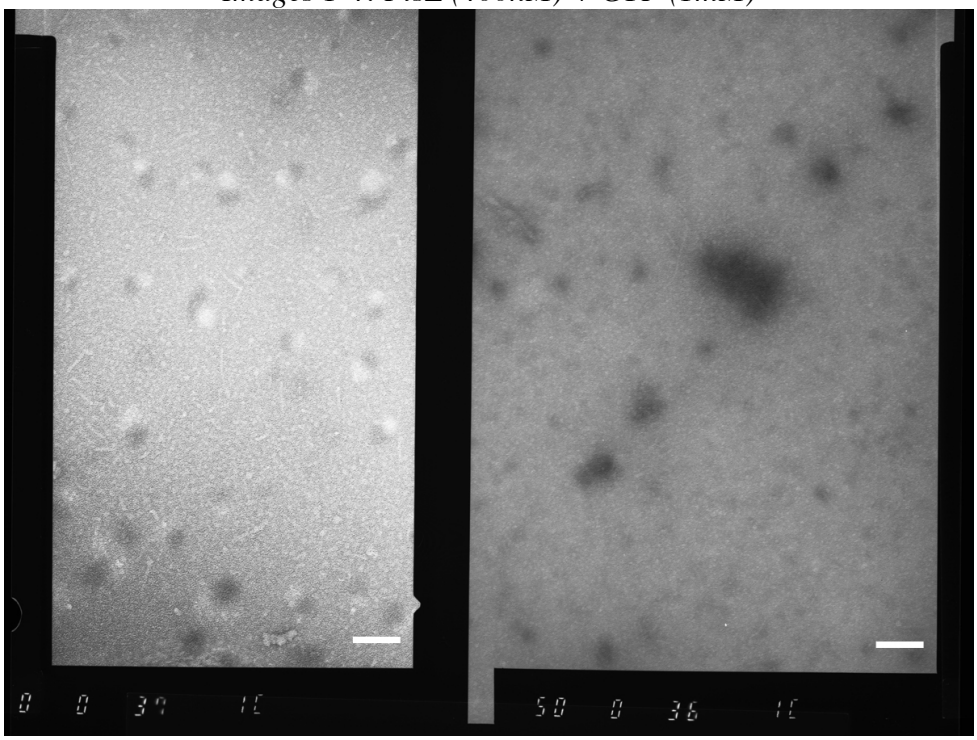

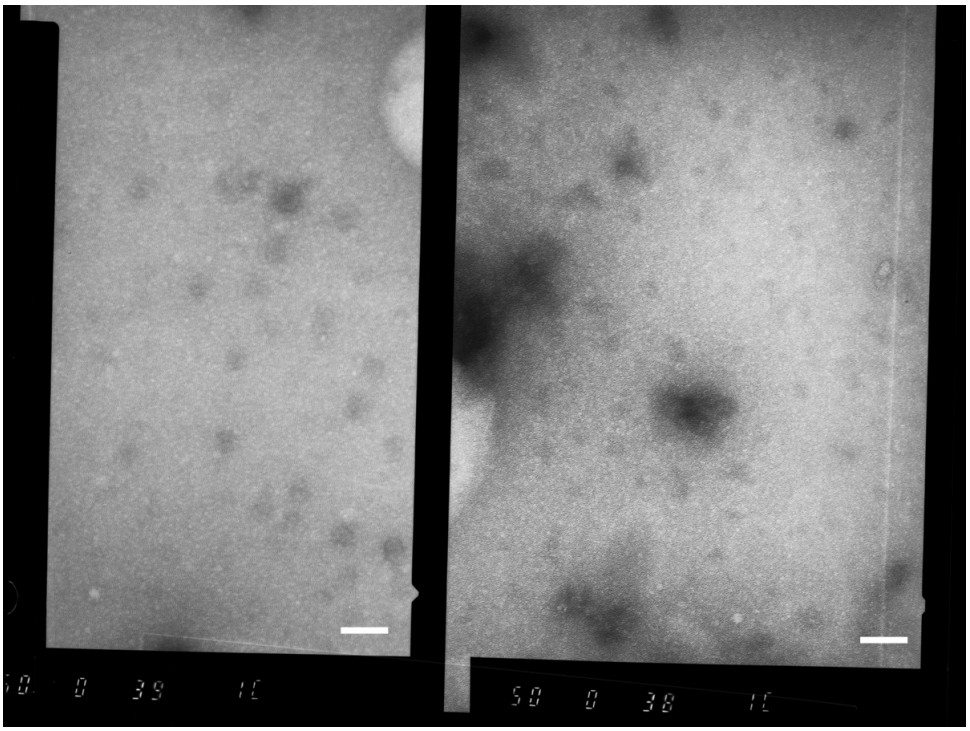

Images 5-8: FtsZ (400nM) +GTP (1mM) + ParA (800nM) + ParB (800nM) + ATP (1mM)

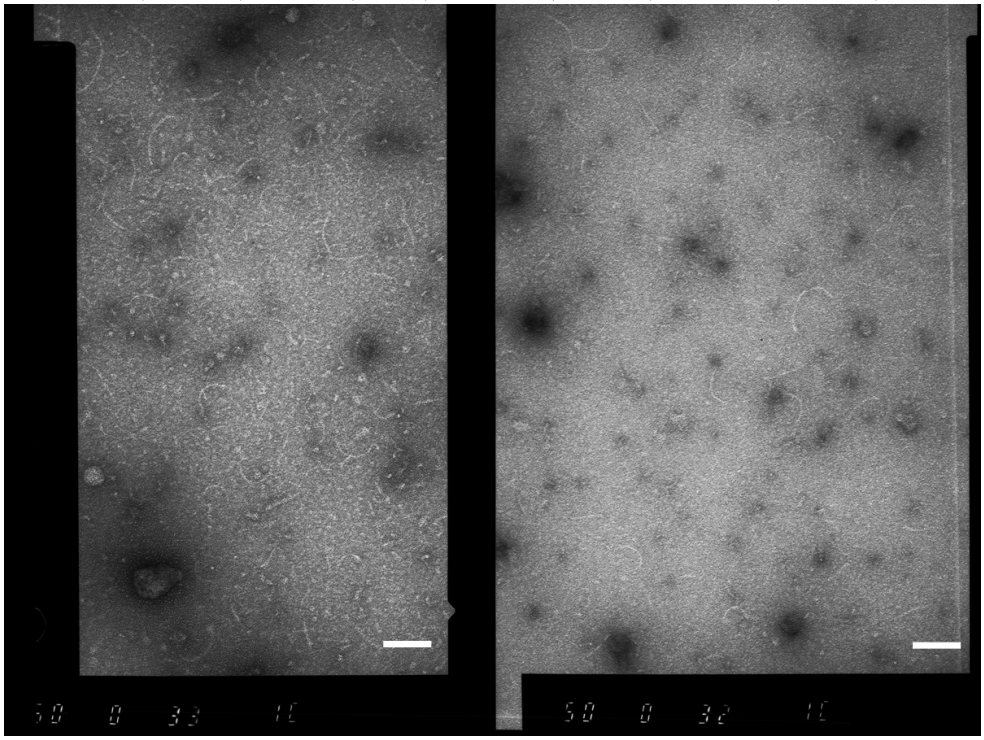

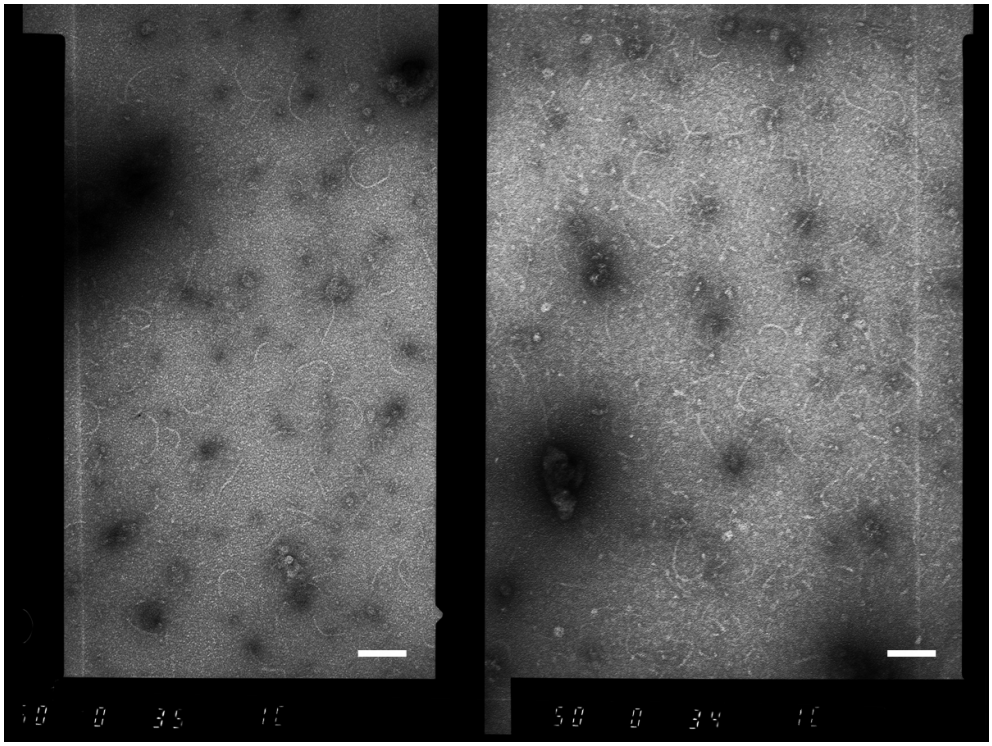

Images 9-12: FtsZ (750nM) + GTP (1mM)

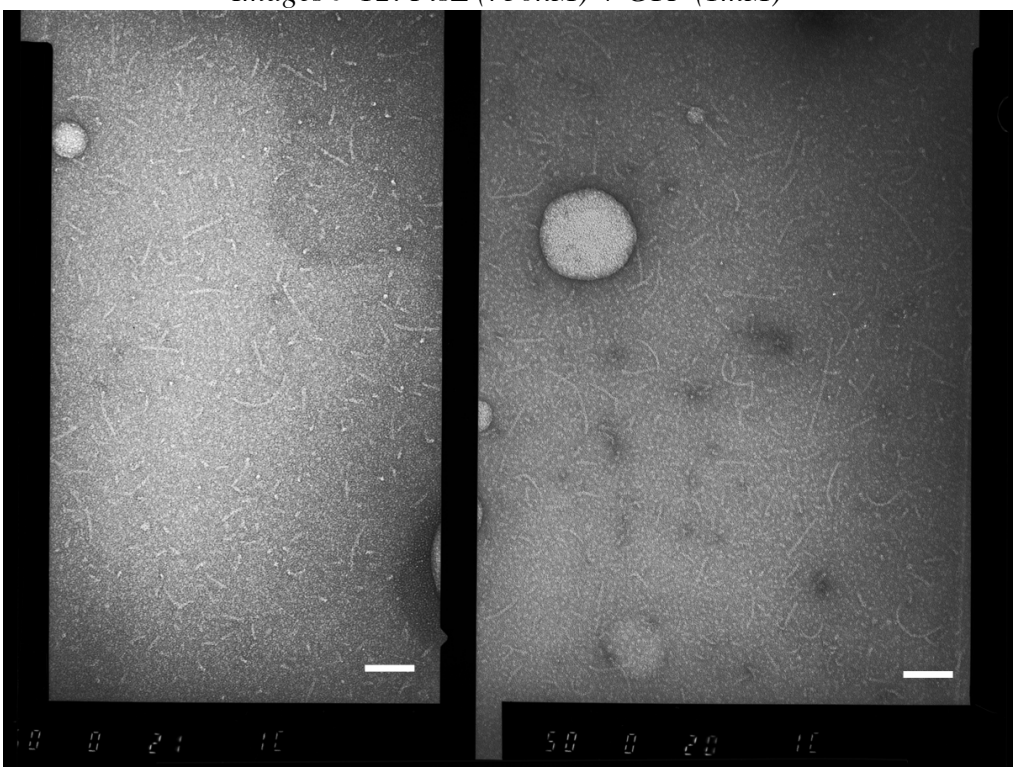

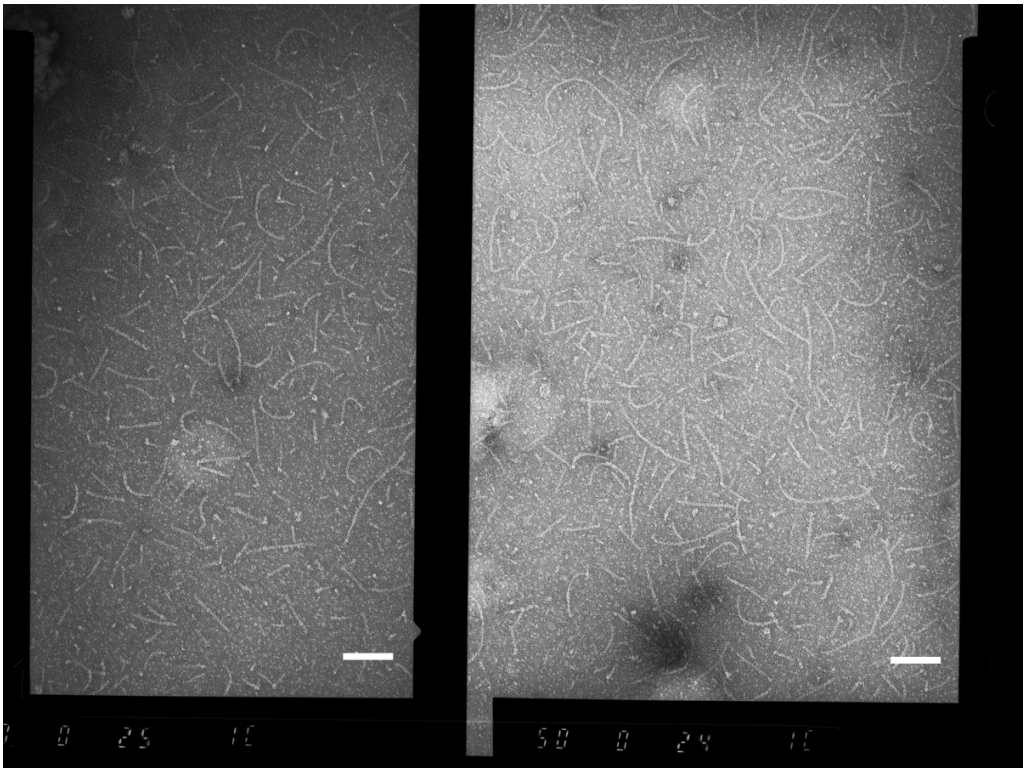

Images 13-16: FtsZ (750nM) + GTP (1mM) + ParA (1.5μM) + ParB (1.5μM) + ATP (1mM)

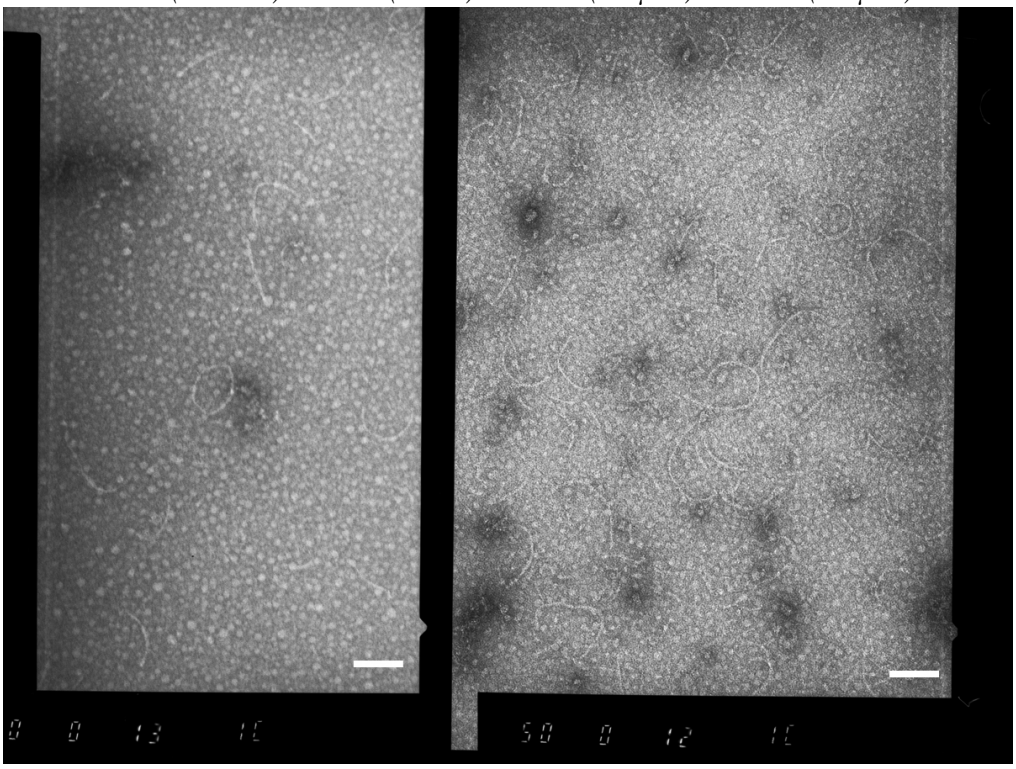

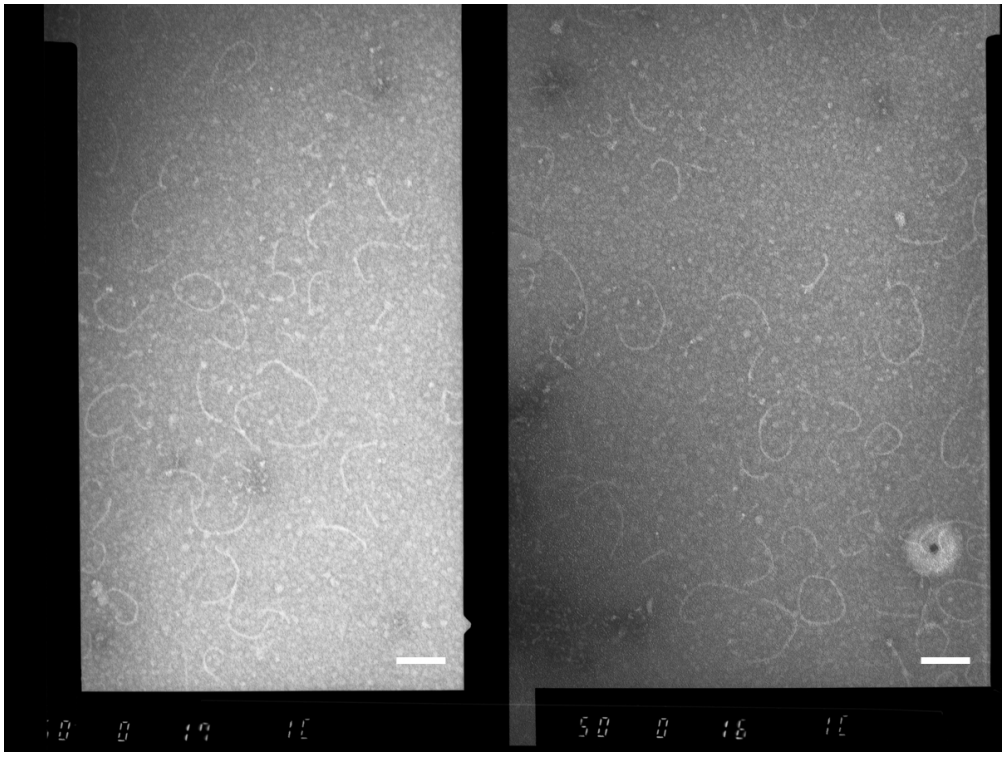

Images 17-20: ParA (1.5μM) + ParB (1.5μM) + ATP (1mM)

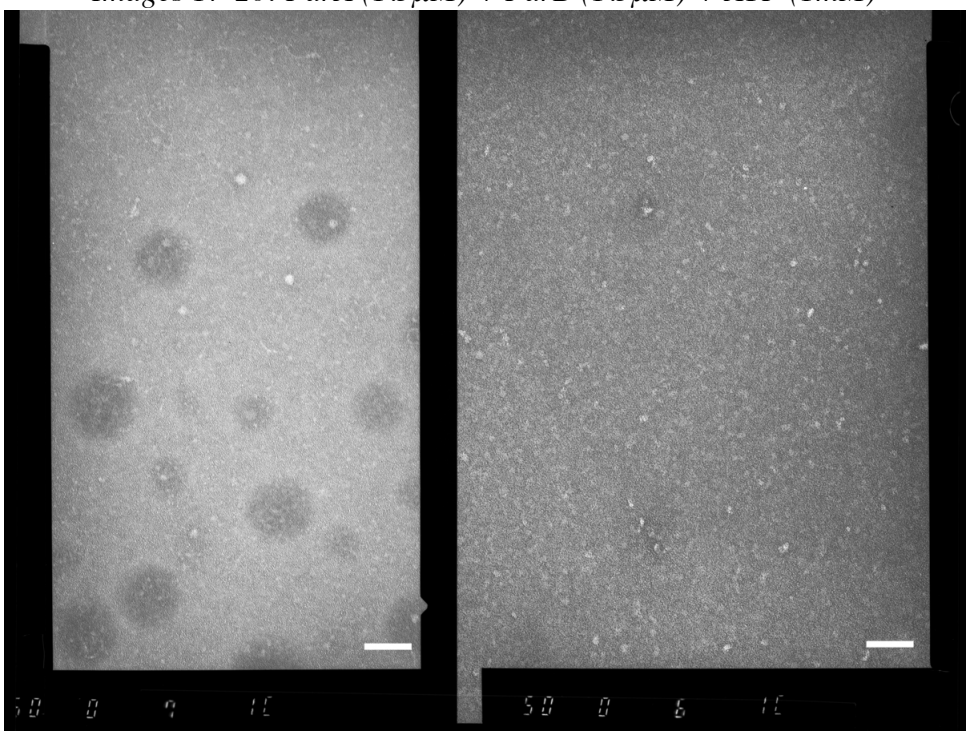

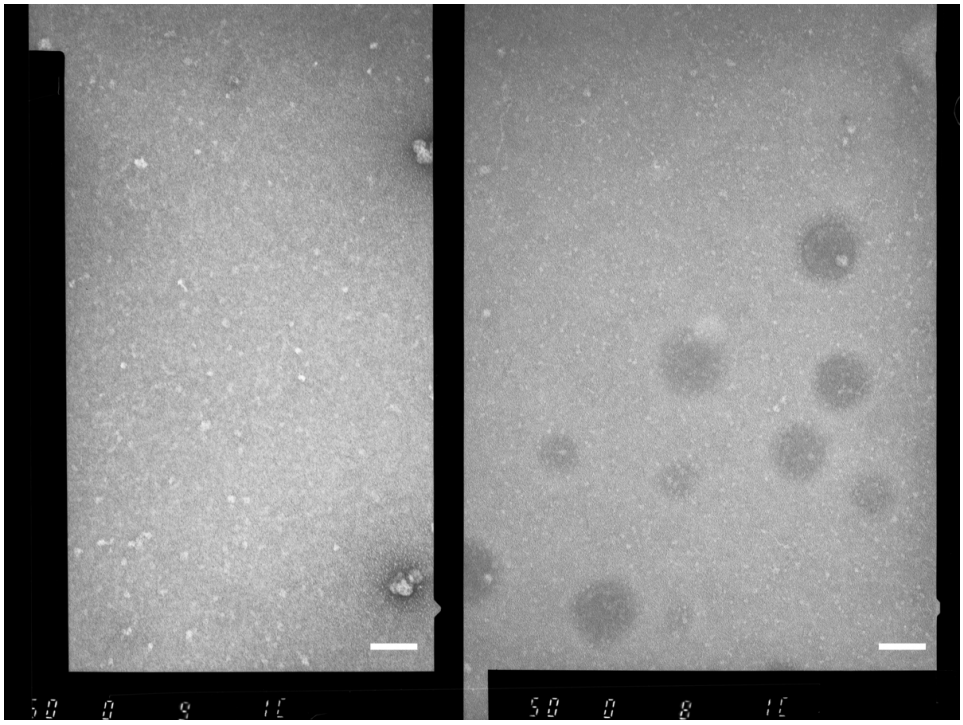

APPENDIX II

The gene products of the operon encoding condensin proteins ScpA and ScpB in *Caulobacter crescentus*

Introduction

Coordination of cytokinesis with the events of chromosomal segregation is likely not limited to the partitioning system of *Caulobacter crescentus*. Genes encoding probable homologues to the condensin proteins ScpA and ScpB have been identified, within an operon that includes a homologue of *Escherichia coli* FtsN protein. FtsN is a conserved and late recruit to the divisome that binds peptidoglycan through a conserved SPOR motif [1, 2, reviewed in 3]. The condensins are a family of proteins homologous to eukaryotic kleisins, which interact with double-stranded DNA and the architectural chromosome binding protein SMC (*Structural Maintenance of Chromosomes*) [4 - 6, reviewed in 7]. Also within this operon is a third gene encoding a protein that has motifs similar to glycosyl-hydrolases, a catalytic motif possibly related to peptidoglycan targeted enzymes. The arrangement of a conserved divisome component and chromosomal organizational proteins within a single operon suggests that these two systems may be functionally linked, or at least that a coordinated transcriptional program is necessary for the proper function of both systems. Compiled within this appendix is preliminary work assessing general features of these proteins, including protein localizations within the cell cycle, work with a null-mutation of the condensin protein ScpA; also provided is a list of bacterial strains created for the study of this operon. Based on CB15-sequence designations [8], the genes of the operon are as follows: *ftsN* (CC_2007), uncharacterized gene with glycosyl-hydrolase homology (CC_2006), *scpA* (CC_2005), *scpB* (CC_2004). During the course of this work, CC_2007 was termed SpoR (*spoR*) and CC_2006 was termed GlyH (*glyH*) as convenient shorthand, due to the uncharacterized nature of these proteins. Concurrent with these experiments, work was published implicating CC_2007 as the *Caulobacter crescentus* homologue of FtsN [2].

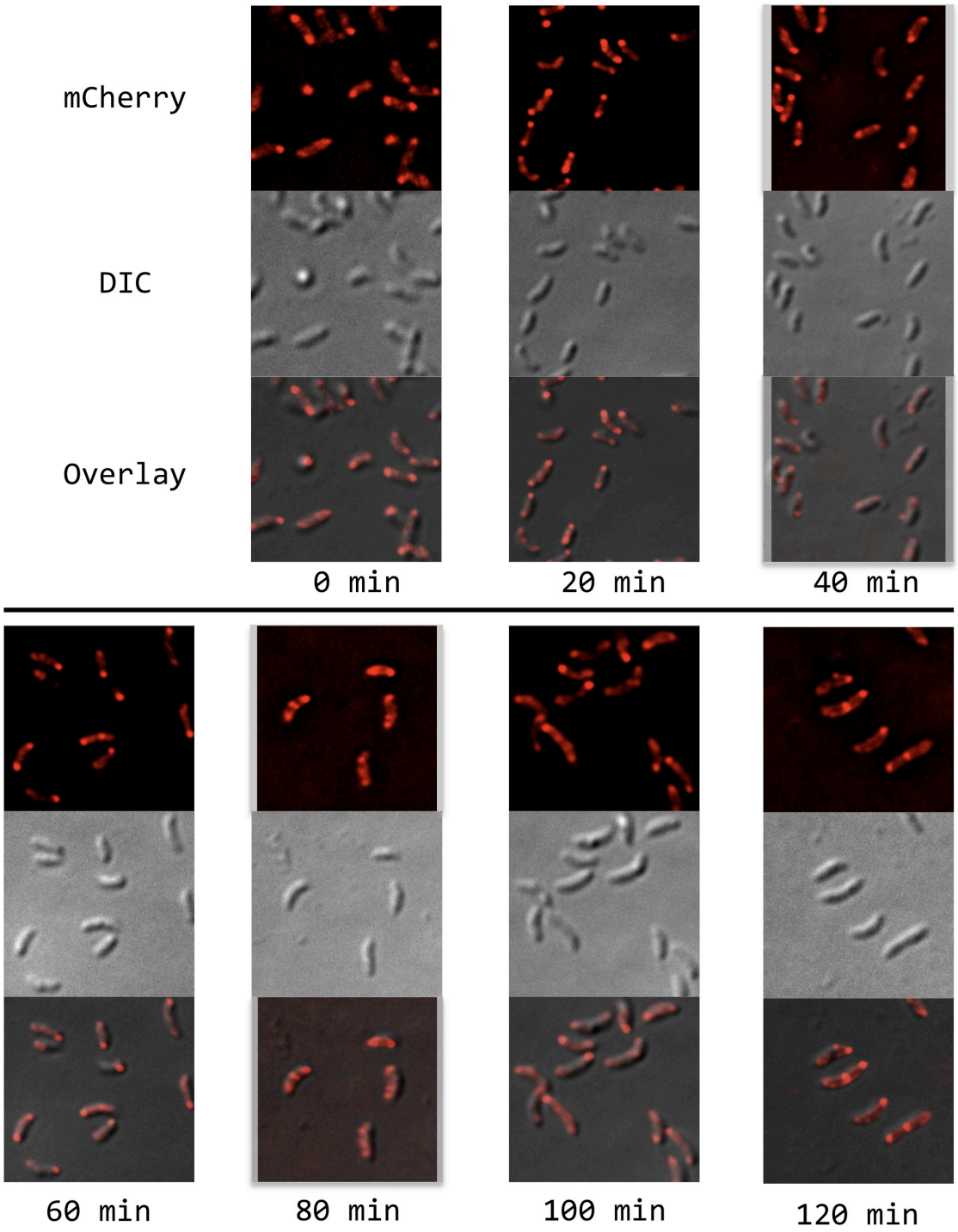

Figure S5: Cell Cycle Dependant Localization mCherry fusions.
Fusion of mCherry to the C-terminus of SpoR expressed from a vanillate inducible promoter on a low-copy plasmid. Cells were grown in M2-minimal media with 200uM vanillate, harvested, washed with M2 mineral salts, and synchronized by centrifugation in 50% Percoll in M2-salts. Swarmer population was isolated, washed with M2-salts, and suspended in M2-media. Samples were taken every 20 minutes and placed on a pre-treated poly-lysine slide for immediate visualization by fluorescence and DIC. Fluorescent images are the deconvolved product of 13 stacks of 0.1μM.

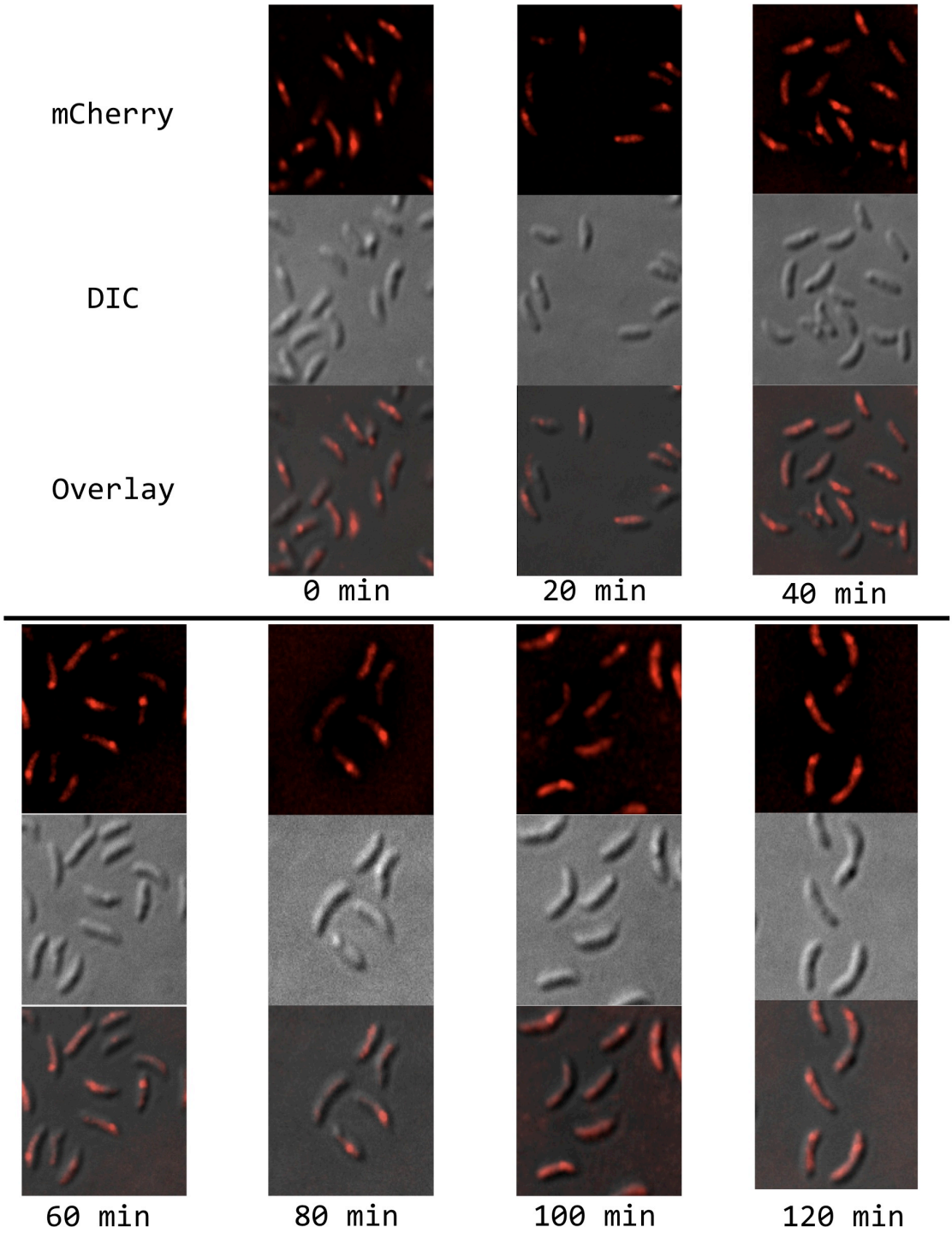

Figure S5: Cell Cycle Dependant Localization mCherry fusions.
Fusion of mCherry to the C-terminus of GlyH expressed from a vanillate inducible promoter on a low-copy plasmid.

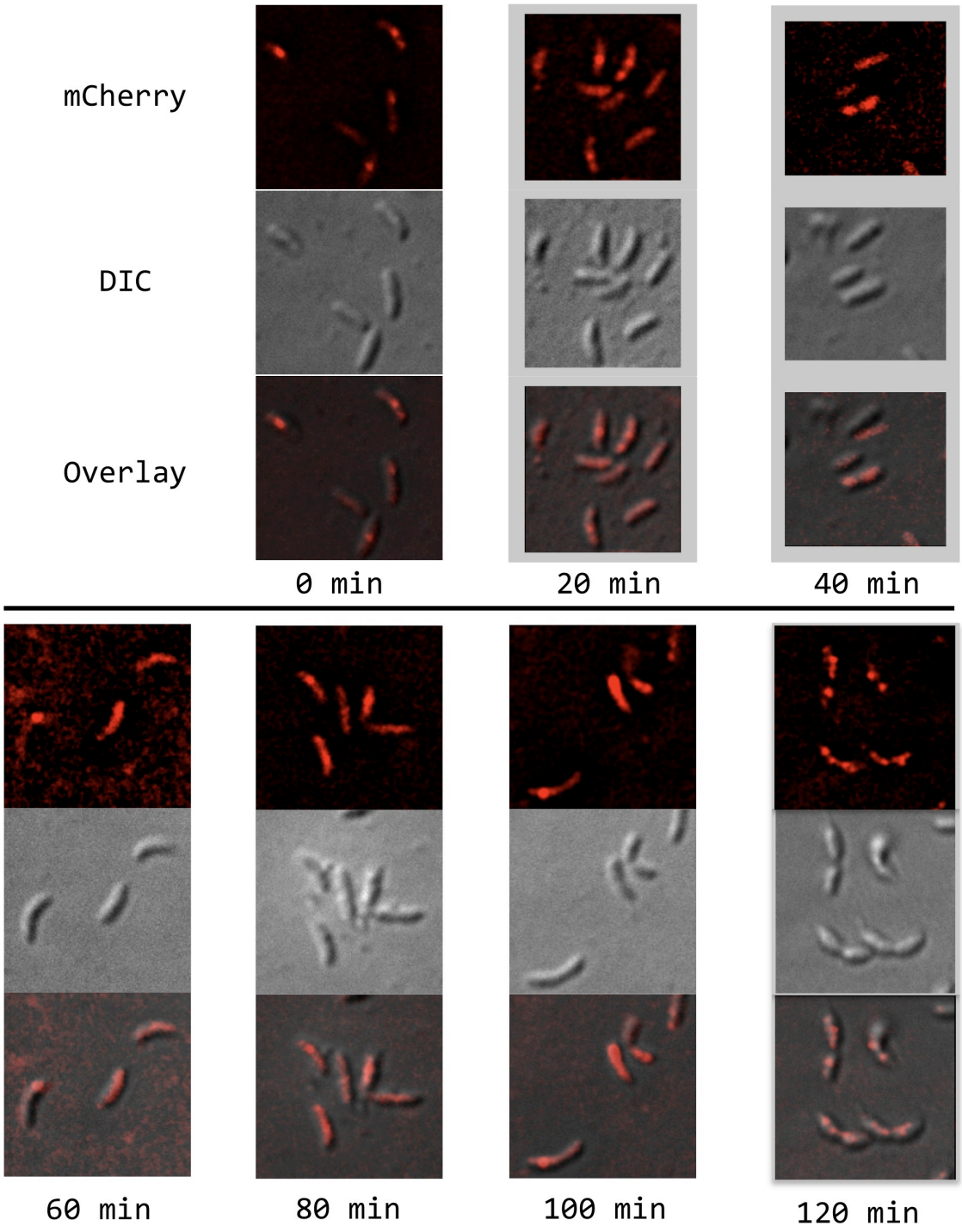

Figure S5: Cell Cycle Dependant Localization mCherry fusions.
Fusion of mCherry to the N-terminus of ScpA expressed from a vanillate inducible promoter on a low-copy plasmid.

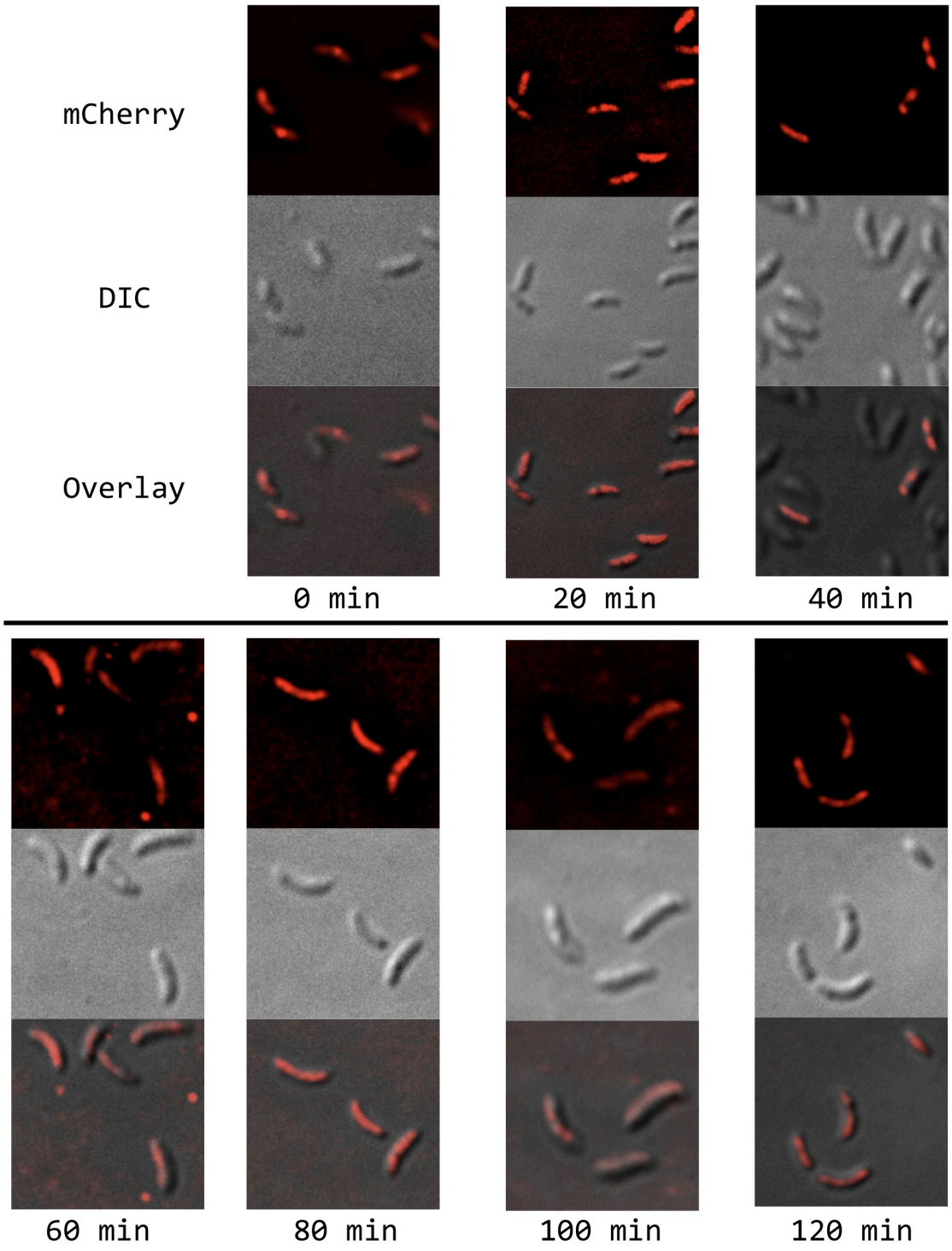

Figure S5: Cell Cycle Dependant Localization mCherry fusions.
Fusion of mCherry to the N-terminus of ScpB expressed from a vanillate inducible promoter on a low-copy plasmid.

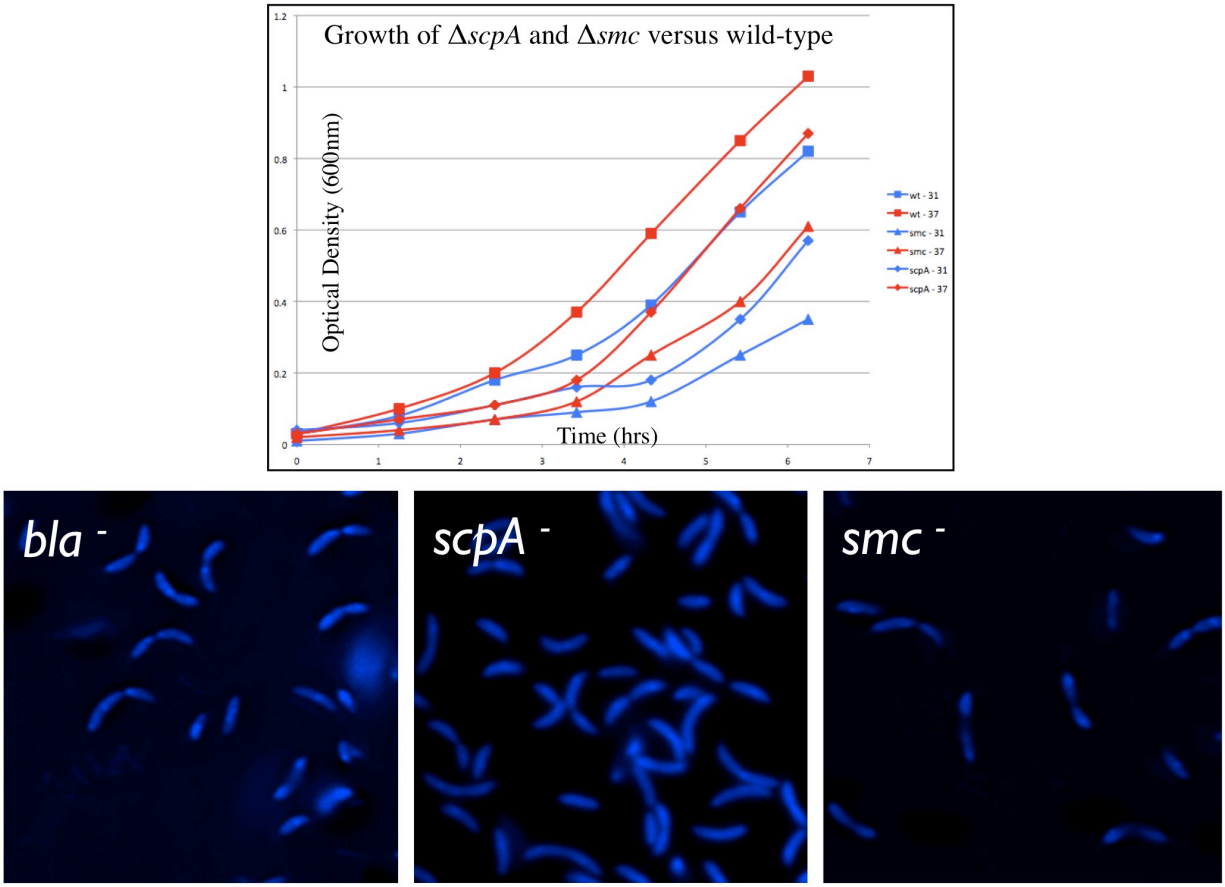

Figure S6: Growth of *smc* and *scpA* mutants at 31°C versus 37°C.
Small batch cultures of mutant *Caulobacter crescentus* were grown to mid-log phase in PYE. Fresh PYE was innoculated with each strain such that all starting cell densities were roughly equivalent. Optical density at 600nm was recorded every hour during the course of growth. Growth at both 31°C (blue) and at 37°C (red) is shown in the graph above: wild-type (*bla*) is represented by squares, a null mutation in *scpA* is indicated by diamonds, and a mutant *smc* by triangles. At the final time-point, each culture grown at 37°C was fixed in 2.5% formaldehyde at room temperature for 1 hour. Samples were washed of fixative with cold 1X PBS and stained with 2.5ng/mL of DAPI to visualize genomic DNA. Samples were imaged using the same microscope and program as the mCherry fusions, and deconvolved over 8 stacks of 0.1μm thickness.

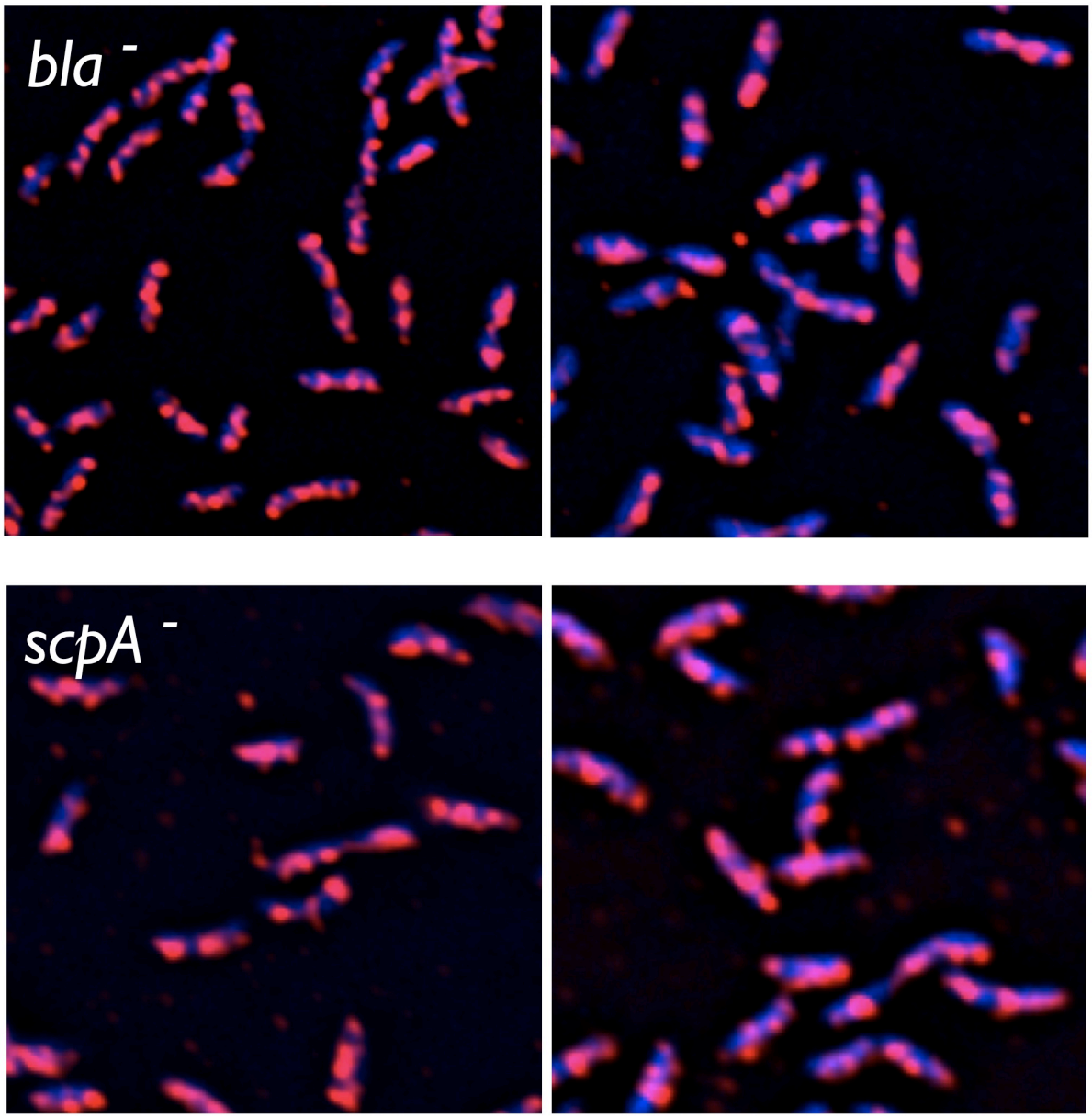

Figure S7: Localization of SMC via Immunofluorescence.
Strains were grown in PYE to mid-log phase. Aliquots of the cultures were fixed in 2.5% formaldehyde for 2 hours. Fixative was washed with 1XPBS, followed by treatment of the samples with 10µg/mL lysozyme in GTE for 15 minutes. Lysozyme was washed with 1XPBS supplemented with 2% BSA (w/v). Samples were placed onto poly-lysine treated slides and incubated for 2 hours with 1:500 dilution of rabbit derived SMC antibody [10] in PBS-T (0.2% w/v Tween-20) with 2% BSA. Samples were washed with PBS-T, followed by treatment with 1:1000 goat derived anti-rabbit IgG antibody conjugated with Cy3 fluorescent marker for 1 hour, supplemented with 2ng/mL DAPI as a counter stain. Samples were washed again with PBS-T, placed under 70% glycerol in water (w/v), and imaged as previously described. Images were deconvolved over 13 stacks of 0.1µm thickness.

Table S1: Bacterial Strains.

Strain Name	*Genotype*	*Notes*
{*Caulobacter crescentus*}		
NA1000	wild-type	[9]
Δ*bla*	wild-type	point mutation in β-lactamase (NA1000 background) conferring broad antibiotic resistance
JG3003	Δ*smc*	[Figure S6] insertion of $Spec^R$ gene into *smc* [10]
MAG2205	*van*::*spoR-mchy*	[Figure S5] Vanillate inducible fluorescent fusion. $Chlor^R$ low-copy replicating plasmid pVCHYC-6 [11]
MAG2206	*van*::*glyH-mchy*	Same as above.
MAG2207	*van*::*mchy-scpA*	Same as above.
MAG2208	*van*::*mchy-scpB*	Same as above.
MAG2209	Δ*scpA*	See note below.
{*Escherichia coli* - DH5α}		
MAG2101	*lac*::*his-spoR*Δ*59*	N-terminal His-tag to periplasmic portion of SpoR(G59→end). Amp^R pET-15b vector.
MAG2102	*lac*::*his-glyH*	N-terminal His-tag to full length GlyH; Amp^R. Expression: positive.
MAG2103	*lac*::*his-scpA*	Same as above.
MAG2104	*lac*::*his-scpB*	Same as above.
MAG2105	*xyl*::*spoR*	Full length gene in integrating xylose inducible plasmid pXTCYC-5 [11] (Tet^R), endogenous stop codon.
MAG2106	*xyl*::*glyH*	Same as above.
MAG2107	*xyl*::*scpA*	Same as above.
MAG2108	*xyl*::*scpB*	Same as above.
MAG2109	*spoR-FLAG*	C-terminal tag to full length gene on integrating plasmid for expression at native locus. $Spec^R$; pFLAG-1 [11]
MAG2110	*glyH-FLAG*	Same as above.

Notes on *scpA* null mutation: The *scpA* gene was deleted in-frame from the full operon leaving 24bp of the *scpA* gene intact on the 5' and 3' end, using by polymerase chain reaction (PCR) of an upstream and downstream fragment. PCR fragments were sub-cloned into pNTPS129 [M.R.K Alley, unpublished]. Isolated plasmid borne mutant operon was transformed into NA1000 by electroporation and selected on media plates containing kanamycin (25μg/mL). Positive transformants were spotted on regular media and additionally on media containing 3% sucrose; sucrose sensitive transformants were grown overnight in liquid culture without any selection, and plated onto media plates containing 3% sucrose. Sucrose resistant mutants were checked for sensitivity to kanamycin. Sucrose resistant and kanamycin sensitive *Caulobacter crescentus* were checked for the in-frame deletion of *scpA* via PCR on purified chromosomal DNA using primers specific to genes flanking the operon, CC_2008 and CC_2003.

References

[1] Kang Dai, Yifan Xu, and Joe Lutkenhaus. Topological characterization of the essential *Escherichia coli* cell division protein FtsN. *J. Bacteriol.* 178: 1328-1334, 1996.

[2] Andrea Möll and Martin Thanbichler. FtsN-like proteins are conserved components of the cell division machinery in proteobacteria. *Mol. Microbiol.* 72: 1037-1053, 2009.

[3] Joe Lutkenhaus. FtsN--trigger for septation [Review]. *J. Bacteriol.* 191: 7381-7382, 2009.

[4] Rasmus B. Jensen and Lucy Shapiro. The *Caulobacter crescentus smc* gene is required for cell cycle progression and chromosome segregation. *Proc. Natl. Acad. Sci. USA* 96: 10661-10666, 1999.

[5] Xindang Wang, Olive W. Tang, Eammon P. Riley, and David Z. Rudner. The SMC Condensin complex is required for origin segregation in *Bacillus subtilis*. *Curr. Biol.* 24: 287-292, 2014.

[6] Weifeng She, Qinhong Wang, Elena A. Mordukhova, and Valentin V. Rybenkov. MukEF is required for stable association of MukB with the Chromosome. *J. Bacteriol.* 189: 7062-7068, 2007.

[7] Sara Cuylen and Christian Haering. Deciphering condensing action during chromosome segregation [Review]. *Trends Cell Biol.* 21: 552-559, 2011.

[8] William C. Nierman, Tamara V. Feldblyum, Michael T. Laub, Ian T. Paulsen, Karen E. Nelson, Jonathan Eisen, John F. Heidelberg, M. R. K. Alley, Noriko Ohta, Janine R. Maddock, Isabel Potocka, William C. Nelson, Austin Newton, Craig Stephens, Nikhil D. Phadke, Bert Ely, Robert T. DeBoy, Robert J. Dodson, A. Scott Durkin, Michelle L. Gwinn, Daniel H. Haft, James F. Kolonay, John Smit, M. B. Craven, Hoda Khouri, Jyoti Shetty, Kriti Berry, Teresa Utterback, Kevin Tran, Alex Wolf, Jessica Vamathevan, Maria Ermolaeva, Owen White, Steven L. Salzberg, J. Craig Venter, Lucy Shapiro, and Claire M. Fraser. Complete genome sequence of *Caulobacter crescentus*. *Proc. Natl. Acad. Sci. USA* 98: 4136-4141, 2001.

[9] Marian Evinger and Nina Agabian. Envelope-Associated Nucleoid from *Caulobacter crescentus* stalked and swarmer cells. *J. Bacteriol.* 132: 294-301, 1977.

[10] Jennifer C. England and James W. Gober. Role of core promoter sequences in the mechanism of swarmer cell-specific silencing of *gyrB* transcription in *Caulobacter crescentus*. *BMC Microbiol.* 5, 2005.

[11] Martin Thanbichler, Antonio A. Iniesta, and Lucy Shapiro. A comprehensive set of plasmids for vanillate- and xylose-inducible gene expression in *Caulobacter crescentus*. *Nuc. Acids Res.* 35, 2007.